Entergy

Entergy Nuclear Northeast
Entergy Nuclear Operations, Inc.
Vermont Yankee
185 Old Ferry Rd.
P.O. Box 500
Brattleboro, VT 05302
Tel 802-257-5271

August 4, 2005

Docket No. 50-271
BVY 05-074
TAC No. MC0761

ATTN: Document Control Desk
U.S. Nuclear Regulatory Commission
Washington, DC 20555-0001

Subject: **Vermont Yankee Nuclear Power Station**
Technical Specification Proposed Change No. 263 – Supplement No. 31
Extended Power Uprate – Response to Request for Additional Information

References:
1) Entergy letter to U.S. Nuclear Regulatory Commission, "Vermont Yankee Nuclear Power Station, License No. DPR-28 (Docket No. 50-271), Technical Specification Proposed Change No. 263, Extended Power Uprate," BVY 03-80, September 10, 2003

2) U.S. Nuclear Regulatory Commission (Richard B. Ennis) letter to Entergy Nuclear Operations, Inc. (Michael Kansler), "Request for Additional Information – Extended Power Uprate, Vermont Yankee Nuclear Power Station (TAC No. MC0761)," July 27, 2005

3) Entergy letter to U.S. Nuclear Regulatory Commission, "Vermont Yankee Nuclear Power Station, License No. DPR-28 (Docket No. 50-271, Technical Specification Proposed Change No. 263, Supplement No. 30 – Response to Request for Additional Information," BVY 05-072, August 1, 2005

This letter provides additional information regarding the application by Entergy Nuclear Vermont Yankee, LLC and Entergy Nuclear Operations, Inc. (Entergy) for a license amendment (Reference 1) to increase the maximum authorized power level of the Vermont Yankee Nuclear Power Station (VYNPS) from 1593 megawatts thermal (MWt) to 1912 MWt.

This submittal responds to the remaining request for additional information questions from NRC's letter of July 27, 2005 (Reference 2). Entergy had previously provided a response to approximately half of those questions in its response dated August 1, 2005 (Reference 3).

AP01

This submittal primarily provides responses to the remaining RAIs not previously provided in Reference 3 including the following major topics:

1) Uncertainties that could exist in the Acoustic Circuit Analysis (ACA); Entergy calculated these uncertainties for both the methodology and the measurement techniques and applied them to the analysis to determine the overall impact on the steam dryer load definition.
2) Adequacy of the GE scale model test (SMT) benchmark of the ACA; Entergy performed additional benchmark data assessment including review of the model setup and operation and the impact of phasing sensitivity.
3) Applicability of knowledge gained from QC2 instrumented dryer tests to VYNPS assumptions, methods and conclusions; Entergy reviewed the QC2 reports for any findings or conclusions that could adversely impact assumptions, methods, or techniques used in the VYNPS analysis.
4) The remaining RAIs on the steam dryer not directly related to one of the topics noted above and three RAIs related to mechanical component evaluations.
5) A supplement to a RAI Response from the Probabilistic Safety Assessment Branch (SPSB).

Attachment 3 of Reference 3 provides an overview of Entergy's understanding of the fundamental issues left to be resolved in order to provide reasonable assurance that steam dryer integrity will be maintained at EPU conditions. These issues are drawn from 129 individual questions posed by the NRC staff. Attachment 3 of Reference 3 provides a restatement of Entergy's overall approach to the steam dryer integrity issue and the framework of Entergy's strategy in addressing the remaining fundamental issues so that the answers to individual questions can be reviewed in that context. Attachments 1, 2, 3, and 4 to this letter provide the remaining responses to the questions raised by the staff about the VYNPS steam dryer analysis.

The responses provided in Attachments 2 and 4 contain Proprietary Information as defined by 10CFR2.390 and should be handled in accordance with provisions of that regulation. Attachments 6 and 7 are non-proprietary versions of Attachments 2 and 4, respectively. Affidavits supporting the proprietary nature of the documents are provided as Attachment 8 (for Continuum Dynamics Inc. (CDI)), and as Attachment 9 (for GE). "Exhibits," which provide supporting information to certain RAI responses are included in Attachment 10. In Attachment 10, a proprietary and a non-proprietary version of Exhibit EMEB-B-143-1 are provided.

Entergy believes this submittal provides the remaining portion of the information needed to support the preparation of the NRC's safety evaluation report for EPU. In compiling and analyzing the information for this submittal, Entergy remains convinced that the VYNPS can be safely operated at up to 120% CLTP. It is our understanding that an audit of the underlying details supporting elements of this submittal will be conducted on or about August 22, 2005. Entergy anticipates that the nature of the audit will be confirmatory and respectfully requests that additional requests for information, if any, be communicated as soon as practical.

The following attachments are included in this submittal:

Attachment	Title
1	Acoustic Circuit Analysis (ACA) Uncertainty
2	GE scale model test (SMT) Benchmark Adequacy (proprietary version)
3	VYNPS Applicability of QC2 instrumented dryer tests
4	Other EMEB RAIs (proprietary version)
5	Supplemental response to SPSB RAI
6	GE scale model test (SMT) Benchmark Adequacy (non-proprietary version)
7	Other EMEB RAIs (nonproprietary version)
8	CDI affidavit for Attachment 4
9	GE affidavits for Attachments 2 and 4 and Exhibit EMEB-B-143-1
10	RAI Response Exhibits (4) Exhibit EMEB-B-143-1 Contains Proprietary Information

This supplement to the license amendment request provides additional information to clarify Entergy's application for a license amendment and does not change the scope or conclusions in the original application, nor does it change Entergy's determination of no significant hazards consideration.

There are no new regulatory commitments contained in this submittal.

Entergy stands ready to support the NRC staff's review of this submittal and suggests meetings (or audits of design files) at your earliest convenience.

If you have any questions or require additional information, please contact Mr. James DeVincentis at (802) 258-4236.

I declare under penalty of perjury that the foregoing is true and correct.

Executed on August 5, 2005.

Sincerely,

Robert J. Wanczyk

Robert J. Wanczyk
Director, Nuclear Safety Assurance
Vermont Yankee Nuclear Power Station

Attachments (10)
Enclosures (2)
cc: (see next page)

cc: Mr. Richard B. Ennis, Project Manager
Project Directorate I
Division of Licensing Project Management
Office of Nuclear Reactor Regulation
U.S. Nuclear Regulatory Commission
Mail Stop O 8 B1
Washington, DC 20555

Mr. Samuel J. Collins (w/o attachments)
Regional Administrator, Region 1
U.S. Nuclear Regulatory Commission
475 Allendale Road
King of Prussia, PA 19406-1415

USNRC Resident Inspector (w/o attachments)
Entergy Nuclear Vermont Yankee, LLC
P.O. Box 157
Vernon, Vermont 05354

Mr. David O'Brien, Commissioner (w/o proprietary information)
VT Department of Public Service
112 State Street – Drawer 20
Montpelier, Vermont 05620-2601

BVY 05-074
Docket No. 50-271

Attachment 1

Vermont Yankee Nuclear Power Station

Proposed Technical Specification Change No. 263 – Supplement No. 31

Extended Power Uprate

Response to Request for Additional Information

Acoustic Circuit Analysis (ACA) Uncertainty

Total number of pages in Attachment 1
(excluding this cover sheet) is 3.

RESPONSE TO REQUEST FOR ADDITIONAL INFORMATION REGARDING APPLICATION FOR EXTENDED POWER UPRATE LICENSE AMENDMENT VERMONT YANKEE NUCLEAR POWER STATION

PREFACE

This attachment responds to the NRC Mechanical and Civil Engineering Branch (EMEB) staff's request for additional information (RAI) dated July 27, 2005. Upon receipt of the RAI, discussions were held with the NRC staff to further clarify the RAI. In certain instances the intent of certain individual RAIs may have been modified based on clarifications reached during these discussions. The information provided herein is consistent with those clarifications.

The individual RAIs are re-stated as provided in NRC's letter of July 27, 2005.

Mechanical and Civil Engineering Branch (EMEB)
Component Integrity and Testing Section (EMEB-A)
Civil and Engineering Mechanics Section (EMEB-B)

RAI EMEB-B-18

On Page 6 of Attachment 1 to Supplement 26, Entergy states that input for the acoustic circuit model is obtained from pressure transducers installed on instrument lines from the four main steamline (MSL) venturi instrument racks and from strain gauges on each of the four MSLs between the reactor pressure vessel (RPV) nozzles and main steam safety relief valves (SRVs). Provide the basis for the assumption that the venturi pressure transducer measurements are capable of detecting very small pressure fluctuations in the MSL flow that will provide accurate and synchronized input for the acoustic circuit methodology in determining the steam dryer loads. Discuss the validation of the accuracy and synchronization of the venturi pressure transducer measurements in comparison to the MSL strain gauge data.

Response to RAI EMEB-B-18

In order to assess the uncertainty in using venturi instrument line pressure data to determine main steam line pressure, the impacts of the following key potential sources of uncertainty were evaluated:

1. The uncertainty acoustic modeling and methodology used to develop the transfer function of the sensing lines.

2. The uncertainty in the Rosemount dynamic properties, referred to here as compliance.

3. The accuracy of the instrumentation used in the mockup testing.

4. The accuracy of the instrumentation used to collect the plant data.

5. The accuracy of the predicted load based on relative location of sensing point in the steam line versus the location of the sampling point used in the benchmark test.

This acoustic load uncertainty evaluation is included in Exhibit EMEB-B-18-1. These uncertainty values described in the evaluation have been incorporated into the VYNPS steam dryer acoustic load definition.

RAI EMEB-B-32

With the uncertainties inherent in the applied FIV (acoustic and computational fluid dynamics) pressure loading, GE indicates on Page 1 of Attachment 6 to Supplement 26 that the time history analysis was performed with a +/-10% time step change to account for uncertainty in the frequency content of the FIV loads. Provide the justification for using the +/-10% uncertainty considering several likely uncertainties involving strain gauge accuracy, instrument leg water temperature, and the assumption of no interaction between acoustic and turbulent flow within the reactor plenum.

Response to RAI EMEB-B-32

The benchmark evaluation identified differences in the predicted ACM and measured SMT frequencies when comparing minor peaks in the frequency response. It was observed that the ACA also over-predicted the amplitude of multiple peaks. The frequency shift of the load can have a marked impact on the structural response as the frequency content of the load changes in relation to the frequency content of the structure. The structural analysis was therefore run with a +/- 10% time step change to shift the frequency content of the ACA projected loads. This process helps differentiate the sensitivity of the peak fatigue stress from uncertainties in the frequency content of the load or response frequency of the structure.

Other uncertainties, including strain gage accuracy that can affect the uncertainty associated with projected dryer loads have been evaluated as discussed in Exhibit EMEB-B-18-1. Responses on reference leg temperature and interaction between acoustic and turbulent flow are addressed in RAI responses EMEB-B-31 and EMEB-B-74.

RAI EMEB-B-40

On Page 22 of Attachment 6 to Supplement 26, GE discusses the sensitivity of the modified dryer analysis results. Discuss the uncertainty of the acoustic circuit analysis pertaining to the formulation equations and parameters including instrument leg water temperature, skirt water level (boundary condition), viscous damping, thermal conductivity, response of Rosemount transmitters, apparent mass, and strain gauge measurement accuracy in transferring pressure data from instrument line to the MSLs and transferring the steamline outer deformation to steam pressure. Also, provide values of parameters mentioned above that were used in the analysis.

Response to RAI EMEB-B-40

Parameters used in the acoustic circuit model are documented in CDI's Design Record File (DRF) R50, which is available in conjunction with the VYNPS steam dryer analysis audit. The impact of these items on uncertainty and the uncertainty assessment that addresses the items listed, is included in the acoustic loads uncertainty analysis provided in Exhibit EMEB-B-18-1.

RAI EMEB-B-52

On Page 38 of Attachment 7 to Supplement 26, CDI states that the work documented in the report meets its Nuclear Quality Assurance Program. Discuss the uncertainties associated with the calculation of the steam dryer loads for VYNPS, including analyses assumptions, correction factors, and instrumentation error.

Response to RAI EMEB-B-52

Please see Exhibit EMEB-B-18-1 for a description of the uncertainty evaluation used in this analysis.

RAI EMEB-B-111

Entergy performed the sensitivity assessment of finite element analysis by varying the time interval between the pressure time steps by +10%. Why were both plus 10% and minus 10% variations in time interval not considered? What is the technical basis showing that ±10% and not larger variations in the time interval are appropriate for steam dryer dynamic stress analysis?

Response to RAI EMEB-B-111

Entergy analyzed both the plus and minus time variation. The +10% results are shown in the report because this condition resulted in an increase in dryer loads, whereas the -10% did not.
From Entergy's review of SMT data, the 10% time shift appeared to be reasonably applicable. Based on the more recent QC2 benchmark, there did not appear to be significant difference in acoustic frequency uncertainty. Based on the available data, Entergy and GE agreed to apply the 10% time step variation in the structural analysis.

Attachment 3

Vermont Yankee Nuclear Power Station

Proposed Technical Specification Change No. 263 – Supplement No. 31

Extended Power Uprate

Response to Request for Additional Information

VYNPS Applicability of QC2 instrumented dryer tests

Total number of pages in Attachment 3 (excluding this cover sheet) is 4.

RESPONSE TO REQUEST FOR ADDITIONAL INFORMATION
REGARDING APPLICATION FOR EXTENDED POWER UPRATE LICENSE AMENDMENT
VERMONT YANKEE NUCLEAR POWER STATION

PREFACE

This attachment responds to the NRC Mechanical and Civil Engineering Branch (EMEB) staff's request for additional information (RAI) dated July 27, 2005. Upon receipt of the RAI, discussions were held with the NRC staff to further clarify the RAI. In certain instances the intent of certain individual RAIs may have been modified based on clarifications reached during these discussions. The information provided herein is consistent with those clarifications.

The individual RAIs are re-stated as provided in NRC's letter of July 27, 2005.

Mechanical and Civil Engineering Branch (EMEB)
Component Integrity and Testing Section (EMEB-A)
Civil and Engineering Mechanics Section (EMEB-B)

RAI EMEB-B-30

On Page 21 of Attachment 3 to Supplement 26, CDI indicates that the acoustic circuit model is validated with data taken in the Quad Cities Unit 2 plant by comparing predictions of the fluctuating pressure at a location in the B MSL with inferred data hoop stress pressure measurements. Explain the basis for the assumed validation of the calculation of steam dryer loads by the acoustic circuit model using strain gauge data from one MSL in Quad Cities Unit 2. Explain the similarities and differences in the pressure and frequency spectra for the various test cases.

Response to RAI EMEB-B-30

Since this report was prepared, additional test data at the subscale test facility and full-scale plant (QC2) have been undertaken to benchmark the acoustic circuit analysis (CDI Report No. 05-10 entitled "Evaluation of Continuum Dynamics, Inc. Steam Dryer Load Methodology Against Quad Cities Unit 2 In-Plant Data").

The measured and predicted pressures on all 27 sensors installed on the QC2 steam dryer are provided in this report. Figure EMEB-B-30-1 shows a comparison between the pressure measured on the dryer at QC2 pressure transducer P-3 and that predicted using the ACM. The comparison in Attachment 3 to Supplement 26 was made with assumptions on phasing which are now not used.

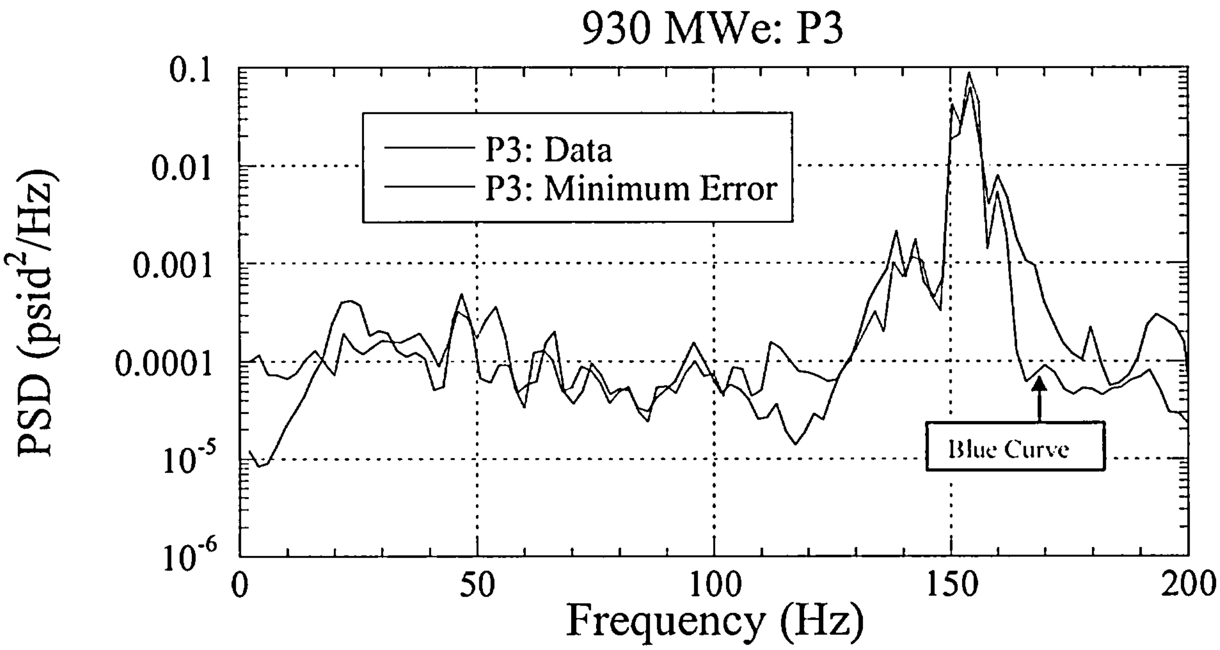

Figure EMEB-B-30-1. PSD comparison between pressure sensor data (blue curve) and the Minimum Error Evaluation (black curve), for QC2 Pressure Sensor P3.

RAI EMEB-B-71

Recently, Exelon indicated that adjustments had been made to the CDI acoustic circuit model in an effort to correct the underprediction of steam dryer pressure loads based on data obtained from the instrumented steam dryer at Quad Cities Unit 2 during EPU operation. Discuss the impact of the determination that corrections were necessary to the acoustic circuit model on the assessment of the VYNPS steam dryer, and the implication of those corrections to the validation effort for the acoustic circuit model applied to the VYNPS steam dryer using the GE SMT facility. Also, discuss the impact on the VYNPS steam dryer analysis of any adjustments made by GE to its SMT facility or test analysis, based on the pressure load data obtained from the Quad Cities Unit 2 instrumented steam dryer.

Response to RAI EMEB-B-71

The Quad Cities in-plant data shows clear discrete frequency phenomena which result in significant stresses on the dryer. The QC2 model was tuned with the aid of dryer data to better match the measured data with the new slant hood designed dryer. Due to the very low signals in the VYNPS steam lines, the VYNPS acoustic loads are controlled by the noise floor of the SG, accuracy of the data acquisition system, and accuracy of the venturi transfer function. VY has reviewed the results of the QC2 790 MWe benchmark and has conservatively quantified the impact to load uncertainties for the VY dryer loads. Further information is included in Exhibit EMEB-B-18-1.

The SMT was not used to develop a load prediction for the VYNPS steam dryer analysis. The SMT was used only to provide a benchmark test for Entergy's use in qualifying the CDI acoustic circuit model. The only modification made to GE's SMT facility following the CDI acoustic circuit model benchmark test was the addition of the steamline flow venturis, which were not available at the time of the benchmark test. The benchmark test evaluated the ability of the CDI acoustic circuit model to characterize the propagation of the injected test signal throughout the piping system and steam dome. The venturis would present a constriction in the pipe that may tend to attenuate the test signal amplitude, but would not be expected to alter the frequency content of the test signal as it is propagated through the piping. Therefore, the adjustments made by GE to the SMT facility are not expected to have a significant effect on the validity of the CDI benchmark test.

RAI EMEB-B-75

In reference to NEDC-33192P, (Attachment 2 to Exelon letter RS-05-053 dated April 28, 2005), "Engineering Report for Quad Cities Unit 1 Scale Model Testing," the Executive Summary (Conclusion 11 for Plant Data and Conclusion 2 for Small Scale Test (SMT) Facility) mentions that the primary sources of the dryer loading are attributed to acoustic resonances in the dryer dome, which are driven by hydrodynamic flow triggers (SRV singing, MSL turbulence at piping discontinuities, vortex flows at the front of the dryer near the MSL, etc.). However, the possibilities of fluid-structure interaction mechanisms are not totally dismissed, and their existence was to be re-evaluated after the Quad Cities Unit 2 plant data is analyzed. Entergy should explain whether the recent startup of the instrumented new dryer in Quad Cities Unit 2 has shown any indication of fluid-elastic instabilities building up with flow at abnormal rates (in its strain gauge, pressure transducer, or accelerometer data).

Response to RAI EMEB-B-75

The Quad Cities Unit 2 plant data has not yet been evaluated with respect to determining the existence of any fluid-structure interaction. A preliminary review of the power ascension trend data for the strain gauges, pressure transducers, and accelerometers does not show indications of fluid-elastic instability. The data from the sensors do show a rapid increase in amplitude in the high frequency range at higher flows. This increase has the characteristics of a SRV resonance. The trend and characteristics observed in Quad Cities Unit 2 are consistent with SRV resonances observed in other BWRs with instrumented dryers.

RAI EMEB-B-79

With respect to its use of MSL strain gauges, Entergy should provide an evaluation of the ability of the strain gauges on the Quad Cities Unit 2 MSLs to provide adequate dynamic pressure input to ACA analysis.

Response to RAI EMEB-B-79

See Response to RAI EMEB-B-78.

RAI EMEB-B-87

Entergy should compare the recently measured dryer surface pressures in the Quad Cities Unit 2 plant to those shown in Figure 15 of Attachment 7 to Supplement No. 26 and establish error bounds between actual and ACA-simulated steam dryer pressures. Entergy should explain whether these error bounds will be applied to the ACA-simulated VYNPS steam dryer pressure loads.

Response to RAI EMEB-B-87

The recently measured dryer surface pressures in the QC2 plant are measured on the new larger steam dryer. Those loads on Figure 15 for QC2 are computed using the ACM on the old dryer. It is not clear that a comparison relevant to the VYNPS dryer analysis is meaningful. Entergy has evaluated the results of the recent Q2 benchmark reports and conservatively assessed the impact of this benchmark on the dryer loads calculated for VYNPS with the ACA methodology.

RAI EMEB-B-93

The Quad Cities Unit 2 MSL acoustic pressures inferred from measured strain gauge data are compared to two ACA simulations in Figures 6.4 - 6.6 on pages 26 - 28 of Attachment 3 to Supplement No. 26. On page 22, it states that the simulated and directly measured frequency spectra are similar. However, examination of those spectra (the bottom plots in Figures 6.4 - 6.6) does not substantiate that assertion. Entergy should explain how accurately the ACA methodology simulates the frequency content of the pressure fluctuations. Entergy should further explain how the discrepancies between the frequency content of the measured and simulated MSL pressures in Quad Cities Unit 2 reflect on the accuracy of the simulated pressures on the VYNPS steam dryer, and whether those inaccuracies are accounted for in the acoustic pressure loads used in the VYNPS steam dryer stress analysis.

Response to RAI EMEB-B-93

See response to RAI EMEB-B-30-1. Examining Figure EMEB-B-30-1, which compares measured and predicted Power Spectral Density function for QC2 steam dryer transducer P3, shows very favorable comparison.

Attachment 5

Vermont Yankee Nuclear Power Station

Proposed Technical Specification Change No. 263 – Supplement No. 30

Extended Power Uprate

Response to Request for Additional Information

Probabilistic Safety Assessment Branch

Total number of page n Attachment 5
(excludina this coversheet) is 1.

RESPONSE TO REQUEST FOR ADDITIONAL INFORMATION REGARDING APPLICATION FOR EXTENDED POWER UPRATE LICENSE AMENDMENT VERMONT YANKEE NUCLEAR POWER STATION

PREFACE

This attachment responds to the NRC Probabilistic Safety Assessment Branch (SPSB) request for additional information (RAI) dated July 27, 2005. Upon receipt of the RAI, discussions were held with the NRC staff to further clarify the RAI. In certain instances the intent of certain individual RAIs may have been modified based on clarifications reached during these discussions. The information provided herein is consistent with those clarifications.

The individual RAIs are re-stated as provided in NRC's letter of July 27, 2005.

Probabilistic Safety Assessment Branch (SPSB)
Containment and Accident Dose Assessment Section (SPSB-C)

RAI SPSB-C-47

The response to RAI SPSB-C-41 is not clear as to why required NPSH values, based on lower pre-EPU suppression pool temperatures, satisfy pump requirements at the higher EPU suppression pool temperatures. Does the increased suppression pool temperature affect the magnitude of the required NPSH or the time period at a given required NPSH, or both?

Response to RAI SPSB-C-47

(Note: This response provides additional information and supplements the previous response to SPSB-C-47 contained in Attachment 7 to Supplement 30 (BVY 05-072, dated August 1, 2005)

Entergy has spoken with the pump vendor, who performed the NPSH testing, who verified the following:

1. As long as other adjustments are made to assure available NPSH is above the required minimum value defined on the curves, the temperature of the fluid is not a limiting parameter.
2. The curves showing required NPSH are not affected by the temperature increase.

Attachment 6

Vermont Yankee Nuclear Power Station

Proposed Technical Specification Change No. 263 – Supplement No. 31

Extended Power Uprate

Response to Request for Additional Information

GE Scale model test (SMT) Benchmark Adequacy

NON-PROPRIETARY VERSION

Total number of pages in Attachment 6 (excluding this cover sheet) is 61.

RESPONSE TO REQUEST FOR ADDITIONAL INFORMATION REGARDING APPLICATION FOR EXTENDED POWER UPRATE LICENSE AMENDMENT VERMONT YANKEE NUCLEAR POWER STATION

PREFACE

This attachment responds to the NRC Mechanical and Civil Engineering Branch (EMEB) staff's request for additional information (RAI) dated July 27, 2005. Upon receipt of the RAI, discussions were held with the NRC staff to further clarify the RAI. In certain instances the intent of certain individual RAIs may have been modified based on clarifications reached during these discussions. The information provided herein is consistent with those clarifications.

The individual RAIs are re-stated as provided in NRC's letter of July 27, 2005.

Mechanical and Civil Engineering Branch (EMEB)
Component Integrity and Testing Section (EMEB-A)
Civil and Engineering Mechanics Section (EMEB-B)

RAI EMEB-B-19

On Page 7 of Attachment 1 to Supplement 26, Entergy states that a test was conducted by Alden Research Labs to determine strain gauge sensitivity and provides a summary of the test results. Provide a detailed description of the sensitivity test, including the test setup, assumptions, applicability, acceptance criteria, and uncertainty analysis.

Response to RAI EMEB-B-19

The purpose of the strain gage sensitivity test was to evaluate the sensitivity of prototypical strain gages attached to a test vessel that is representative of main steam line installation at VYNPS. This test is applicable to VYNPS strain gage sensitivity determination based on use of a test vessel representative of VYNPS main steam line piping, the use of strain gage instruments of the same model as installed at VYNPS and use of the same DAS from VY used to collect in-plant data.
The test setup included the following:

Facility
A section of 18 inch diameter schedule 80 carbon steel pipe with pipe cap ends. The assembly was built in conformance with ASME VIII.

Strain gages
Hitec Products Inc., Model No. HBWAK-12-125-6-10FG-F. Installed by Hitec Products Inc. personnel.

Dead Weight Tester
Ashcroft deadweight gage tester (2000 psi capacity). Gram Weight set ARL 463.

Pressure Sensor
Sensotec Model FPG/G621-02 pressure transmitter.

Data Acquisition
Data Acquisition System (DAS), provided by Entergy, consisting of: PC with recording software and National Instruments interfacing hardware for recording the Sensotec gage and two strain gage signals configured as either a ¼ or a ½ bridge. The DAS was operated according to the procedure provided by Structural Integrity Associates, Inc.

Test Procedure:
Strain Gage testing was done at approximately 1000 psig to simulate the mean strain of strain gages used at the plant. The pipe was filled with water for the test.
Static Testing: Acquisition System in DC Mode.
Dynamic Testing: step change pressure, to measure the performance of the Sensotec and SG for a large dP. (The load ramp was performed by venting the vessel.)
Dynamic Testing: Acquisition System in AC Mode
Dynamic Testing. Apply a small amplitude (~.10 psi) oscillatory load for ~60 seconds to assess the ability of the SG to match pressure transmitter data. (The oscillations were added by cycling the dead weight tester by hand while watching the FFT plot of the transmitter.)

Assumptions applied for the testing and results evaluation included the following:
Pipe used in the test was representative of VYNPS MS piping where strain gages are installed.
DC versus AC setup.

Acceptance criteria for the testing included:
No acceptance criteria were used. Results were interpreted to determine how low strain gages could resolve detection of fluctuating pressures.

Uncertainty analysis results:
SG (and balancing resistors) is very sensitive to temperature changes. This resulted in drift if used in the DC mode. Dynamic testing and load ramp changes would be required to measure sensitivity.

In dynamic testing the strain gages were tested in AC mode as used in the plant. The test apparatus allowed for testing of the strain gages under oscillating pressure signals as low as 0.1 psi and at frequencies up to 4 Hz. This was sufficient to provide dynamic response data for signal processing. This was significant noise in the strain gage signal including random noise as well as electrical 60 Hz noise. The electrical conditions were similar to the plant conditions. PSD were developed over multiple 60 sec test runs. Comparison of PT and strain gage PSDs, demonstrated that the strain data continued to correlate to pressure as a function of the hoop strain at oscillating pressures close to the VYDAS noise floor.

RAI EMEB-B-20

On Page 7 of Attachment 1 to Supplement 26, Entergy states that a benchmark test was performed using the General Electric (GE) Scale Model Test (SMT) facility in San Jose, California, to evaluate the ability of the acoustic circuit methodology to predict steam dryer loads. Provide the basis for the assumption that the GE SMT facility provides a reasonable representation of the sources, types, distribution, amplitude, and frequency spectra of the loads on a steam dryer installed in a boiling water reactor (BWR) nuclear power plant operating at EPU conditions.

Response to RAI EMEB-B-20

Please refer to GENE-0000-0042-7471-01-P. This report demonstrates that the GE Scale Model Test apparatus and methodology adequately replicates the majority of the frequency content and amplitudes observed in the Quad Cities Unit 2 plant data. Although some differences exist between the model and plant data in the high frequency range there are distinct differences between the QC1 and QC2 plant configurations that may explain these differences. Where differences do exist additional work is ongoing to understand the cause. Also, as shown in NEDC-33192P the fluctuating loads measured at three different BWRs are observed to exhibit similar characteristics such as trends with power level and frequency content. The BWRs from which these data were obtained contained both square and curved hood dryers as well as substantially different RPV diameters. Considering these two points, the SMT is considered to provide a reasonable representation of the sources, types, distributions, amplitude, and frequency spectra of the loads expected on a BWR steam dryer.

RAI EMEB-B-21

On Page 8 of Attachment 1 to Supplement 26, Entergy states that pressure measurements from eight points in the SMT piping were provided as input for the acoustic circuit methodology in calculating the steam dryer loads. At VYNPS, Entergy indicates that the input for the acoustic circuit methodology is obtained from four venturi pressure transducers and four MSL strain gauge locations. Discuss the consideration of the differences in input sources and their uncertainties in evaluating the acoustic circuit methodology using the SMT facility and when calculating the steam dryer loads at VYNPS using the acoustic circuit methodology.

Response to RAI EMEB-B-21

Please refer to the acoustic load uncertainty evaluation in Exhibit EMEB-B-18-1. This evaluation addresses the difference between benchmark test SMT sensing locations and the methods used to obtain VYNPS main steam line measurement data.

RAI EMEB-B-53

On Page 6 of Attachment 2 to Supplement 27, Entergy describes the 1:17.3 sub-scale GE SMT facility. Discuss the steamline geometry and component differences between the GE SMT facility and the VYNPS as-built configuration, and the potential for different sources of steam dryer loading being present in VYNPS.

Response to RAI EMEB-B-53

As discussed in the response to RAI EMEB-B-20 the fluctuating loads for three different instrumented BWRs show similar characteristics. From these data GE expects that all BWR fluctuating loads will exhibit characteristics similar to those shown in NEDC-33192P. Also documented in NEDC-33192P are the results of source identification testing performed with the QC1 scale model test apparatus. These tests showed that the steam system components observed to control the loading on the steam dryer are: [[

]] Both the Vermont Yankee and Quad Cities plant configurations contain these components; therefore, the VYNPS as-built configuration is not considered susceptible to a source mechanism not present in the plant configurations from which data already exists.

RAI EMEB-B-54

On Page 6 of Attachment 2 to Supplement 27, Entergy states that microphones were installed in the SMT piping, dryer, and inlet plenum to measure unsteady pressure oscillations in the system. Discuss the potential for differences in source identification and measurement from the microphones in the GE SMT air lines compared to the VYNPS instrumentation.

Response to RAI EMEB-B-54

The acoustic circuit analysis accounts for the presence or absence of sources in the system. The benchmark against SMT data in several cases introduced a deterministic source downstream of the microphone to test the models ability to predict dryer loads. The SMT was not a simulation of VYNPS configuration or operating conditions but provided a test platform and data set from which the capabilities of the acoustic circuit model could be evaluated.

VYNPS has the required number of independent measurements made on each steam line to compute dryer loads. The measurement capabilities of the SMT microphones are different from the capabilities of the VYNPS strain gages and pressure sensors. Each of these measurement systems was adequate for obtaining circuit analysis input data. The differences in the VY and Benchmark instrumentation are addressed in the acoustic load uncertainty evaluation in Exhibit EMEB-B-18-1.

RAI EMEB-B-55

On Page 6 of Attachment 2 to Supplement 27, it is not clear as to how the GE SMT facility in this validation was set up regarding the vibration sources associated with the MSL (i.e., SRVs, electromatic relief valves, main steam isolation valves, high pressure coolant injection lines, reactor core isolation cooling lines). Confirm whether all 13 test cases were performed at ambient pressure. Discuss how these 13 test cases were performed to simulate the VYNPS systems pertaining to the pressure on the steam dryer. Discuss why the testing is considered valid in that the test conditions deviate from the VYNPS operating conditions.

Response to RAI EMEB-B-55

Section 4.0 of NEDC-33192P contains digital images of the scale model test apparatus. The system configuration used for the benchmark testing was comparable to that shown in NEDC-33192-P. Also contained in Section 4.0 is a detailed description of the level of detail included in the scale model test apparatus. This document should provide adequate description of the test setup.

The no-flow tests were performed close to ambient pressure. With flow the pressure at the dryer inlet at 81.5 CFM flow was 15.2-14.7=0.5 psig, with 114.7 CFM flow 15.8-14.7= 1.1 psig. See the response to RAI EMEB-53.

The scale model benchmark tests were not performed to simulate VYNPS dryer loads. The scale model benchmark tests were performed to obtain representative data from a BWR configuration that could be used to benchmark the acoustic circuit methodology. The scale model tests were performed with both flow induced noise and an external source so that a variety of excitations could be evaluated.

RAI EMEB-B-56

On Page 6 of Attachment 2 to Supplement 27, Entergy indicates that CDI developed an analytical model of the GE SMT for use in predicting loads on the model dryer. Explain the CDI acoustic circuit model that was used in predicting the loads on the dryer in comparison with the SMT data. For each acoustic circuit analysis, describe the input data including microphone numbers and locations, and analytical results in comparison to the corresponding scale model test data. Provide the user's manual and theoretical manual pertaining to the computer analysis code for review by the NRC staff.

Response to RAI EMEB-B-56

The acoustic circuit model used in predicting the loads on the dryer to compare with SMT data is documented in CDI Report No. 04-09 (Proprietary) and has been previously supplied to the staff.

Microphone Locations in SMT in feet (scale factor = 17.3)

	P1	P2
A MSL	1.474	4.438
B MSL	1.391	5.094
C MSL	1.391	5.161
D MSL	1.474	4.438

The code is proprietary and is used only by CDI staff. Descriptions of input variables and instructions on operation are detailed in CDI's DRF R50, which has previously been made available to the staff in conjunction with the Exelon dryer analysis. The DRF could be brought to a future Entergy/NRC audit for review, if required.

RAI EMEB-B-57

On Page 7 of Attachment 2 to Supplement 27, Entergy states that the 81 cubic feet per minute (cfm) flow rate in the GE SMT facility represented approximately 50% OLTP for Quad Cities Unit 2. Discuss the scaling of the SMT flow rate up to the VYNPS EPU flow rate, and the potential for excitation of additional frequencies at significantly higher flow rates than achieved in the SMT facility.

Response to RAI EMEB-B-57

Please refer to Figures 10 and 39 of NEDC-33192P which show that the majority of the frequency content observed both in the available plant data and the SMT data [[

]] The only exception to this observation is the behavior of the [[

]]

RAI EMEB-B-58

On Page 10 of Attachment 2 to Supplement 27, Entergy states that data from microphone M30 at the outlet of the muffler in the GE SMT facility was provided to CDI in addition to air line instrumentation data. Discuss the influence of the muffler outlet data on achieving a blind benchmark of the acoustic circuit analysis.

Response to RAI EMEB-B-58

Microphone M30 was at the outlet of the blower muffler and at the inlet at the large transition that channeled the air to the bottom of the SMT dryer. CDI asked for this information to allow them to determine how much noise was entering or reflecting at the muffler exit. This allowed CDI to establish a boundary condition at the inlet to the dryer. Upon review and comparison of this data with the vertical face and skirt regions, Entergy concluded that the signals in this region had negligible coherence with the vertical face or skirt regions and that there was little pressure signal in this region. Providing this data to CDI would not compromise the blindness of the benchmark test. Entergy subsequently agreed to provide the M30 data along with steam line data to CDI.

RAI EMEB-B-59

On Pages 13 and 14 of Attachment 2 to Supplement 27, Entergy indicates that the averaged maximum CDI acoustic analysis predicted loads ranging from 162% to 91% of the SMT microphone measured loads in four test runs (two runs with no air flow and two runs with air flow). In one test run with flow (VY6RUN2), the average value of the pressure load predicted by the acoustic circuit analysis is indicated to have underestimated the microphone measured pressures with a CDI/SMT ratio of 91%. In the other test run with flow (VY12R1), the acoustic circuit analysis is indicated to have overestimated the measured pressures with a CDI/SMT ratio of 109%. Entergy states that, therefore, the "CDI acoustic analysis model would appear to be a reasonable tool for predicting steam dryer peak loads." Discuss the acceptance criteria for the validation of the steam dryer load definition calculated by the acoustic circuit model, and the uncertainty range in applying the acceptance criteria in light of the underestimation and overestimation of the average pressure loads in the two test runs with air flow.

Response to RAI EMEB-B-59

The purpose of the benchmark was to evaluate the ability of the CDI acoustic load methodology to predict loads on the SMT dryer using only data measured on the main steam lines. Entergy compared the calculated loads to the measured loads at key SMT locations and concluded that the methodology provided a reasonably close prediction. Quantitative acceptance criteria for the benchmark were not defined prior to the evaluation, nor did Entergy intend to "tune" the ACA as a result of SMT measured versus predicted results. Rather, it was Entergy's intent to use the results of the benchmark to establish the uncertainty of the methodology. The uncertainty of the ACA was evaluated based on model predictions and data from the ACA benchmarks. Exhibit EMEB-B-18-1 provides the results of this evaluation and establishes the uncertainty of the ACA. Exhibit EMEB-B-18-1 also addresses application of the total ACA uncertainty value and provides responses to related RAI's EMEB-B-40 and 52.

RAI EMEB-B-60

On Page 17 of Attachment 2 to Supplement 27, Figure 3C shows the maximum pressure and standard deviation for SMT steam dryer loads for the acoustic circuit analysis and SMT data for a burst random and 81 cfm flow. Discuss the underestimation by the acoustic circuit model of the maximum pressure measurements obtained from multiple SMT microphones and the uncertainty of the acoustic circuit model.

Response to RAI EMEB-B-60

In the process of assessing the ACA load uncertainty in response to RAI EMEB-B-18, it was concluded that that the non-conservative RMS and maximum pressure conditions shown in the Supplement 27, Attachment 2 plots involved test case conditions with flow; VY6RUN2, Burst with 81 CFM Flow and VY12R1, Chirp with 81 CFM Flow. Review of the PSDs suggested that the under-predictions occurred at microphones with significant frequency content less than 240 Hz. To assess further, the SMT data for VY6RUN2 and VY12R1 were reprocessed applying a 240 Hz high pass filter. The revised filtered Max and RMS signal plots are included in Exhibit EMEB-B-18-1 as Figures EMEB-B-18-1-E1, EMEB-B-18-1-E2, EMEB-B-18-1-G1 and EMEB-B-18-1-G2. With the low frequency turbulence signal removed, the RMS and Maximum ACA predictions always bound the measured data.

RAI EMEB-B-61

On Page 20 of Attachment 2 to Supplement 27, Entergy notes that the acoustic model does not predict an SMT peak at 800 Hz. Discuss the absence of the 800 Hz (67 Hz full scale) frequency peak from the acoustic circuit analysis, including the source of frequency peak in the SMT facility and the impact of its omission on the validity of the acoustic circuit analysis.

Response to RAI EMEB-B-61

The application of the +/- 10 % time step variation was used to assess the uncertainty introduced by differences in the ACA and SMT at closely spaced frequencies. As depicted on Figure 7 of Supplement 27 Attachment 2, when the +/- 10 time step is applied the peak at ~750 Hz effectively bounds the shortcoming at ~800 Hz. The load phasing was evaluated in conjunction with response to RAI EMEB-B-107. For the vertical face where VYNPS dryer loads are high, the ~750 and ~800 Hz load phasing is very similar. Therefore, the application of a +/-10% time step in the structural analysis is effective in addressing the frequency response under prediction at ~800 Hz.

It should also be noted that based on VYNPS steam line data, the loads projected on the dryer are very low in the range 10^-5 psid^2/Hz from 0 through 125 Hz. As shown in the PSD of the ANSYS model stress [see response to RAI EMEB-B-110] there is no significant structural response to any of the loads in the 0 Hz to 125 Hz frequency range. Therefore, the structural dryer analysis indicates that the VYNPS dryer has significant margin for load uncertainty at the equivalent full scale frequency, 67 Hz.

RAI EMEB-B-62

On Page 20 of Attachment 2 to Supplement 27, Entergy states that, in general, the acoustic model did well under GE SMT flow conditions from 240 to 3200 Hz (20 to 267 Hz full scale), but some mismatches existed at narrow frequency bands. To address the uncertainty, Entergy generated additional power spectral density data sets varying the frequency sample rate by about 10% and established an enveloping curve by using the maximum of the three separate curves. Discuss the basis for broadening the power spectra density spectra in a benchmarking assessment of the acoustic circuit model.

Response to RAI EMEB-B-62

The basis for use of a +/-10% time step change is to account for uncertainty in the frequency content of the SMT dryer FIV loads. This is the same time step change as used in the VYNPS dryer load definition. See the response to RAI #32, which addresses the time step change relative to the VYNPS loads.

The benchmark evaluation identified differences in the predicted ACM and measured SMT frequencies when comparing minor peaks in the frequency response. It was observed that the ACA also over-predicted the amplitude of multiple peaks. The frequency shift of the load can have a marked impact on the structural response as the frequency content of the load changes in relation to the frequency content of the structure. The structural analysis was therefore run with a +/- 10% time step change to shift the frequency content of the ACA projected loads. This process helps differentiate the sensitivity of the peak fatigue stress from uncertainties in the frequency content of the load or response frequency of the structure.

RAI EMEB-B-63

On Pages 20 and 21 of Attachment 2 to Supplement 27, Entergy states that "it is likely that under predicting the frequency content below 20 Hz (full scale, 240 Hz SMT scale) and shifting the peak response to higher frequencies below 77 Hz would have a conservative impact on stress in the structural assessment." Entergy also states that, "[a]lternatively, other methods could be employed to better define low frequency forces." Discuss the differences in the acoustic circuit model and the SMT at low frequencies, and whether the acoustic circuit model or SMT provides more appropriate representation at low frequencies in a full size steam dryer operating at EPU conditions in a nuclear power plant. Also, discuss the possible application of the higher of the SMT measurements or acoustic circuit predictions to generate a bounding design load case over the entire frequency range.

Response to RAI EMEB-B-63

The ACA was determined to be non-conservative in predicting SMT dryer loads below 240 Hz (20 Hz full scale). The source of the signals below 240 Hz appears to be SMT flow turbulence and is not associated with acoustic signals. Exhibit EMEB-B-18-1 provides a discussion of the differences between the SMT and ACA at low frequencies.

Based on this determination, Entergy developed an unsteady CFD Large Eddy Simulation analysis to serve as the VYNPS hydrodynamic load definition at 0 – 20 Hz. Application of the CFD load definition is more appropriate than use of either the SMT or ACA low frequency loads, since the CFD model is specific to VYNPS (whereas the SMT is not) and the ACA was shown to under-predict low frequency, hydrodynamic loads. Both the ACA and CFD loads were used in the structural evaluation of the VYNPS dryer.

Regarding the possible application of the higher of the SMT measurements or acoustic circuit predictions to generate a bounding design load case over the entire frequency range, neither the measured nor predicted SMT dryer loads associated with the ACA benchmark are appropriate for development of a VYNPS load case, since the SMT model was not intended to be representative of VYNPS configuration or operating conditions.

RAI EMEB-B-64

On Page 24 of Attachment 2 to Supplement 27, Figure 6 compares the power spectral density (PSD) versus frequency plots for Microphone M16 obtained from the SMT facility and predicted by the acoustic circuit analysis during a burst signal with flow. Discuss the lack of consistency between the SMT measured data and the acoustic circuit analysis throughout the entire frequency range in terms of the PSD amplitude and specific excited frequencies.

Response to RAI EMEB-B-64

The comparison of the measured versus predicted data from 240 Hz to 2000 Hz matches very well. The ACA accurately identifies the frequency response at 400 Hz. It over-predicts the amplitude at the peak by [~sqrt (200%)-100% =] ~40%. The ACA does not accurately predict the low frequency turbulent flow pressure below 240Hz. (Entergy is applying CFD loads to adequately represent these forces). The model over-predicts the loads above 2000 Hz. The load magnitude at this frequency range is very low. There is a secondary peak that is an order of magnitude lower that the 400 Hz peak that was not captured at ~800 Hz. This has been addressed in our response to RAI EMEB-B-61.

RAI EMEB-B-65

On Page 26 of Attachment 2 to Supplement 27, Figure 8 compares the PSD for a pipe measured signal with the dryer face measured signal and the acoustic model prediction at Microphone M16 over the entire frequency range during a burst signal with flow. Figure 8 shows (a) the pipe signal higher than the dryer signal and acoustic model prediction throughout the frequency range; (b) the absence of alignment of frequency peaks for the three plots; and (c) the dryer signal exceeding the acoustic model prediction at low frequencies and at certain higher frequencies. From this information, discuss the source of steam dryer loads, the fidelity of the acoustic circuit model, and reliability of the acoustic circuit model in providing a bounding steam dryer load definition.

Response to RAI EMEB-B-65

This figure was intended to provide a broad view of the benchmark performance of the ACA. Microphone 16 was selected to demonstrate that the flow and sound source excite numerous system frequencies in the pipe. The benchmark against SMT data in this case introduced a deterministic source downstream of the microphone to test the models ability to predict dryer loads. The SMT was not a simulation of VYNPS configuration or operating conditions but provided a test platform and data set from which the capabilities of the acoustic circuit model could be evaluated. This figure demonstrates that the pressure measured in the steam line and the pressure measured on the dryer differ by varying orders of magnitude throughout the frequency range, thereby appropriately exercising the ACM. The figure demonstrates that the ACA adequately predicts these changes above 240 Hz and below 2000 Hz. Based on our assessment of the SMT benchmark data, for frequencies above 240 Hz the ACA provides conservative dryer load data based on steam line data.

RAI EMEB-B-66

On Page 27 of Attachment 2 to Supplement 27, Entergy states that the "acoustic model does a reasonable job of predicting pressure amplitude and energy at the dryer face." Describe the acceptance criteria and their basis for evaluating the validity of the acoustic circuit model.

Response to RAI EMEB-B-66

Please see response to RAI EMEB-B-59.

RAI EMEB-B-67

On Page 27 of Attachment 2 to Supplement 27, Entergy states that, "[i]f a 10% load step uncertainty is applied to the data the acoustic model predictions are conservative." Explain this statement in light of the information on Page 20 and Figure 7 (as well as other figures) that the acoustic load predictions are nonconservative at low frequencies.

Response to RAI EMEB-B-67

Entergy concluded that the ACA did not accurately predict SMT dryer loads below 240 Hz (20 Hz full scale). The evaluation of SMT data in response to RAI EMEB-B-107 indicates that the data at this frequency has low compliance and is indicative of turbulent rather than acoustic loads. To address the issue of load definition adequacy at < 20 Hz, Entergy used the CFD analysis to provide the turbulent load definition for the VYNPS dryer.

RAI EMEB-B-68

On Page E1 of Appendix E in Attachment 2 to Supplement 27, the figure shows the acoustic circuit model underpredicting the maximum pressure measured by numerous microphones on the SMT steam dryer outer surface. Discuss the evaluation of the acoustic circuit model in light of this underprediction of maximum SMT steam dryer surface pressure.

Response to RAI EMEB-B-68

In the process of assessing the ACA load uncertainty in response to RAI EMEB-B-18, it was concluded that the non-conservative RMS and maximum pressure conditions shown in the Supplement 27, Attachment 2 plots involved test case conditions with flow; VY6RUN2, Burst with 81 CFM Flow and VY12R1, Chirp with 81 CFM Flow. Review of the PSDs suggested that the under-predictions occurred at microphones with significant frequency content less than 240 Hz. To assess further, the SMT data for VY6RUN2 and VY12R1 were reprocessed applying a 240 Hz high pass filter. The revised filtered Max and RMS signal plots are included in Exhibit EMEB-B-18-1 as Figures EMEB-B-18-1-E1, EMEB-B-18-1-E2, EMEB-B-18-1-G1 and EMEB-B-18-1-G2. With the low frequency turbulence signal removed, the RMS and Maximum ACA predictions always bound the measured data.

RAI EMEB-B-69

The figures of the pressure loading of specific microphone locations in Appendix E in Attachment 2 to Supplement 27 show the acoustic circuit model underpredicting the pressure loading at various low, medium, and high frequencies for certain microphones. For example, see the figures on pages E3, E5, E7, E9, E11, E13, E15, E17, E19, E21, E23, E25, E27, E29, and E31. Discuss the evaluation of the acoustic circuit model in light of this underprediction of pressure loading at various frequencies over the entire spectra.

Response to RAI EMEB-B-69

Although the figures contained in Attachment 2 to Supplement 27 show underprediction for certain microphone locations, the +/- 10 % time step variation was applied to assess the uncertainty introduced by differences in the ACA and SMT at closely spaced frequencies. As described in response to EMEB-B-61, application of the +/- 10 time step effectively bounds the nearby peak.

RAI EMEB-B-70

The figures of the pressure loading of specific microphone locations in Appendix F in Attachment 2 to Supplement 27 show the acoustic circuit model with +/-10% uncertainty applied. Although more bounding than the acoustic circuit model without the 10% uncertainty, the expanded acoustic circuit model continues to underpredict loading at various low, medium, and high frequencies for certain microphones. For example, see the figures on pages F1, F4, F5, F8, F12, and F13. Discuss the evaluation of the expanded acoustic circuit model in light of this underprediction of pressure loading at particular frequencies.

Response to RAI EMEB-B-70

The expanded acoustic circuit model is considered to provide good prediction of measured SMT loads. In figures F1, F5, F8 and F13, other than limited points of underprediction, the overall match on the predicted curves is good, with no points between 240 and 2400 Hz critical range that are below the +/- 10% time step bound. There is an insignificant amount of underprediction across the total frequency spectra. In figures F4 and F12 the results reflect generally conservative predictions, other than small mismatches at 900 – 1100 Hz where the ACA was slightly underpredictive but at an order of magnitude below the peak frequency response. Review of phasing between the measured and predicted SMT loads to support response to RAI EMEB-B-107 did not indicate any generic deficiency in acoustic phasing versus SMT phasing. With the determination that the phasing is confirmed, Entergy concludes that these results demonstrate sufficiently accurate ACA predictive capability.

RAI EMEB-B-86

In the ACA SMT benchmark report (Attachment 2 to Supplement No. 27, "VYNPS Acoustic Model Benchmark - Dryer Acoustic Load Methodology," VY-RPT-05-00006), the Conclusion section on page 27 states that the ACA systematically underpredicts low frequency differential pressures on the steam dryer (below 20 Hz at VYNPS scale). Entergy should explain why correction factors based on the discrepancies between low-frequency ACA and directly measured steam dryer pressure spectra from the SMT benchmark are not applied in order to simulate the acoustic pressure loading on the steam dryer.

Response to RAI EMEB-B-86

As stated in response to RAI EMEB-B-63, the ACA was non-conservative in predicting SMT dryer loads below 240 Hz (20 Hz full scale) due to SMT flow turbulence not associated with acoustic signals. Exhibit EMEB-B-18-1 provides a discussion of the differences between the SMT and ACA at low frequencies.

Entergy developed an unsteady CFD Large Eddy Simulation analysis to serve as the VYNPS hydrodynamic load definition at 0 – 20 Hz. Application of the CFD load definition is more appropriate than use of a correction factor based on the difference in SMT versus ACA low frequency loads. The CFD model is specific to VYNPS, whereas the SMT model was not intended to be representative of VYNPS configuration or operating conditions. Use of a correction factor based on the non-representative SMT and the under-predicting ACA would not necessarily provide accurate low frequency, hydrodynamic loads. Both the ACA and CFD loads were used in the structural evaluation of the VYNPS dryer.

RAI EMEB-B-96

As discussed in Attachment 1 to Supplement No. 27, "VYNPS Acoustic Model Benchmark - Dryer Acoustic Load Methodology," a "blind" benchmark test was performed using the GE SMT facility to evaluate the ability of CDI's acoustic circuit methodology to predict dryer loads. The purpose of the evaluation is not clear because of the use of terms, like the "viability of the methodology." Entergy should clearly state the purpose of the evaluation. If a purpose of the report is to use the SMT results to show that a bounding pressure loading can be obtained for the VYNPS dryer using the CDI ACA methodology, then Entergy should demonstrate that the SMT adequately represents the VYNPS steam dryer, the associated steam space, and the VYNPS MSLs.

Response to RAI EMEB-B-96

The purpose of the benchmark was to evaluate the ability of the CDI acoustic load methodology to predict loads on the SMT dryer using only data measured on the main steam lines. The SMT model was not intended to be representative of VYNPS configuration or operating conditions. The SMT also was not intended to be used to develop bounding or nominal VYNPS steam dryer loads. Entergy compared the benchmark ACA calculated loads to the measured loads at key SMT locations and concluded that the ACA methodology provided a reasonably accurate prediction. It was Entergy's intent to use the results of the benchmark to establish the uncertainty of the methodology. The uncertainty of the ACA was evaluated based on model predictions and data from the SMT benchmark. Exhibit EMEB-B-18-1 provides the results of this evaluation and shows that the uncertainty of the ACA can be established as 78%. This uncertainty value has been applied to the VYNPS ACA load definition (see responses to RAI EMEB-B-40 and 52).

RAI EMEB-B-97

The SMT was performed with flow rates, as shown in the table on page 7 of Attachment 1 to Supplement No. 27, well below EPU conditions (i.e., flow rates equivalent to half Quad Cities Unit 1 pre-EPU power). Entergy should justify why the SMT provides acceptable benchmarking (i.e., explain why SMT testing was not performed up to and including EPU conditions).

Response to RAI EMEB-B-97

As discussed in the response to RAI 57 the available plant data and SMT data show that the majority of the frequency content of the BWR steam dryer loads becomes apparent [[

]] For the SMT benchmark tests both flow noise and external sound sources were used to provide a diversity of excitations to the scale model system.

RAI EMEB-B-98

Attachment 1 to Supplement No. 27 does not appear to constitute a typical benchmark analysis. Entergy should define what benchmarking means in this report. In addition, it should provide criteria for benchmarking the predicted pressures, and justify why the criteria were selected based on their intended use of predicting steam dryer structural dynamic stresses. In particular, pressure amplitudes and frequency content from SMT and ACA are compared at specific locations on the dryer face, but phasing of the pressures across the dryer face is not. Also, comparisons of maximum and RMS pressures are given for each frequency, but frequency domain comparisons of the spatial distribution of pressures are not considered. All these characteristics of pressure loading (frequency, amplitude, phase, and spatial distribution) are important to the excitation of structural modes and the resulting stresses.

Response to RAI EMEB-B-98

The purpose of the benchmark was to evaluate the ability of the CDI acoustic circuit model to predict loads on the SMT dryer using only data measured on the main steam lines. Quantitative acceptance criteria for the benchmark were not defined prior to the evaluation, nor did Entergy intend to "tune" the ACA as a result of SMT measured versus predicted results. Rather, it was Entergy's intent to use the results of the benchmark to establish the uncertainty of the methodology, one component of the overall VYNPS dryer load definition uncertainty. Exhibit EMEB-B-18-1 provides a description of the evaluation of uncertainty associated with the acoustic circuit model. The phasing of the predicted versus measured pressures across the SMT dryer face and frequency domain comparisons of spatial pressure distributions are provided in response to RAI EMEB-B-107.

RAI EMEB-B-99

The selection of the burst random and chirp noise sources (listed in the table on page 7 of Attachment 1 to Supplement No. 27) are not explained, other than to show a graph of their time history. Entergy should define the noise sources, elaborate on why they were used, how they were chosen, and provide comparisons of the SMT dryer pressures and spectrums with and without the noise.

Response to RAI EMEB-B-99

The PSD's for the burst random and chirp noise sources are provided in Figures EMEB-B-99-1 and EMEB-B-99-2. The burst random noise source was selected to provide a broad bandwidth continuous signal over one second time duration to permit a wide range of frequency excitation. The chirp also included a broad bandwidth and was selected to introduce a source with a different phase relation than the burst random.

In Figures EMEB-B-99-3 through 18, Entergy provides comparisons of PSD's for the 81 CFM flow case with no source and the 81 CFM flow case with chirp source.

Figure EMEB-B-99-1

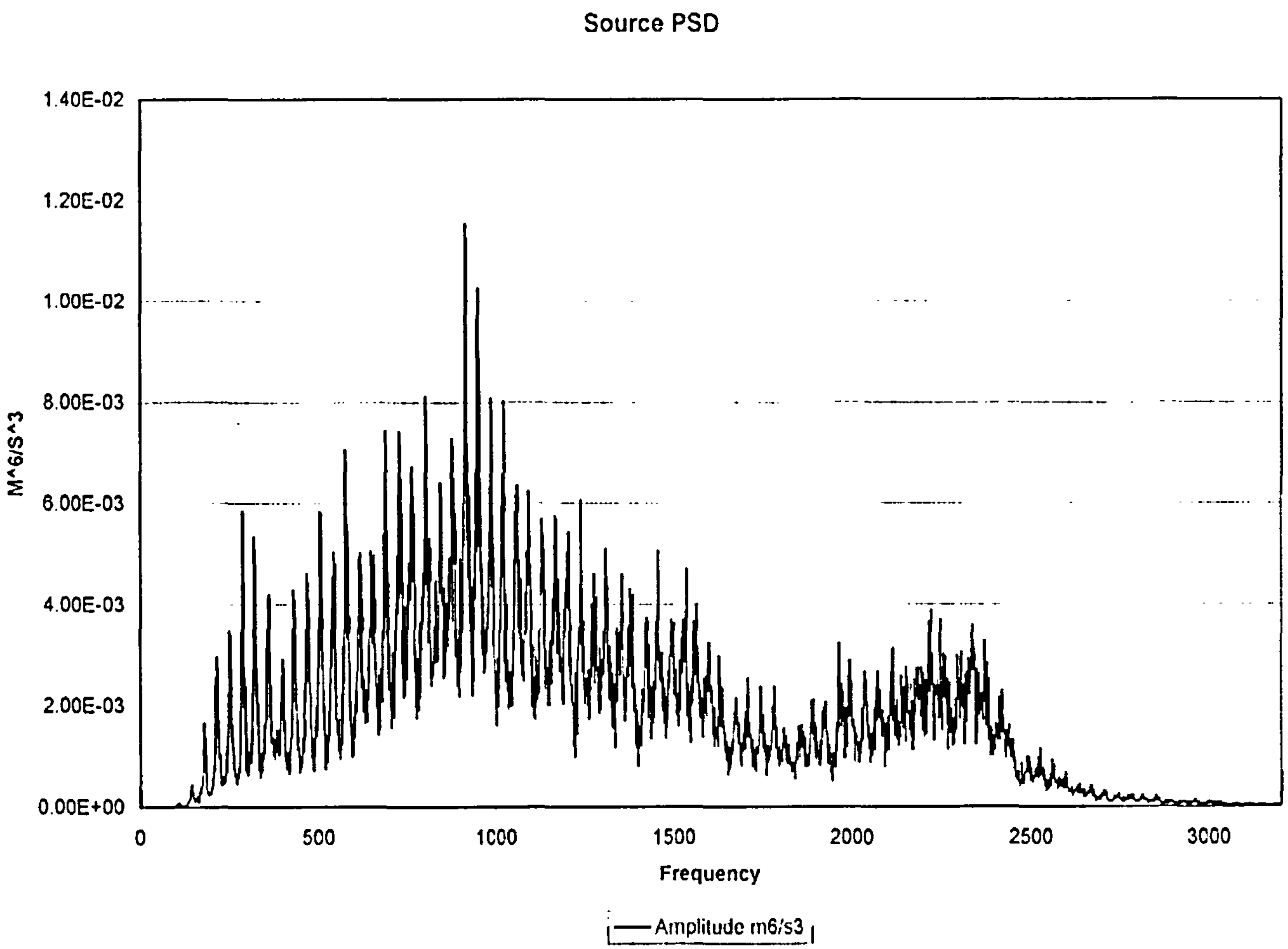

Non-Proprietary Version

Figure EMEB-B-99-2

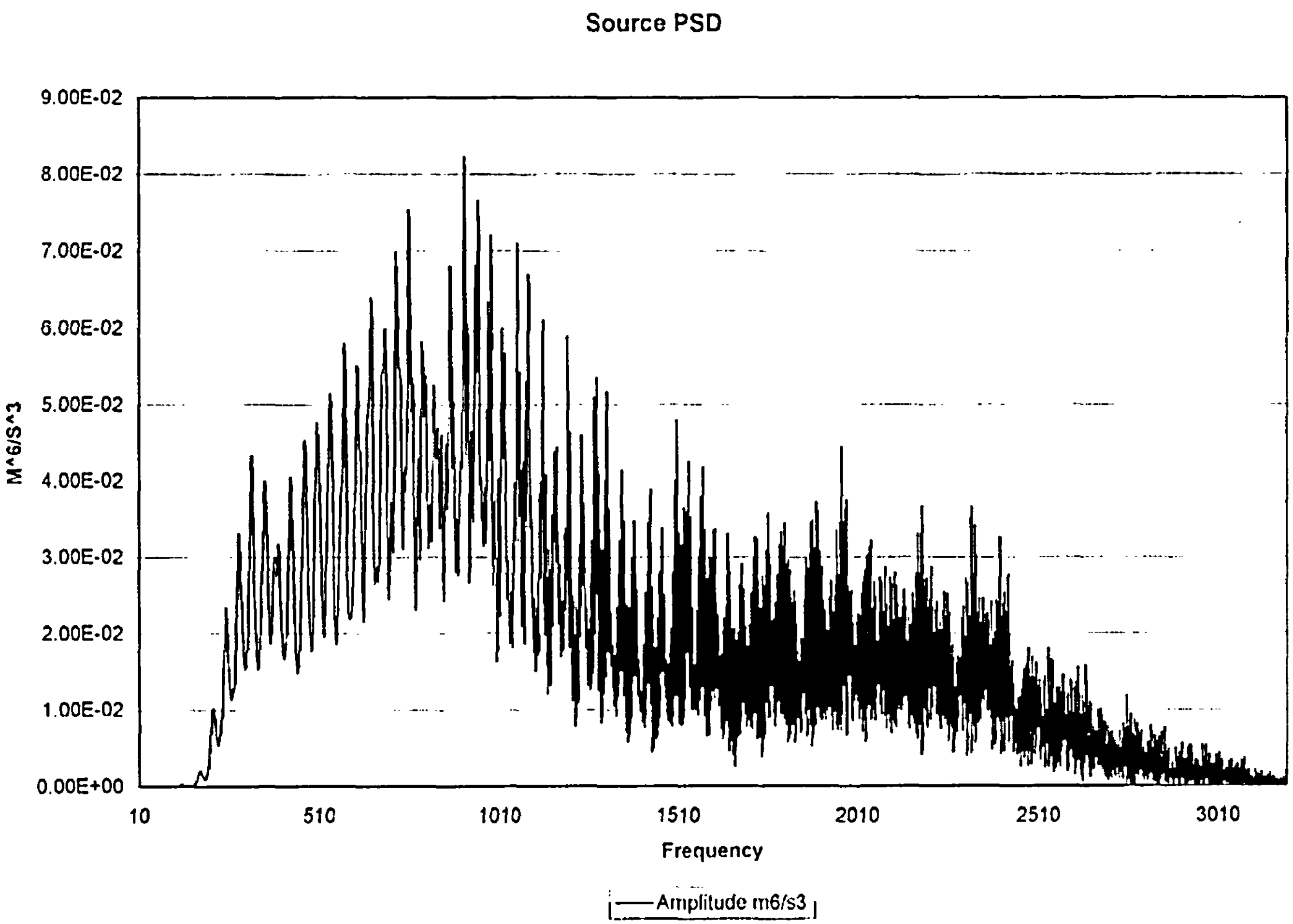

Non-Proprietary Version

Figure EMEB-B-99-3

Comparison Mic PSDs Flow vs Source

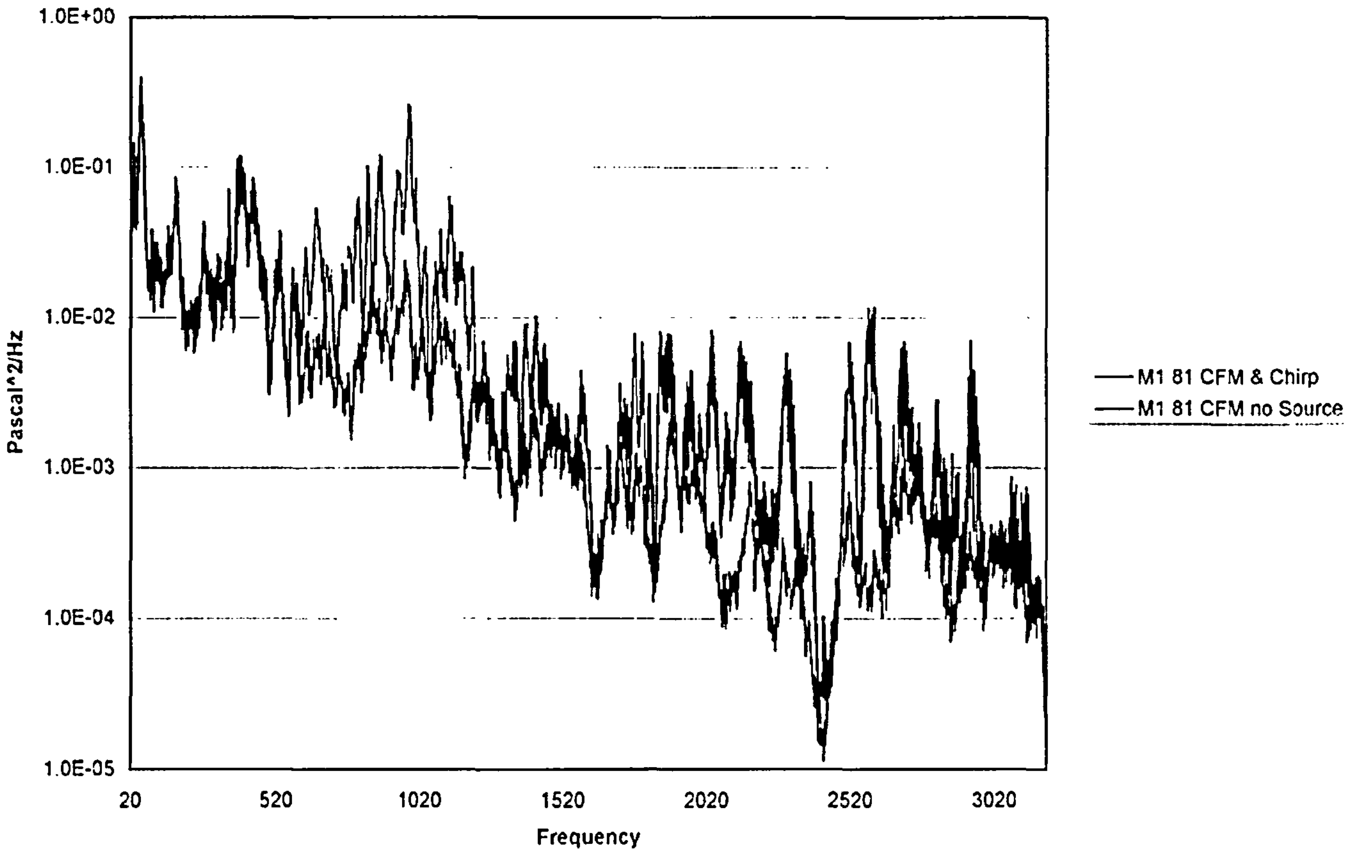

Non-Proprietary Version

Figure EMEB-B-99-4

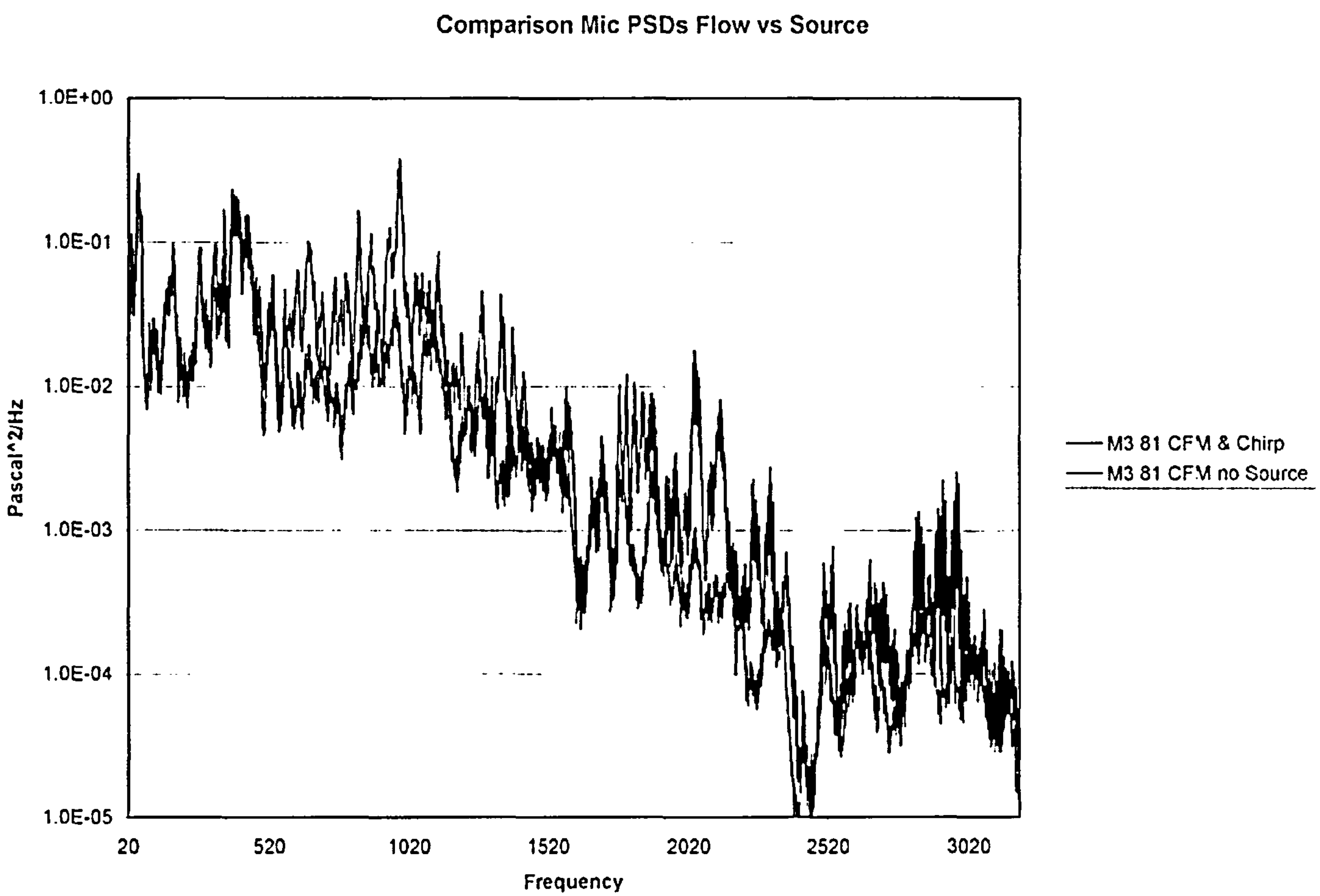

Non-Proprietary Version

Figure EMEB-B-99-5

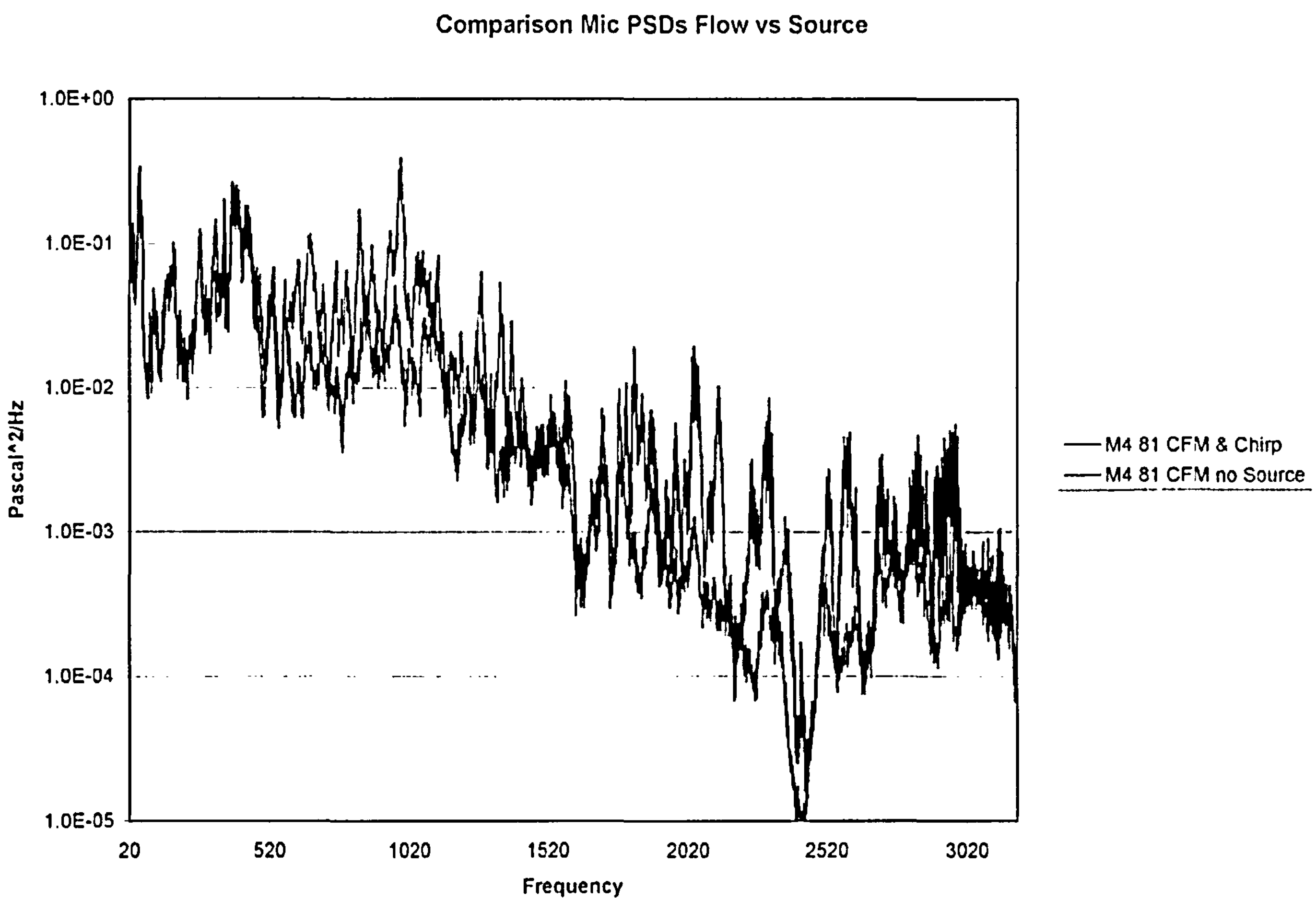

Figure EMEB-B-99-6

Comparison Mic PSDs Flow vs Source

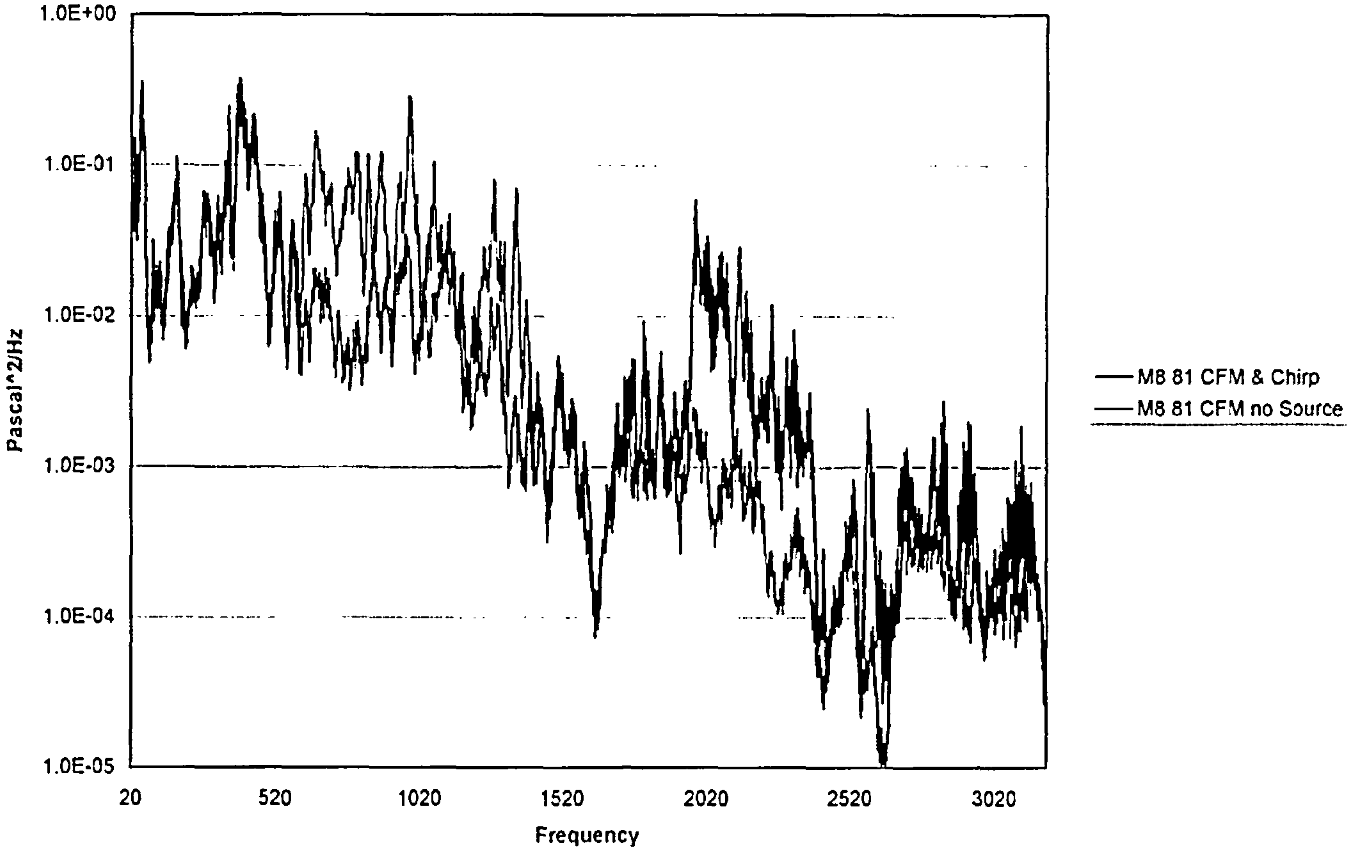

Non-Proprietary Version

Figure EMEB-B-99-7

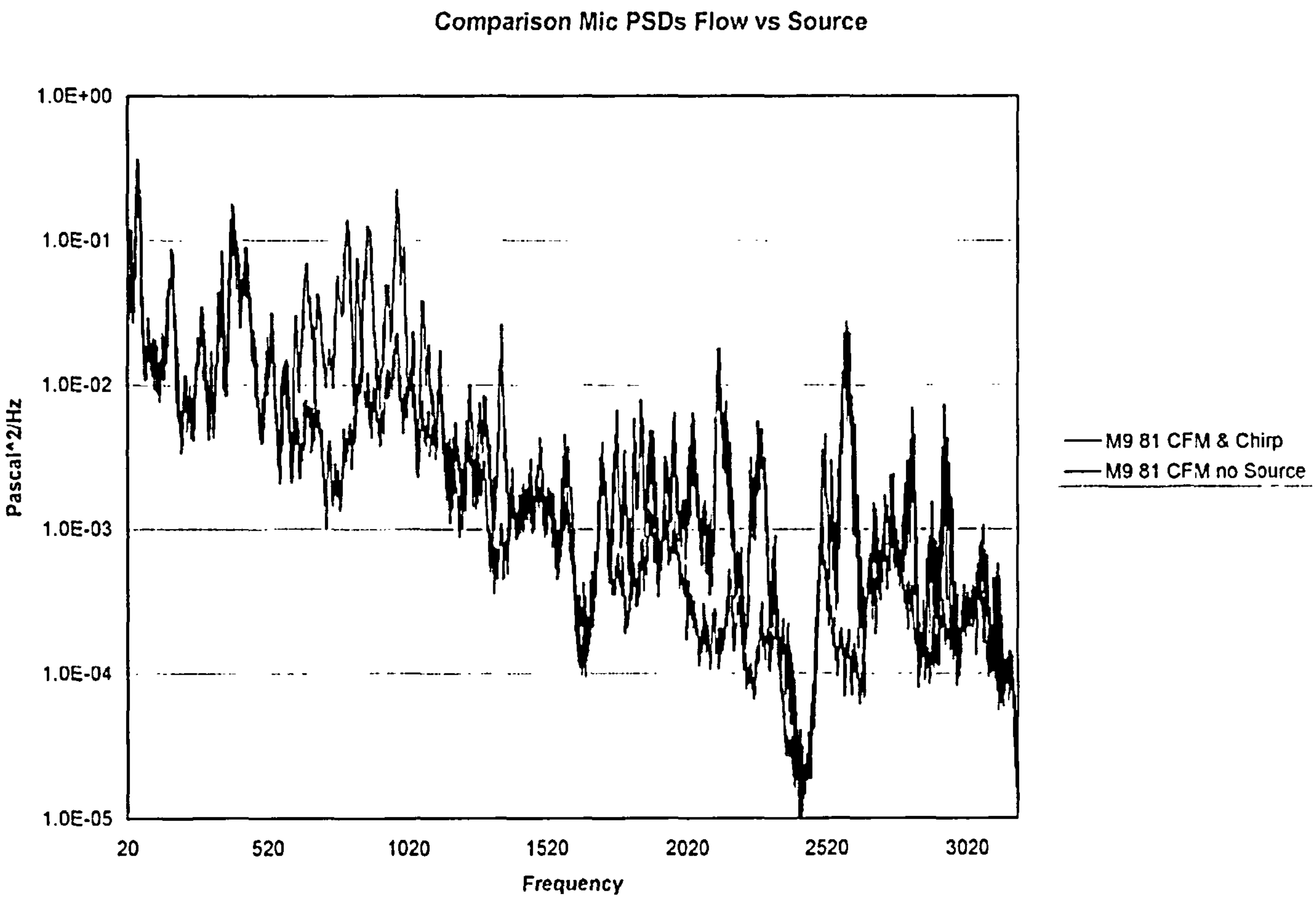

Figure EMEB-B-99-8

Comparison Mic PSDs Flow vs Source

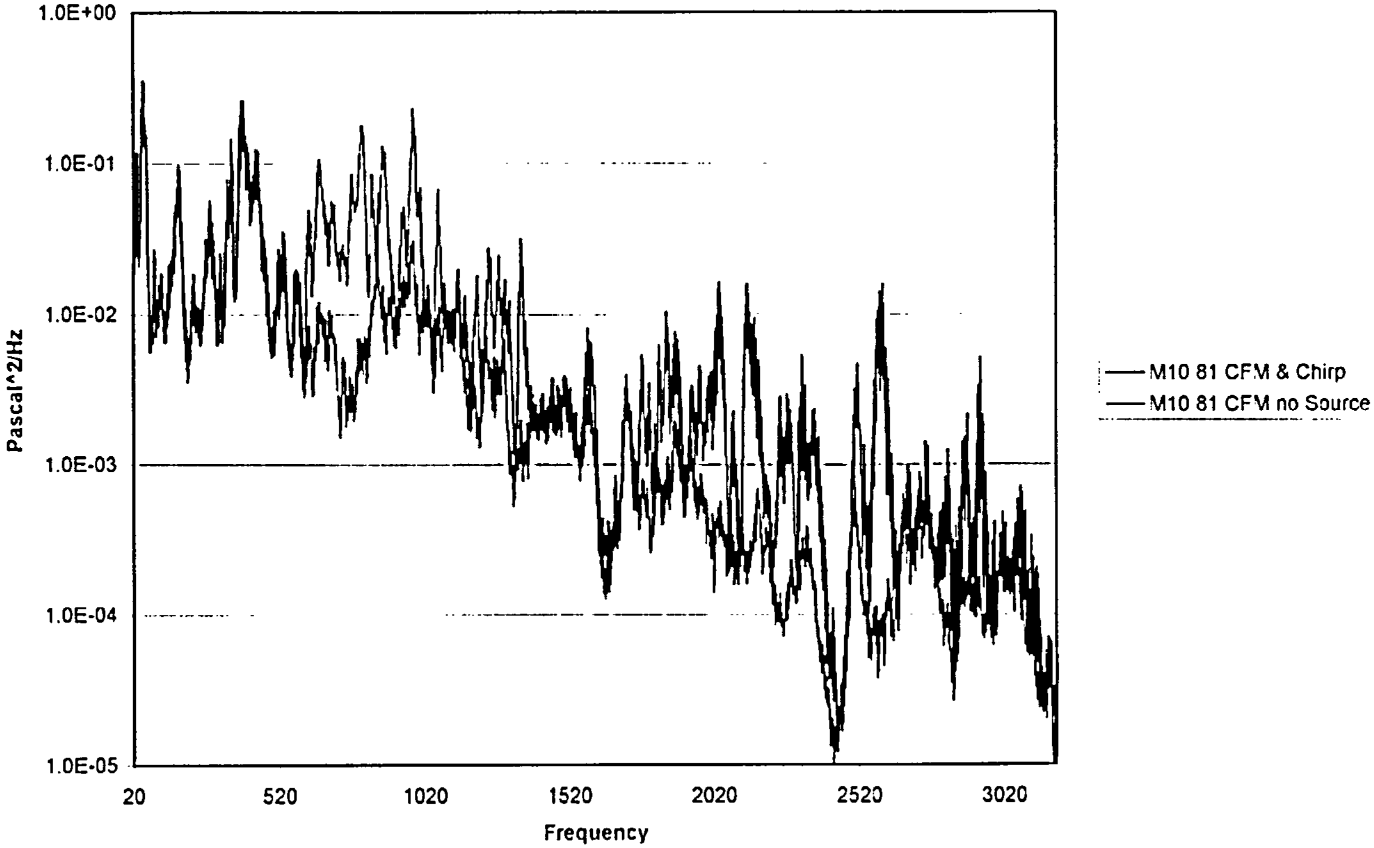

Non-Proprietary Version

Figure EMEB-B-99-9

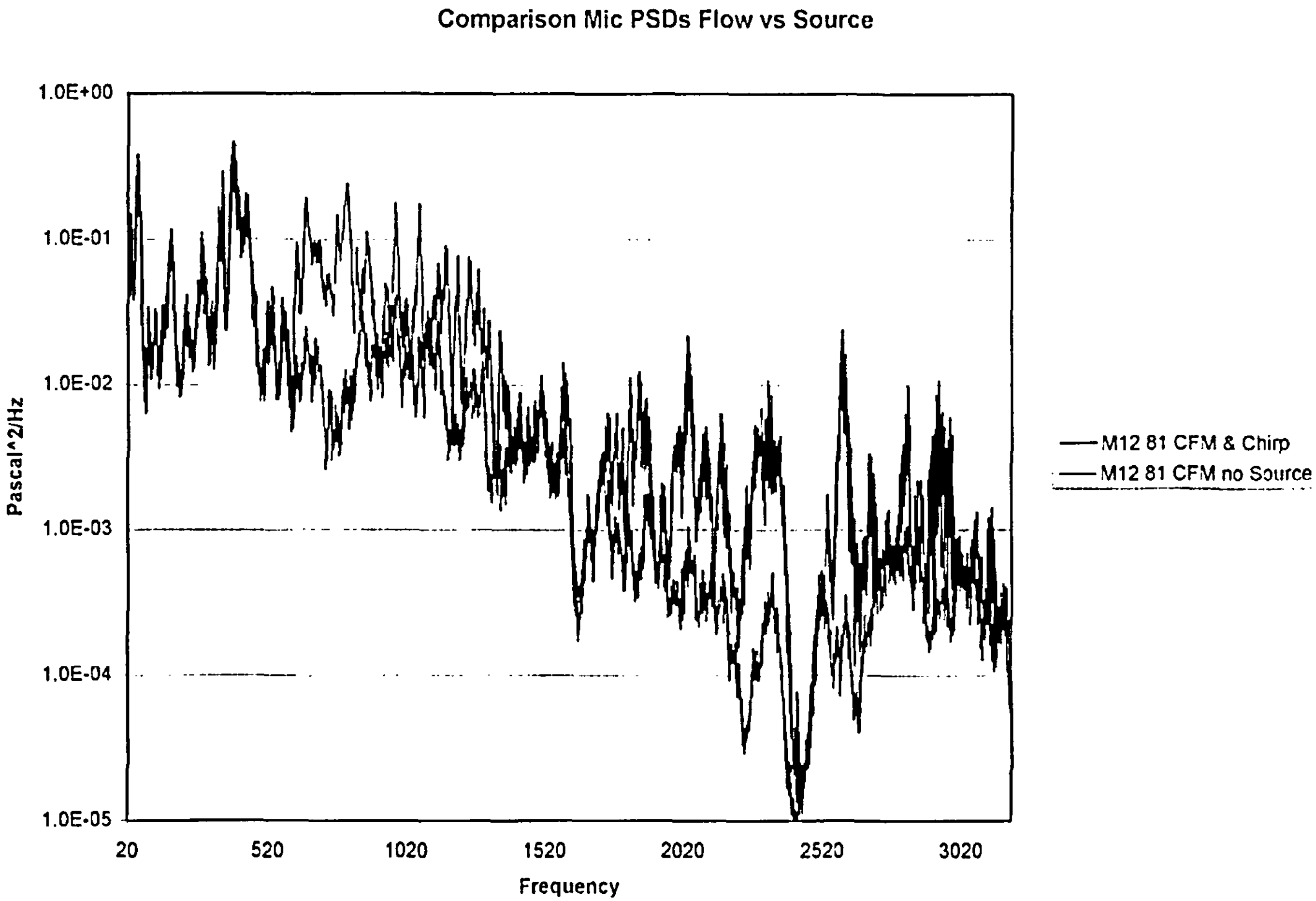

Non-Proprietary Version

Figure EMEB-B-99-10

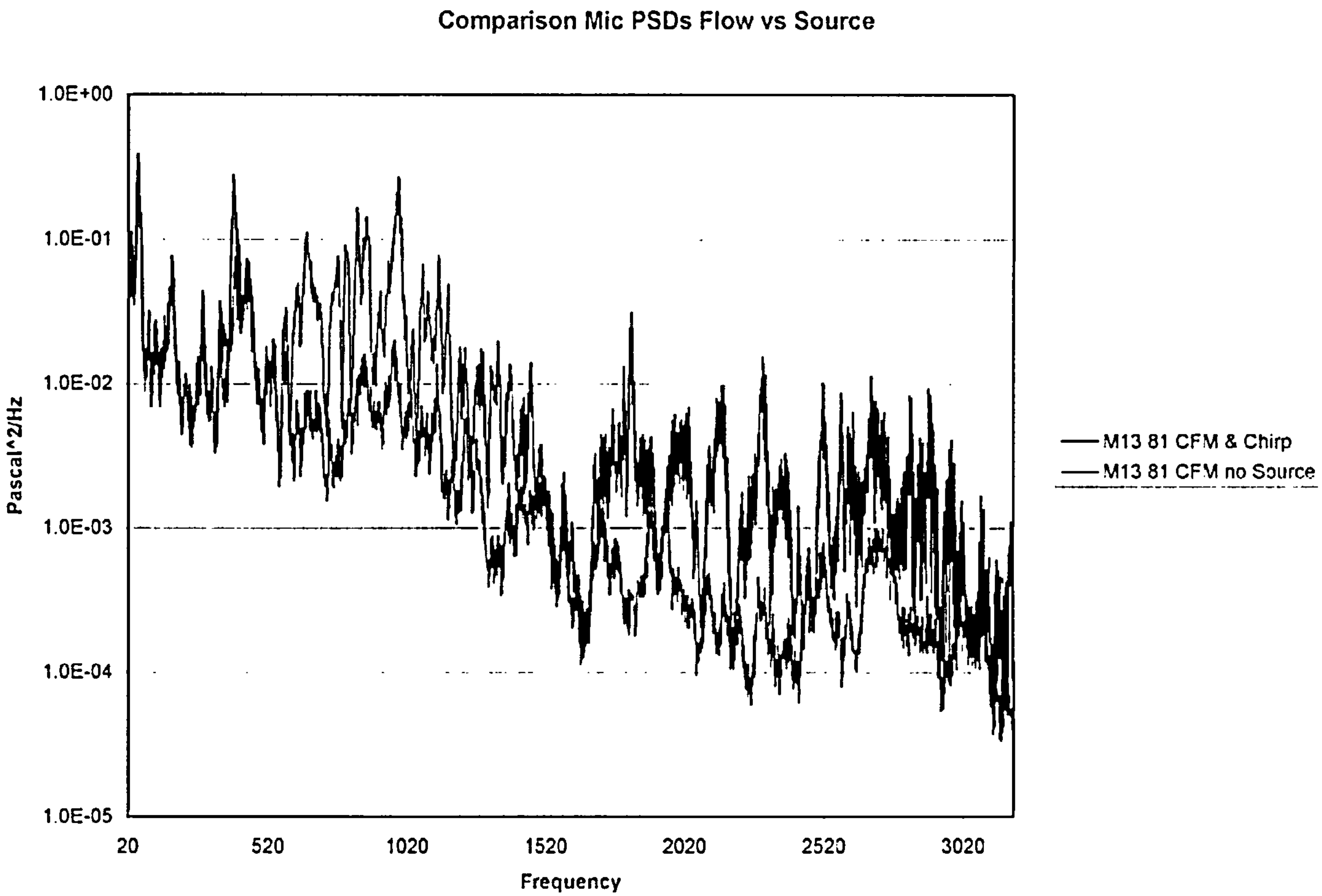

Non-Proprietary Version

Attachment 6
BVY 05-074
Docket No. 50-271
Page 26 of 61

Figure EMEB-B-99-11

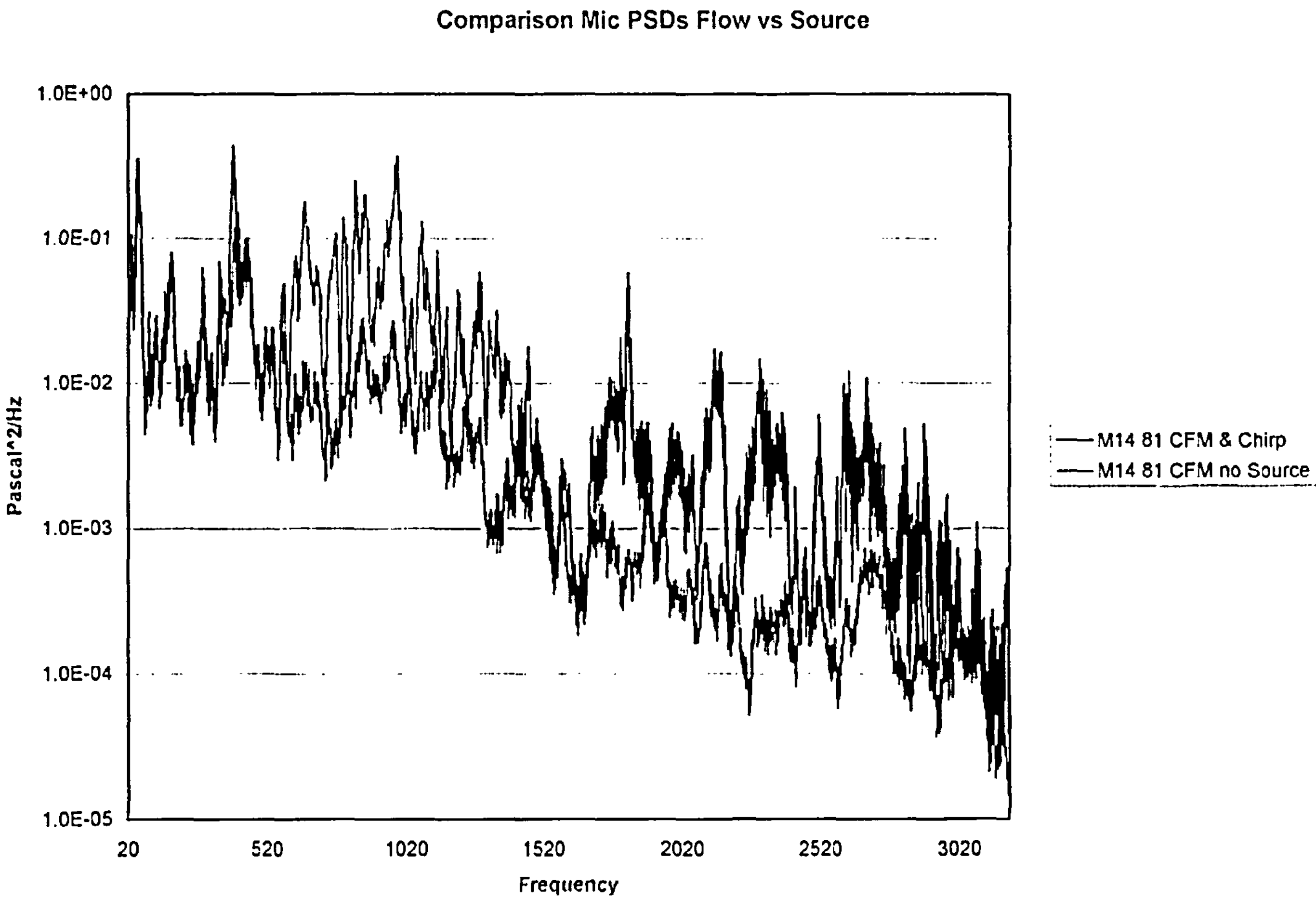

Non-Proprietary Version

Figure EMEB-B-99-12

Comparison Mic PSDs Flow vs Source

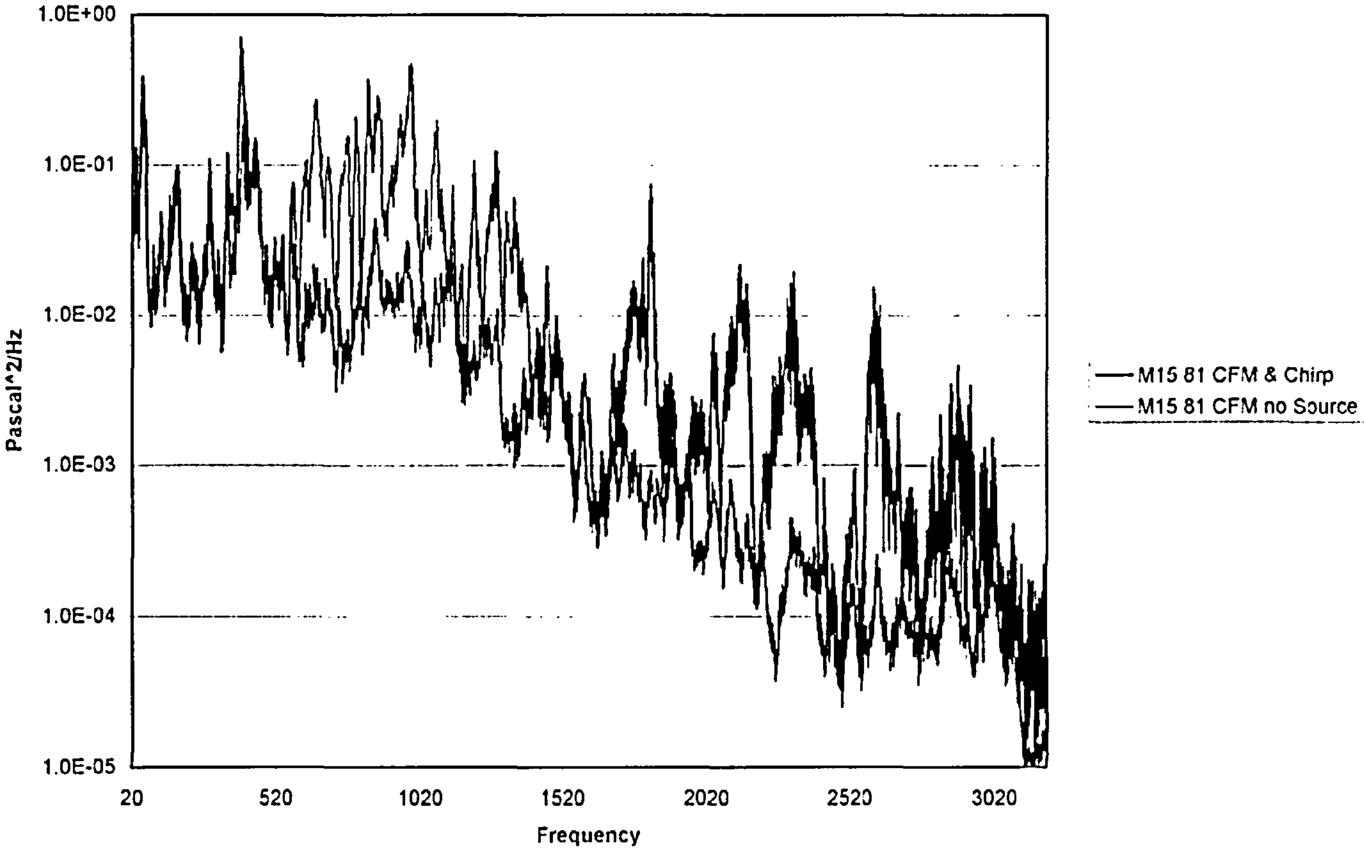

Non-Proprietary Version

Figure EMEB-B-99-13

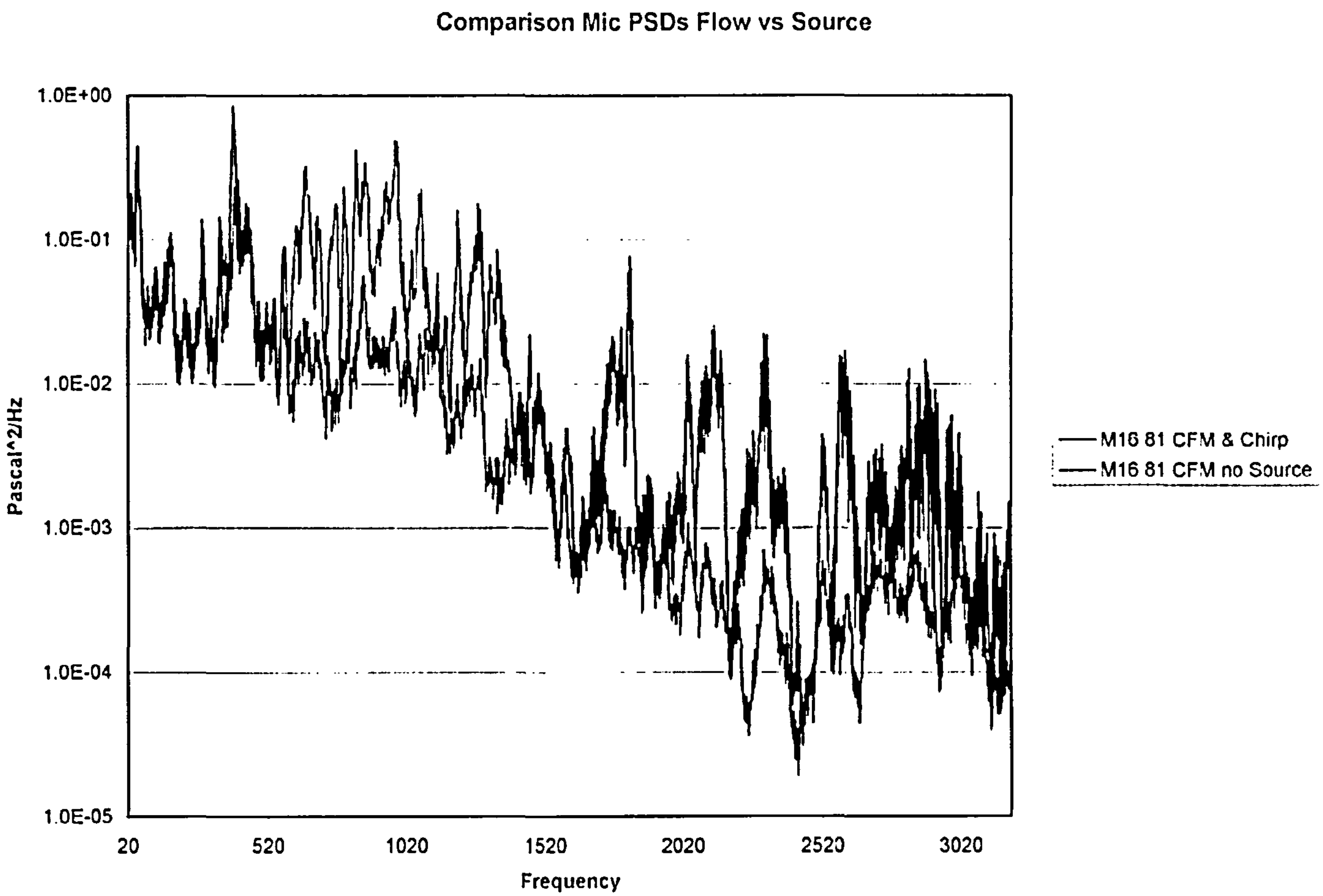

Figure EMEB-B-99-14

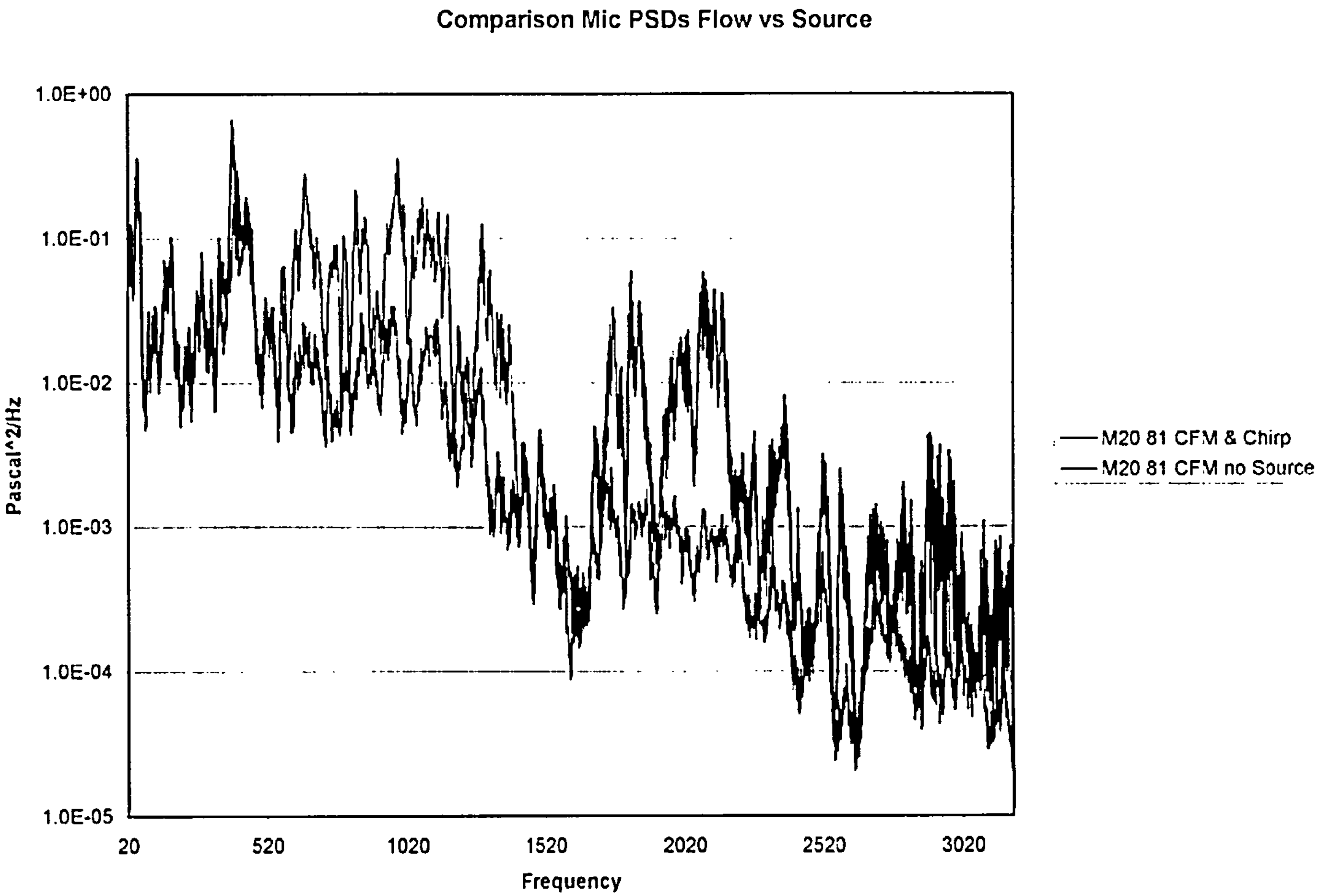

Figure EMEB-B-99-15

Comparison Mic PSDs Flow vs Source

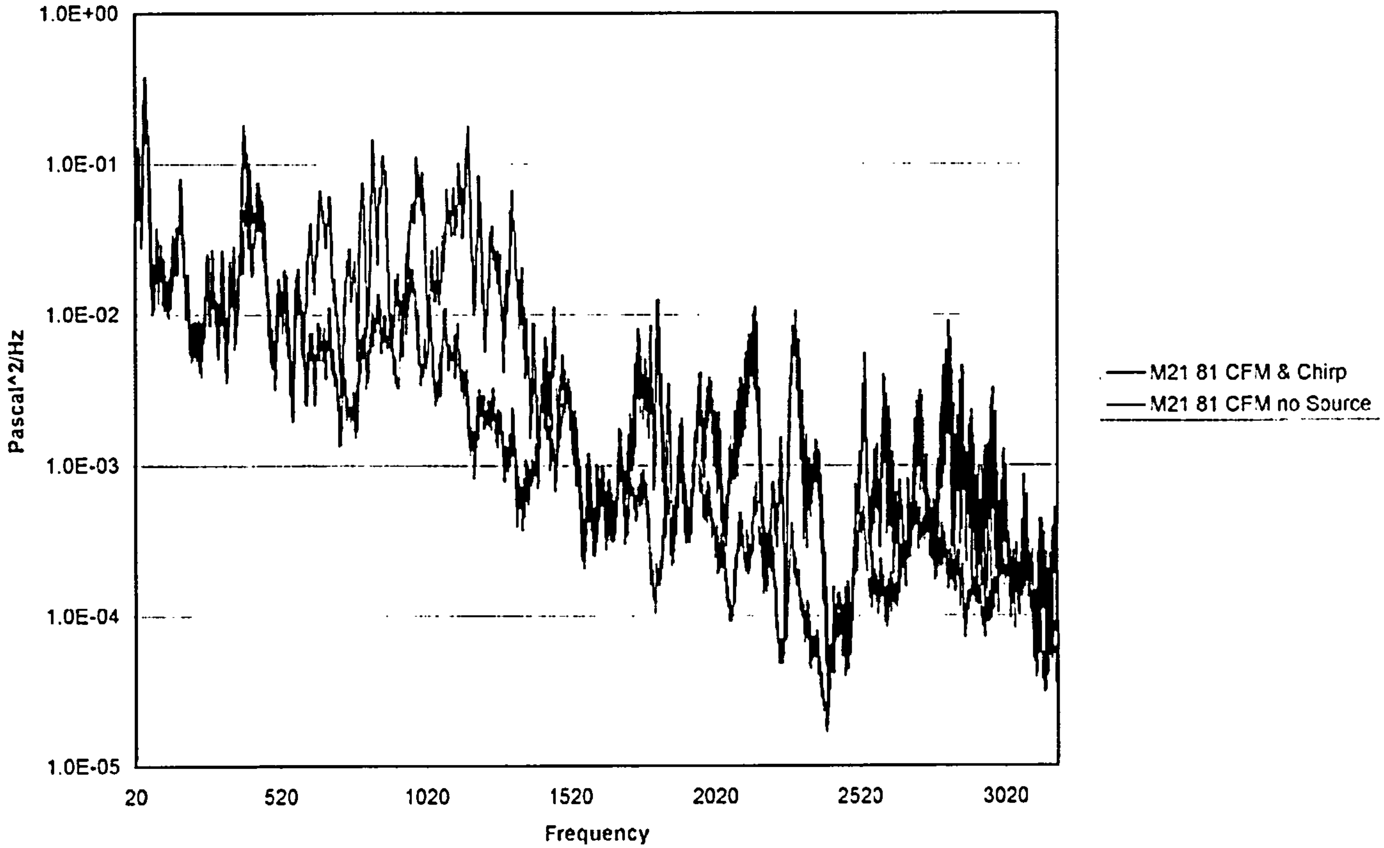

Figure EMEB-B-99-16

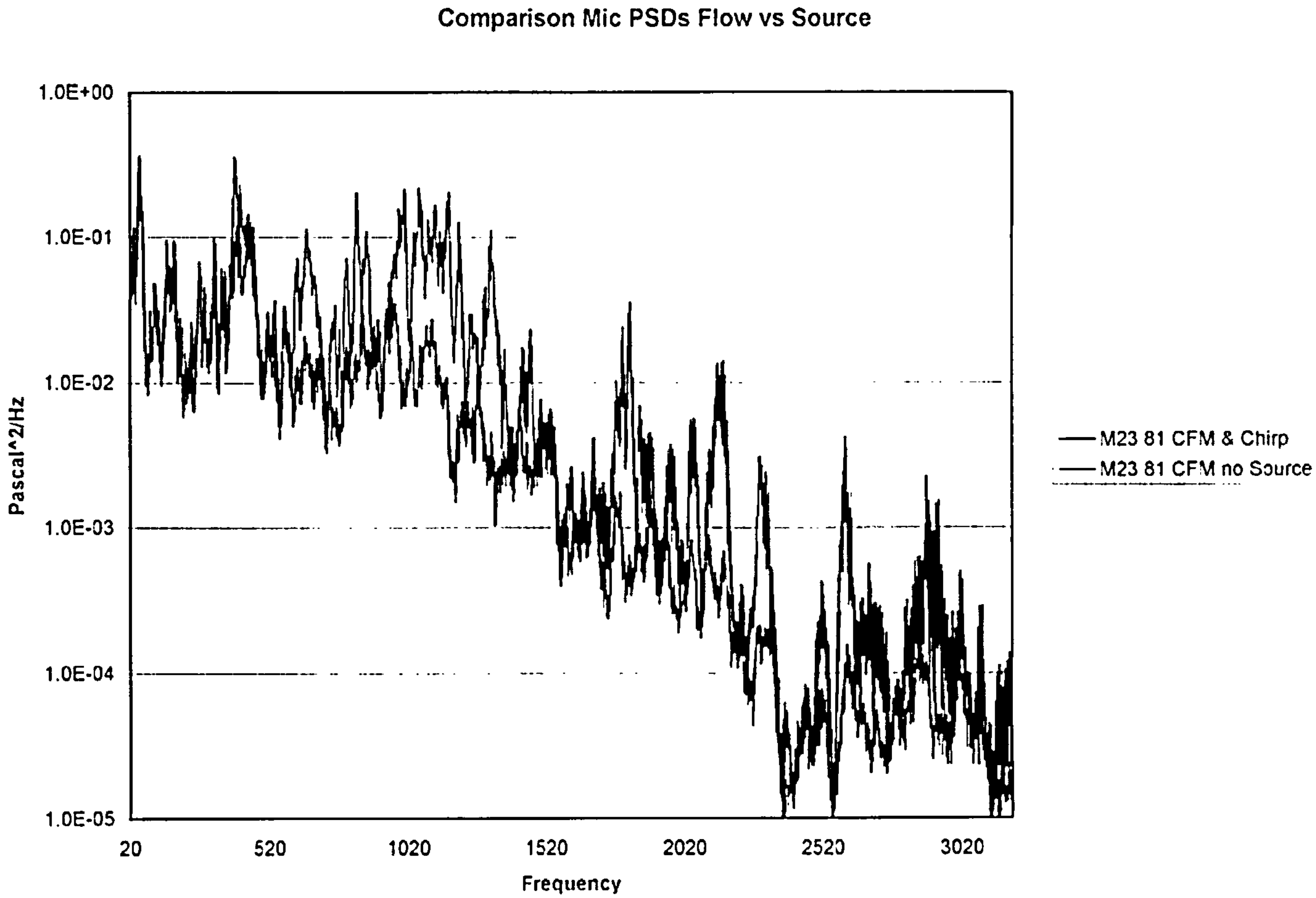

Non-Proprietary Version

Figure EMEB-B-99-17

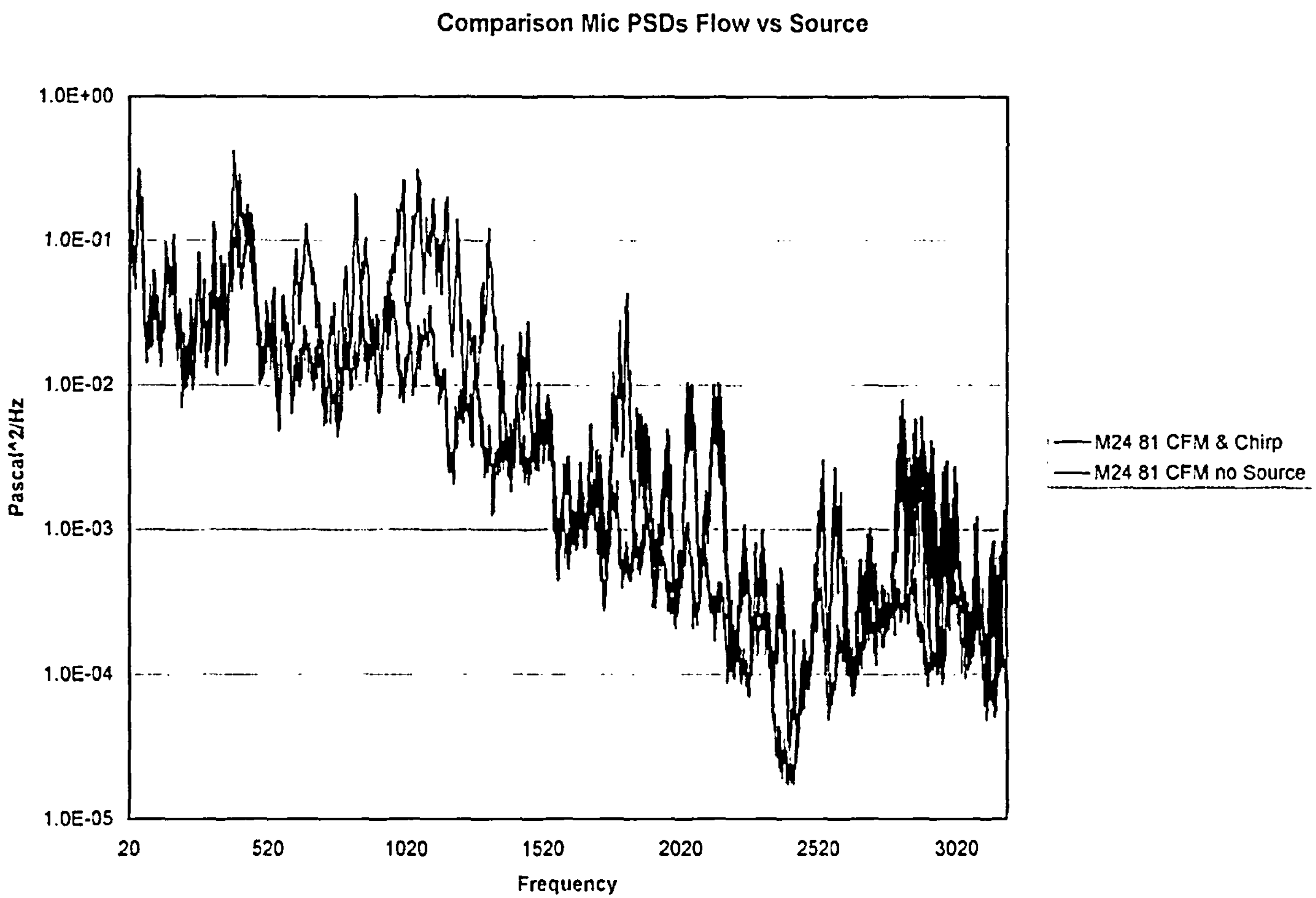

Non-Proprietary Version

RAI EMEB-B-100

The SMT was performed at reduced flow and included noise sources in the MSL, apparently to provide data that could be analyzed with confidence. However, no noise sources were included in the scale model steam dome. Entergy should elaborate on how this SMT has the ability to benchmark the ACA for FIV noise sources created in the steam dome.

Response to RAI EMEB-B-100

The acoustic circuit analysis accounts for the presence or absence of sources in the system, whether in the main steam system or the steam dome. Based on CFD model results, there is no evidence of significant acoustic sources in the VYNPS steam dome. Rather, according to the CFD model, the important acoustic noise source is at the RPV nozzle. Entergy's benchmark relied on SMT flow energy to excite noise sources in the steam dome and elsewhere in the system. The SMT benchmark introduced a deterministic source in the main steam system to replicate an acoustic resonator in the full scale plant. The benchmark exercised the acoustic circuit model's ability to predict the impact on the dryer due to deterministic and flow noises in the system. Since this benchmark was performed, a full scale benchmark of the QC2 instrumented dryer provided additional validation of the CDI ACA. The results demonstrate that the ACA assumption on location of noise source is appropriate.

RAI EMEB-B-101

The microphones on the dryer front surface chosen for SMT did not include any of those located in the center of the dryer (see Figure 2 on page 12 of Attachment 1 to Supplement No. 27). Entergy should explain the basis for selection of the microphone locations, including considerations that were given for investigating pressure distribution and phasing.

Response to RAI EMEB-B-101

Sensors were chosen on both outer hoods, around the skirt and on the top plates. The selected locations provide a sample of all regions on the dryer. More sensors were placed on the outer hoods because the most significant dryer failures have occurred on the outer hoods.

The sensor locations chosen allow identification of both symmetric and asymmetric loading on the dryer outer hoods. A symmetric load can be identified by observing the phase of the measurements obtained on different sides of the same hood to be in phase; whereas, an asymmetric load would be observable by out of phase measurements. Relationships between the outer hoods on each side of the dryer can also be identified.

RAI EMEB-B-102

The reported pressures from the SMT are quite low. At 50% flow and an added noise chirp, the maximum and RMS pressures are less than 70 pascal (Pa) (0.01 psi) and 12 Pa (0.002 psi), respectively (see Figure 3D on page 18 of Attachment 1 to Supplement 27). Assuming a quadratic increase in pressures with flow rate, the extrapolated pressure would be less than 403 Pa (~ 0.06 psi) and 69 Pa (0.015 psi), respectively for 120% simulated Quad Cities Unit 1 pre-EPU power. In the prototype, the maximum pressure would be ~ 3.8 psi and the RMS would be 0.65 psi at 120% pre-EPU power, assuming a scaling factor of 65. Entergy should justify why benchmarking at such low pressure and noise levels is a valid evaluation of the ability of the ACA to predict dryer pressures in the presence of high noise levels.

Response to RAI EMEB-B-102

The flow used in the SMT during the benchmark test provided pressures that were of equivalent amplitude to the sound source used during the benchmark. The combined sources were also balanced against the dynamic range of the microphones. It was also important to Entergy that the selected flow condition was different from that previously used in the ACM. With the exception of external acoustic sources such as branch line resonators, testing experience prior to the benchmark date had indicated that the flow frequency signature correlated reasonably well with flow velocity. Therefore, as long as flow noise sources and sound sources were within the dynamic range of the microphones, Entergy concluded that the conditions in the SMT were adequate for a valid benchmark. The subsequent QC2 benchmark evaluation provides validation of the ACA for flow conditions on a full scale plant that will envelope the VYNPS EPU flow conditions.

RAI EMEB-B-103

Both the ACA predicted maximum and RMS pressure levels for SMT with 50% flow and an added noise chirp are significantly less than the pressures predicted for no flow and the same noise chirp (see Figures 3B and 3D on pages 16 and 18 of Attachment 1 to Supplement No. 27). The SMT results do not exhibit this trend. Entergy should explain why the ACA predicts higher pressure-levels on the front surface of the dryer when flow is not present, in the presence of the same noise chirp.

Response to RAI EMEB-B-103

The purpose of the ACM benchmark no flow test was to evaluate the transmission and distribution capability of the model without the impact of flow. Review of the SMT data indicates that the flow noise suppresses the transmission of higher frequency acoustic signals on the dryer, resulting in a relative reduction in high frequency dryer loads compared to the no-flow case. The predicted SMT dryer loads replicate this behavior well. The ACA under-predicts the flow noise at frequencies less than 240 Hz. This is the primary reason for the difference in pressure amplitude predictions in the cited figures. Entergy is applying CFD loads to define the turbulent loads on the dryer.

RAI EMEB-B-104

Comparisons of the time data reveals that the ACA pressure predictions are up to 40% lower than SMT results for several microphone locations. These differences are discussed by stating that "... in a structural analysis of the modified full scale VYNPS steam dryer, these loads would be effectively 'integrated' by the 1" face plate and heavy 5/8" cover plate and 1/2" gussets" (see page 13 of Attachment 1 to Supplement No. 27). Entergy should explain whether such a statement is appropriate for a benchmark analysis intended to demonstrate the ability of the ACA to predict pressures. Also, Entergy should explain the meaning of 'effectively integrated' and how it is applicable when pressures contain significant energy at a natural frequency and the pressure distribution and phasing result in a high participation factor.

Response to RAI EMEB-B-104

In response to RAI's EMEB-B-18, EMEB-B-60 and EMEB-B-107, Entergy has reevaluated the SMT data and determined that the major source of differences in the microphone comparisons were due to the acoustic model's inadequate prediction of flow turbulent energy at less than 240 Hz. The phasing and participation factor issues have been addressed in response to EMEB-B-61 and EMEB-B-107.

RAI EMEB-B-105

Using its benchmark criteria formulated in response to RAI EMEB-98, Entergy should justify the conclusion that this analysis constitutes a benchmark for ACA analysis. Several differences are noted in the main body of the report (Attachment 1 to Supplement No. 27). These differences are more apparent in the data provided in the Appendices. Most importantly:

a) Many significant pressure peaks measured at frequencies in the range of dryer structural natural frequencies are not predicted by CDI model. These discrepancies occur for many microphone locations. For example, see the PSD comparison at about 1,000 Hz for Microphone M8 located on the cover plate (Appendix E, page E9). The SMT data provides several times higher value for PSD than CDI model.

b) The CDI model predicts peaks at frequencies that do not exist in the data or greatly overpredicts the pressures at many frequencies. These discrepancies occur for almost all microphone locations.

Using its benchmark criteria formulated in response to RAI EMEB-98, Entergy should discuss the significance of the above-mentioned differences and justify the conclusion that this analysis constitutes a benchmark for ACA analysis.

Response to RAI EMEB-B-105

a) Microphone M8 is located on the top of the SMT dryer cover plate. Based on the phasing evaluation performed to support response to EMEB-B-107, the acoustic model predicts the phasing of the loading and predicts the amplitude of the balance of other face microphones well, at this frequency. This region of the VYNPS dryer is at the junction of the ring girder, cover plate, gussets and vertical plate. Pressure loading in this area has limited impact on the dryer response or peak stress.

b) Entergy agrees that the acoustic model over-predicts the pressures at many frequencies. Applying the +/- 10% time variation adds additional conservatism, as described in response to RAI EMEB-B-61. This benchmark provides confidence that the application of the acoustic model to VYNPS results in a conservative load definition for dryer acoustic forces above 20 Hz.

RAI EMEB-B-106

The benchmark test shown in Attachment 1 to Supplement No. 27 minimizes the differences between the predictions by the CDI model and SMT results by a technique more appropriate for determining conservative load bounds, not for benchmarking a prediction method. Essentially, the predictions in the frequency domain are broadened to bound and envelope the peaks not predicted in the ACA blind benchmark analysis. Even with this broadening, several significant peaks are not predicted. Entergy should provide the theoretical basis for broadening.

Response to RAI EMEB-B-106

For the VYNPS dryer analysis, the significant acoustic model loads act primarily on the vertical face of the dryer. Even though the complete dryer structure includes many mode shapes and frequencies, there are limited frequencies affected by the ACA and CFD loads (refer to response to RAI EMEB-B-110 and Exhibit EMEB-B-143-1). Broadening the PSD results provides indication of how well +/- 10% time step changes in the structural analysis will capture uncertainties in amplitude differences of closely spaced modal response.

RAI EMEB-B-107

The benchmark test shown in Attachment 1 to Supplement No. 27 did not make any frequency-by-frequency comparisons of pressure phasing or distribution, nor investigate the correlation, coherence, or phasing between the pressures at different locations investigated. Entergy should explain why benchmarking pressure phasing between different dryer locations is not important, for the ACA methodology intended to provide the loading for structural dynamic analysis.

Response to RAI EMEB-B-107

The following pages are comparisons of scale model test results to acoustic circuit predicted results for the following conditions:

1. No flow with burst random excitation (VY3Run2)
2. 81 CFM with burst random excitation (VY6Run2)
3. No flow with periodic chirp excitation (VY13Run1)
4. 81 CFM with periodic chirp excitation (VY12Run1)

- The following slides contain comparisons of Crosspower Amplitude, Crosspower Phase, and Coherence Between Scale Model Test and Acoustic Circuit Prediction.
- Frequency Limitations; the volume velocity source used as sound excitation has a useable lower frequency limit of 200 Hz.
- The Quad Cities Original Design Dryer model was installed in the test rig for this testing.
- The crosspower spectrum shown is a measure of the mutual power between 2 signals at each frequency of the analysis band.
- The crosspower amplitude is high when the amplitudes of both signals are high.
- The crosspower phase is the relative phase between the signals.
- In the spectra presented, the 2 signals are time histories of pressure from different locations on the steam dryer scale model, the upper right location on each dryer face to an observer looking at the face serving as the reference or input.
- The coherence function shown in the following plots is a measure of how the output is linearly related to the input or reference at each frequency of the analysis band.
- In this case a pressure signal at 1 location (upper right) is considered the input and a pressure signal at another location is considered the output.
- Its value ranges between 0 and 1, 0 indicating no linear dependence and 1 indicating perfect linear dependence.
- The crosspower average comparisons among the following slides show:
  [[

  ]]
- This comparison is a global comparison of the measured points
  [[

]]

Non-Proprietary Version

[[

]]

Figure EMEB-107-1: Average of Crosspowers and Reference Autopowers for No Flow with Burst Random Acoustic Excitation near D-ring of MSL A.

[[

]]

Figure EMEB-107-2: Crosspower Amplitude, Crosspower Phase and Coherence for No Flow with Burst Random Acoustic Excitation near D-ring of MSL A 90° Face, Middle Right Location with Respect to Upper Right Location

[[

]]

Figure EMEB-107-3: Crosspower Amplitude, Crosspower Phase and Coherence for No Flow with Burst Random Acoustic Excitation near D-ring of MSL A 90° Face, Lower Left Location with Respect to Upper Right Location

[[

]]

Figure EMEB-107-4: Crosspower Amplitude, Crosspower Phase and Coherence for No Flow with Burst Random Acoustic Excitation near D-ring of MSL A 270° Face, Middle Right Location with Respect to Upper Right Location

[[

]]

Figure EMEB-107-5: Crosspower Amplitude, Crosspower Phase and Coherence for No Flow with Burst Random Acoustic Excitation near D-ring of MSL A 270° Face, Lower Left Location with Respect to Upper Right Location

[[

]]

Figure EMEB-107-6: Average of Crosspowers and Reference Autopowers for 81CFM Flow with Burst Random Acoustic Excitation near D-ring of MSL A

[[

]]

Figure EMEB-107-7: Crosspower Amplitude, Crosspower Phase and Coherence for 81CFM Flow with Burst Random Acoustic Excitation near D-ring of MSL A 90° Face, Middle Right Location with Respect to Upper Right Location

[[

]]

Figure EMEB-107-8: Crosspower Amplitude, Crosspower Phase and Coherence for 81 CFM Flow with Burst Random Acoustic Excitation near D-ring of MSL A 90° Face, Lower Left Location with Respect to Upper Right Location

[[

]]

Figure EMEB-107-9: Crosspower Amplitude, Crosspower Phase and Coherence for 81CFM Flow with Burst Random Acoustic Excitation near D-ring of MSL A 270° Face, Middle Right Location with Respect to Upper Right Location

[[

]]

Figure EMEB-107-10: Crosspower Amplitude, Crosspower Phase and Coherence for 81 CFM Flow with Burst Random Acoustic Excitation near D-ring of MSL A
270° Face, Lower Left Location with Respect to Upper Right Location

[[

]]

Figure EMEB-107-11: Average of Crosspowers and Reference Autopowers for No Flow with Periodic Chirp Acoustic Excitation near D-ring of MSL A

[[

]]

Figure EMEB-107-12: Crosspower Amplitude, Crosspower Phase and Coherence for No Flow with Periodic Chirp Acoustic Excitation near D-ring of MSL A 90° Face, Middle Right Location with Respect to Upper Right Location

[[

]]

**Figure EMEB-107-13: Crosspower Amplitude, Crosspower Phase and Coherence for No Flow with Periodic Chirp Acoustic Excitation near D-ring of MSL A
90° Face, Lower Left Location with Respect to Upper Right Location**

[[

]]

Figure EMEB-107-14: Crosspower Amplitude, Crosspower Phase and Coherence for No Flow with Periodic Chirp Acoustic Excitation near D-ring of MSL A
270° Face, Middle Right Location with Respect to Upper Right Location

[[

]]

**Figure EMEB-107-15: Crosspower Amplitude, Crosspower Phase and Coherence for No Flow with Periodic Chirp Acoustic Excitation near D-ring of MSL A
270° Face, Lower Left Location with Respect to Upper Right Location**

[[

]]

Figure EMEB-107-16: Average of Crosspowers and Reference Autopowers for No Flow with Periodic Chirp Acoustic Excitation near D-ring of MSL A

[[

]]

Figure EMEB-107-17: Crosspower Amplitude, Crosspower Phase and Coherence for 81CFM Flow with Periodic Chirp Acoustic Excitation near D-ring of MSL A 90° Face, Middle Right Location with Respect to Upper Right Location

[[

]]

**Figure EMEB-107-18: Crosspower Amplitude, Crosspower Phase and Coherence for 81 CFM Flow with Periodic Chirp Acoustic Excitation near D-ring of MSL A
90° Face, Lower Left Location with Respect to Upper Right Location**

[[

]]

Figure EMEB-107-19: Crosspower Amplitude, Crosspower Phase and Coherence for 81CFM Flow with Periodic Chirp Acoustic Excitation near D-ring of MSL A 270° Face, Middle Right Location with Respect to Upper Right Location

[[

]]

Figure EMEB-107-20: Crosspower Amplitude, Crosspower Phase and Coherence for 81 CFM Flow with Periodic Chirp Acoustic Excitation near D-ring of MSL A 270° Face, Lower Left Location with Respect to Upper Right Location

[[

]]

Figure EMEB-107-21: Plots of Average Crosspower for each Case being Analyzed

- The accompanying animations (Enclosure 3) are depictions of operating pressure shape comparisons from the scale model test results and the acoustic circuit predictions
- All of the possible measurement points for this scale model are shown; however, only a subset of the points (those that move in these animations) was measured for this set of tests
- The pressure is defined as normal to the dryer surface
- The wireframe connects the points that were measured. The remaining points are shown as markers and are left to provide some sense of the dryer geometry except for M:39, which is one of the measured points but is not connected to the wireframe.
- A sampling of animations from the highest amplitudes in the averaged crosspower measurements is provided

[[

]]

Figure EMEB-107-22: Undeformed Geometry

Attachment 7

Vermont Yankee Nuclear Power Station

Proposed Technical Specification Change No. 263 – Supplement No. 31

Extended Power Uprate

Response to Request for Additional Information

Other Mechanical and Civil Engineering Branch RAIs

NON-PROPRIETARY VERSION

Total number of pages in Attachment 4
(excluding this cover sheet) is 49.

RESPONSE TO REQUEST FOR ADDITIONAL INFORMATION REGARDING APPLICATION FOR EXTENDED POWER UPRATE LICENSE AMENDMENT VERMONT YANKEE NUCLEAR POWER STATION

PREFACE

This attachment provides responses to the NRC Mechanical and Civil Engineering Branch (EMEB) individual requests for additional information (RAIs) in NRC's letter dated July 27, 2005.[1] Upon receipt of the RAI, discussions were held with the NRC staff to further clarify the RAI. In certain instances the intent of certain individual RAIs may have been modified based on clarifications reached during these discussions. The information provided herein is consistent with those clarifications.

The individual RAIs are re-stated as provided in NRC's letter of July 27, 2005.

Mechanical and Civil Engineering Branch (EMEB)
Component Integrity and Testing Section (EMEB-A)
Civil and Engineering Mechanics Section (EMEB-B)

RAI EMEB-B-22

On Pages 1 and 2 of Attachment 2 to Supplement 26, Entergy describes a two-step power ascension for VYNPS if the EPU request is granted. In the first step, Entergy would increase power from 100% to 115% of the original licensed thermal power (OLTP) with 4-hour hold periods after each 2.5% power increase and a 168-hour hold period at each 5% plateau. Discuss the evaluation of the steam dryer loads that will be performed at each 5% plateau based on the acoustic circuit analysis using MSL data input and the plans to provide that information to the NRC staff.

Response to RAI EMEB-B-22

Table 1 of Attachment 2 specifies the frequency of main steam system data collection. This data will serve as the input for evaluating steam dryer loading at each test plateau. The initial evaluation will consist of the surveillance which will compare the Fast Fourier Transforms (FFT) for the measurements to the spectra performance criteria described in Table 2. If the Level 2 surveillance performance criteria are met at the test plateau, no additional evaluation will be performed. If the Level 2 performance criterion for spectra is not met, power ascension will be suspended and an engineering evaluation performed to justify resumption of power ascension. This evaluation will

[1] U.S. Nuclear Regulatory Commission (Richard B. Ennis) letter to Entergy Nuclear Operations, Inc. (Michael Kansler), "Request for Additional Information – Extended Power Uprate, Vermont Yankee Nuclear Power Station (TAC No. MC0761)," July 27, 2005

involve comparison of data points and trends to confirm the validity of spectra changes. If the Level 1 performance criterion for spectra is not met, power will be reduced to a previously acceptable level. An engineering evaluation will be performed which will include validation of the spectra and use of the VYNPS acoustic circuit model to generate updated acoustic loads. The dryer load definition will be revised based on the re-calculated acoustic loads and run through the VYNPS dryer finite element model. The resulting stresses will be compared to the structural limit to determine whether any dryer component exceeds the limit. If no components exceed the limit, a new acceptance curve will be defined based on the methodology used for establishing the previous limit, using the updated spectra. The results of the analysis will be documented and reviewed by the on-site safety review committee. Entergy will make the engineering evaluation available to NRC on-site at VYNPS. As stated on Page 2 of Attachment 2 to Supplement 26, if a license amendment is not granted before the next refueling outage, the power uprate will be accomplished in a single step, and the Steam Dryer Monitoring Plan, including power increase steps, hold points and operating specifications, will be carried out throughout the power ascension process.

RAI EMEB-B-23

On Page 1 of Attachment 2 to Supplement 26, Entergy states that, if the EPU request is granted during the current operating cycle, the second step of the power ascension for VYNPS would increase power to 120% OLTP following the refueling outage scheduled for the fall of 2005. Discuss the startup test plan that would be followed upon restart from the refueling outage with appropriate hold points at 2.5% and 5% plateaus and the evaluation of plant data at those hold points. Discuss the impact on the power ascension test plan if the EPU is not granted during the current operating cycle.

Response to RAI EMEB-B-23

If the first step of the power ascension to 115% OLTP is completed during the current operating cycle, the second step would increase power to 120% following the fall 2005 refueling outage. The startup test plan for increasing power from 115% to 120% will include the same actions as used for the first step, including two 2.5% power increase steps with 4-hour holds and a 5% final plateau, bringing the plant to the 120% OLTP operating condition. The operating specifications provided in Attachment 2 to Supplement 26 will pertain to the second step of power ascension. As stated on Page 2 of Attachment 2 to Supplement 26, if a license amendment is not granted before the next refueling outage, the power uprate will be accomplished in a single step, and the Steam Dryer Monitoring Plan, including power increase steps, hold points and operating specifications, will be carried out throughout the power ascension process.

RAI EMEB-B-24

On Page 3 of Attachment 2 to Supplement 26, Table 1 indicates that the plant parameters to be monitored for steam dryer surveillance are moisture carryover, MSL pressure data from strain gauges, and MSL pressure data from pressure transducers. Discuss the monitoring of MSL pressure data in assessing the performance of the steam dryer at VYNPS during plant operation.

Response to RAI EMEB-B-24

See response to RAI EMEB-B-22.

RAI EMEB-B-25

In Footnote 1 on Page 5 of Attachment 2 to Supplement 26, Entergy states that the Level 1 and 2 spectra for steam dryer performance criteria will be determined and documented in an engineering calculation or report. Provide the engineering calculations or reports that describe the development and bases for the steam dryer performance criteria.

Response to RAI EMEB-B-25

The actual Level 1 and 2 spectra to be used during Power Ascension for the steam dryer performance criteria have not yet been calculated. The spectra will be based on VYNPS main steam system pressure fluctuation measurement spectrum at CLTP, used as a component of the dryer load definition. The acceptance criteria is calculated based on the extrapolation of the CLTP spectrum by the margin of the limiting dryer component to the ASME stress limit, minus the uncertainty associated with FIV loads (see EMEB-B-143). The Level 1 and 2 steam dryer performance criteria spectra will be developed based on the factors described in Exhibit EMEB-B-143-1. These limit curves will be available at VYNPS for NRC review.

RAI EMEB-B-26

On Page 5 of Attachment 2 to Supplement 26, Entergy specifies 0.35% as the Level 1 performance criterion for moisture carryover. Discuss the basis for the selection of 0.35% as the Level 1 performance criterion for moisture carryover. If 0.35% moisture carryover represents indications of steam dryer damage, discuss the basis for allowing continued power ascension or operation.

Response to RAI EMEB-B-26

The square hood dryer design used at VYNPS was not optimized for moisture removal. The steam moisture content for this dryer design is typically in the 0.1-0.3% range. The criterion of 0.35% was selected based on moisture carryover predictions for potential core operating conditions at EPU. The moisture carryover is expected to remain below 0.35%; however, a value of 0.35% does not necessarily indicate steam dryer damage. If the moisture carryover exceeds 0.35%, activities would be initiated to eliminate the high probability causes for a high moisture carryover indication. For example, steam moisture content is dependent on core power, core flow and local core power peaking and is usually the cause of high moisture carryover. The moisture carryover predictions may be refined based on the actual core operating conditions in order to determine if local core conditions are exceeding the capability of the steam dryer to effectively remove the moisture. Steam moisture content is typically monitored by comparing the Na-24 concentration in the condenser hotwell to the concentration in the reactor water. Any reactor water reaching the condenser through paths other than the steamlines (e.g., through the reactor water cleanup system or through sample lines) will result in a moisture measurement that is higher than actual. Confirmatory samples would be taken after ensuring that these other paths were closed off. The trends of other reactor parameters (e.g., individual steamline flows, reactor water level, reactor pressure) would also be evaluated for anomalies that may indicate dryer degradation. Continued power ascension or operation would depend on the results and conclusions of these evaluations.

RAI EMEB-B-27

On Page 6 of Attachment 2 to Supplement 26, Entergy discusses data that will be collected during the power ascension for evaluation of steam dryer performance. Discuss the monitoring of additional plant parameters (such as MSL flow mismatch and loose parts noise) to identify degraded steam dryer conditions and the prompt action to be taken in response to adverse indications. Also, discuss the monitoring and walkdown inspections of plant equipment (other than the steam dryer) that could be impacted by increased flow-induced vibration (FIV) during EPU operations, such as main steam and feedwater system piping and components.

Response to RAI EMEB-B-27

Entergy's Steam Dryer Monitoring Plan (SDMP) specifies collection of data that are pertinent to the evaluation of the VYNPS dryer structural integrity during power ascension to EPU conditions. The parameters listed in the SDMP are consistent with the data collection recommendations of SIL 644 Revision 1. VYNPS does not have a loose parts monitoring system. The following is a complete listing of the parameters to be monitored at VYNPS during power ascension per SIL 644 Revision 1:

- Reactor power (MWt)
- Core flow (Mlb/hr)
- Core inlet subcooling (deg F)
- Reactor water level
- Individual main steam line flows (Mlb/hr)
- Individual main steam line pressures (venturi)
- Total feedwater flow (Mlb/hr)
- CRD flow

The first four parameters listed are discussed in SIL 644 Revision 1 Appendix D as affecting moisture carryover levels. The trend in measurements for these parameters would be used to assess changes in moisture carryover measurement trends. Changes in flow distribution between the four main steam lines may result if dryer damage occurs, according to SIL 644. As stated on

Page 6 of Supplement 26 Attachment 2, it is Entergy's intent to monitor plant parameters that may be influenced by steam dryer integrity, such as flow distribution between individual main steam lines. Similarly, changes in main steam line venturi differential pressures may be evident if moisture content changes resulting from a loss of dryer structural integrity. SIL 644 Revision 1 states that increased feed-to-steam mismatch (i.e., total feedwater flow plus CRD flow minus total steam flow, with reactor water level constant) may validate an increase in moisture carryover. Entergy would take action as a result of a changing trend in these parameter values only in conjunction with the Level 1 and Level 2 SDMP actions described in Attachment 2 to Supplement 26.

Entergy described the FIV monitoring and walkdown plan for feedwater and main steam systems in Supplement 15, BVY 04-100. The submittal contained details on piping and system component FIV monitoring, including acceptance criteria.

RAI EMEB-B-28

On Page 4 of Attachment 3 to Supplement 26, the Entergy contractor Continuum Dynamics Inc. (CDI) indicates that, because the steam velocity in the MSL is on the order of 200 ft/sec and the speed of sound in steam is approximately 1600 ft/sec, the flow Mach number is on the order of 0.1, and pressure oscillations, if they occur, are expected to be acoustic in nature. Note that this does not mean that the incompressible portion of the flow field plays no role in the oscillations but instead provides the source where mean flow energy is transferred into acoustic oscillations in the system. For structural loadings, however, the acoustic component to the overall pressure fluctuation is most significant. Specify which portion of the flow used in the formulation is considered incompressible. Provide all assumptions used throughout the report.

Response to RAI EMEB-B-28

In the acoustic circuit formulation the entire flow is assumed to be compressible.

The following assumptions are stated or implied in the acoustic circuit analysis methodology

- steam behaves isentropically and can be approximated as an ideal gas
- in the main steam lines the flow field is approximated by one dimensional, convective, compressible flow
- acoustic sources which may be present are compact
- the acoustic field in the steam dome is fully three dimensional, unsteady but convection by the mean flow is neglected
- fluctuating pressures are not so large that nonlinear effects are important
- the steam-water interface may be approximated as a partially reflective / partially absorptive surface
- frequencies are low so that acoustic wave lengths are long compared to transverse dimensions in the main steam lines

RAI EMEB-B-29

On Page 21 of Attachment 3 to Supplement 26, CDI indicates that the assumption of an out-of-phase vortex shedding in calculating the pressure resulted in non-physical results. Discuss those findings and the physical implications that were drawn from the stated mathematical results. CDI also indicates that the gusset splitter plate installed between adjacent steamlines had no affect on reducing dryer damage. Provide the technical basis for this conclusion.

Response to RAI EMEB-B-29

Since the time Attachment 3 to Supplement 26 was issued, sufficient independent data have been measured on main steam lines such that assumptions on source phasing are no longer necessary in application of the ACM. That being said, it can be shown that pressure pulses from the inlets of two steam lines on the same side of the dryer will result in the highest dryer load when the pulses are in phase. When the pulses are out of phase, the dryer load is at or near a minimum loading condition.

Exelon modified the original QC dryer by installing two gusset plates at the outer bank hood with the purpose of structurally strengthening the outer bank hood and with the potential benefit of straightening the flow entering the main steam lines. If sources exist in the steam lines that propagate up the main steam lines and load the dryer, the splitter plates/gussets between the steam lines will have no effect on dryer loads if the acoustic pulses are in phase. Alternately, if the pulses are out of phase, the splitter plate will actually raise the dryer load. By introducing a barrier between the inlets to the steam lines, cancellation of a pulsation from one inlet by the other is reduced or eliminated.

RAI EMEB-B-31

On Page 22 of Attachment 3 to Supplement 26, CDI compares results between the strain gauge data and predicted pressure associated with different instrument leg temperatures. Given that this step is intended to be a validation of the methodology, it seems more appropriate to predict the expected temperature based on a best estimate, rather than tabulating results using different temperatures. There will likely be a temperature which results in agreement, but if that temperature cannot be predicted accurately, then how does this represent a validation? Confirm whether the calculation requires varying the bulk acoustic speed in the instrument lines in the acoustic circuit analysis.

Response to RAI EMEB-B-31

At the time the transfer function model was developed it was believed that the venturi line temperature and hence acoustic speed in the venturi line would introduce large uncertainty into the venturi correction. Presently, the temperature of the lines is well known since it corresponds to the ambient temperature in the component where the line passes. The sensitivity of the corrections to this temperature is now determined to be of lesser importance. However, three acoustic speeds are used in the venturi correction. They are the acoustic speed of steam, the acoustic speed of water corresponding to the temperature in the drywell, and the acoustic speed in water corresponding to the reactor building in the area of the instruments based on VYNPS plant temperature data.

RAI EMEB-B-33

On Page 7 of Attachment 6 to Supplement 26, GE provides a summary of the computational fluid dynamics (CFD) analysis for the VYNPS steam dryer using large-scale eddy simulation (LES) to assess the turbulence and shedding. Provide the details of that analysis for NRC staff review. For example, confirm whether the CFD analysis was performed considering an incompressible flow and the eddies were assumed to have frequencies similar to those detected in the MSL piping by VYNPS instrumentation. Discuss how the CFD results were benchmarked. Also, provide a description of the model, methodology (computer code, version and year), assumptions, input values of key parameters, boundary conditions, and results.

Response to RAI EMEB-B-33

Entergy submitted details of the Phase 2 CFD analysis in a report prepared by Fluent that was provided in Supplement 29. The submittal contained description of the CFD model including features such as methodology, assumptions, input values, boundary conditions and results. The report explains that a compressible fluid was assumed in the LES model. The CFD model did not incorporate an assumption that the eddies had frequencies similar to VYNPS main steam line piping measurement data.

RAI EMEB-B-34

On Page 9 of Attachment 6 to Supplement 26, GE states that vortex pressures have a localized effect resulting in lateral bending loads on the steam dryer gussets. Discuss the consideration of these loads in the steam dryer analysis and modifications.

Response to RAI EMEB-B-34

Entergy employed the computational fluid dynamics (CFD) analysis to calculate hydrodynamic loads on the dryer. The vortex shedding unsteady forces in the plenum are included in the flow induced vibration stresses for each component of the modified steam dryer. The stresses from the hydrodynamic pressure loading were combined with the stresses calculated from the acoustic pressure loading for each component in the modified VYNPS steam dryer.
Therefore, the effects of lateral bending loads and other turbulent loads in the plenum have been included in the results provided. The local effect of vortex loads on the gussets is depicted in the CFD load summary.

RAI EMEB-B-35

On Page 11 of Attachment 6 to Supplement 26, GE states that weld quality factors were not applied in its analysis. Provide the basis for the exclusion of the consideration of weld strength in the stress analysis of the VYNPS steam dryer.

Response to RAI EMEB-B-35

The weld quality factors are relevant only in the evaluation of primary stresses. [[

]] Thus, the weld quality factors need not be used in the evaluation of primary stresses in the steam dryer stress analyses. The only observed failures in steam dryers were fatigue related. The alternating fatigue stresses in the evaluation are calculated using stress intensity or concentration factors that are consistent with the NG 'f' factors.

RAI EMEB-B-36

On Page 13 of Attachment 6 to Supplement 26, GE indicates that the seismic loads on VYNPS steam dryer are documented and unchanged for EPU conditions. Address the seismic evaluation impact on the internal structural response including the dryer and its support brackets due to the increase of the total dryer weight from the modifications.

Response to RAI EMEB-B-36

As discussed below, a seismic evaluation is not required. With the exception of the dryer assembly and the dryer support brackets on the RPV vessel wall, none of the existing RPV internals seismic responses will significantly change due to the modified dryer assembly increased weight of 2.6 kips. The added weight of the modification is 2.6 kips, in contrast to the weight of the dryer assembly, before modification, which was approximately 47.5 kips and the weight of the RPV vessel, with dryer assembly, which is of the order of 1,000 kips. Also, the load path for the modification added weight is through the dryer assembly, through the dryer support brackets on the RPV vessel wall, down through the RPV vessel wall and into the RPV skirt.

It then follows that the added weight of the repair will increase the vertical load on the vessel brackets by approximately 5.47%. The evaluation of the steam dryer support brackets was previously transmitted to the NRC in the Entergy response to RAI EMEB-B-10. In that evaluation of the RPV support brackets, a conservative weight of 60 kips was used for the modified steam dryer assembly.

The percent increase in the vertical load in the RPV skirt, due to the repair added weight, will be less than 0.25%. This increase is not significant considering that there is approximately 30% margin to the ASME stress limits for the RPV skirt at EPU conditions. Everywhere else in the RPV internals, the percentage change will be significantly less because the load path of the steam dryer modification added weight does not pass through those RPV internals components.

Applying the NRC Subsystem Decoupling Criteria[2], also corroborates this fact. Per Criterion (i) of the Decoupling Criteria pertaining to the mass ratio, if the modification added mass is less than 1% of the mass of the dryer assembly, plus the mass of the RPV vessel wall, the added mass of the repair can be neglected in the primary structure analysis. The VYNPS dryer modification meets this criterion. It then follows that seismic reanalysis of the VYNPS primary structure, due to the added mass associated with the steam dryer repair, is not required.

RAI EMEB-B-37

On page 15 of Attachment 6 to Supplement 26, GE indicates that, in final verification of the model and completed analysis cases, one node was found in the modified hood that was inappropriately constrained by the beam below. The node was corrected and a static case was run to assess the stiffness changes. The modified hood stress decreased as a result and the attached end plate stress increased. FIV stresses were scaled in these two components. Confirm whether this additional restraint at the hood changes the fundamental frequency of the analytical model.

Response to RAI EMEB-B-37

Modification of the node constraints has a very local effect on the stresses and only a very little effect on the natural frequencies that are integral characteristics of the system.

In order to investigate the effect of the constraint modification on the fundamental frequencies of the analytical model, ANSYS modal analysis was run on the model with modified constraints. Calculated frequencies have been subsequently compared with frequencies calculated for the original model before the alternation.

The model has 234 fundamental frequencies calculated in the range from 0 to 200 Hz. Only one of those frequencies has shown a deviation of 3% with respect of its original value. The average deviation calculated through the frequency range is 0.09%. This effect is negligible.

2 US NRC Subsystem Decoupling Criteria in Subsection II.3.b of US NRC Standard Review Plan (SRP) Section 3.7.2

RAI EMEB-B-38

On Page 15 of Attachment 6 to Supplement 26, GE states that the stress intensity was conservatively used as the acoustic contribution to the FIV stress amplitude. Explain the basis for this assumption.

Response to RAI EMEB-B-38

Stress intensity is a scalar non-negative parameter. By definition, the amplitude of the fluctuating fatigue stresses (which is then compared with the fatigue threshold stress) should be less than the calculated maximum stress intensity on a time scale. Therefore, the use of stress intensity to estimate fatigue alternating stress from acoustic loading is conservative and technically justified.

RAI EMEB-B-39

In Attachment 6 to Supplement 26, the modified dryer is shown in Figures 3.1-1 (Page 17) and 3.7.1 (Page 21) for CFD analysis and ANSYS analysis, respectively. The recent hammer test performed for a new steam dryer at Quad Cities indicated that significant coupling exists between the upper portion of the dryer and the skirt with pressure loading applied to the full dryer including the skirt. Confirm whether the full steam dryer model in the CFD and ANSYS analyses consists of both upper dryer banks, supporting ring, and the skirt. If the skirt is not included in the analysis, provide a justification.

Response to RAI EMEB-B-39

The ANSYS models for the VYNPS steam dryer analysis include the dryer support ring, dryer hoods, end plates, cover plates, upper dryer banks, cross beams, bottom support plates, tie bars and gussets The ANSYS model does not include the dryer skirt. Details of the ANSYS model were previously supplied in the response to RAI EMEB-B-1.

As discussed below, the VYNPS steam dryer upper structure is more likely to be dynamically isolated from the dryer skirt through the support ring. This is a result of the overall flexibility of the support ring structure with its cross bracing from the dryer support plates, and bottom beams. It is noted that the support ring construction for the VYNPS steam dryer is significantly different than that of the new steam dryer at Quad Cities. The support ring and cross beams in the VYNPS steam dryer are constructed of solid forgings, while the support ring and cross beams for the new steam dryer at Quad Cities are constructed of induction bent tube steel with much smaller section properties (bending stiffness about both major and minor axes and torsional rigidity about tangential axis). The reason for the difference in construction is that the support ring for the new steam dryer at Quad Cities serves a dual purpose for providing added dryer structural support and for providing part of the steam dryer moisture removal drain path.

The effect of the skirt on the natural frequencies of the front hood and the cover plate has been studied. The skirt provides additional stiffness to the dryer ring in the vertical direction. The gussets are welded on the cover plate and the front hood and supported at the dryer ring. If the skirt is included in the model, the gusset support stiffness at the dryer ring is significantly increased. The fundamental frequencies of the front hood and cover plate are increased commensurately. This is due to the fact that the skirt improves the structural effectiveness of the gusseted support of the cover.

Because the dryer skirt thickness is 0.25" and the dryer ring has a solid, rectangular cross section of 6" height by 3" wide and is stiffened by the cross beams, the horizontal modes of the skirt are isolated by the dryer ring. Consequently, in the horizontal direction, there is no significant dynamic interaction between the dryer skirt and the dryer cover plate and front hood.

Furthermore, there are no significant acoustic sources identified in the steam system at 100% CLTP. The transient loads from the CFD loads evaluation are hydrodynamic loads that have frequency content up to approximately 62 Hz. Entergy has run a load step uncertainty assessment for this CFD loading. This assessment demonstrated that stiffening the structure would reduce the stress. See EMEB-B-143-1 for further information.

The acoustic signals in the VYNPS steam lines are very low. The calculated acoustic loads that were projected on the dryer are driven by the noise floor of the instruments. The stress and model excitation from these loads is very low. The peak stress from acoustic loads is 1070 psi, less than 10% of the Code allowable. The mode shapes and stress PSD are presented in more detail in EMEB-110-4.

The Acoustic analysis was run for a +/- 10% load step uncertainty. The load identified by this sensitivity evaluation has been combined with other load uncertainties resulting in a 78% ACM load uncertainty in the limit factor evaluation. The major portion of this uncertainty is driven by the venturi signal input to ACA model; doubling the load step uncertainty would have only a small impact in the total uncertainty. Entergy has calculated a 580% margin to Code allowable and a 270% margin after applying load uncertainty. (See RAI EMEB-B-143.)

In summary, a stiffer model would reduce CFD stress and increase ACM stress. Entergy has considered a +/- 10% frequency uncertainty in the analysis. The VYNPS Level 1 and 2 power ascension performance spectra will be conservatively reduced to account for the ACM and CFD load uncertainty. Based on the factors described in Exhibit EMEB-B-143-1, the VYNPS performance spectra would require re-evaluation of the dryer at strain gage readings at a level equivalent to 10% of the PSD amplitude experienced by QC2. Further sensitivity analysis is not warranted until a discernable VYNPS acoustic signature is observed.

RAI EMEB-B-42

On Page 22 of Attachment 6 to Supplement 26, GE states that, with the exception of FIV stresses, the other stresses are calculated for EPU conditions. Explain the basis for this statement.

Response to RAI EMEB-B-42

In response to RAI EMEB-B-41, Entergy explained that an analysis of VYNPS steam dryer EPU loads has not yet been performed. This is a consequence of the fact that the acoustic circuit model relies on measured main steam system fluctuating pressure data as input. Any attempt to predict EPU measurements is subject to uncertainty due to the potential non-linear nature of hydrodynamic and acoustic loads resulting from increasing steam flow at EPU conditions. The dryer load definition methodologies are not designed to predict the frequency or amplitude of the potential resonant spikes at new levels of operation. There is currently no evidence of acoustic resonance detected by either the strain gages or accelerometers on main steam piping. GE calculated the other stresses for EPU based on predicted extrapolation of operating condition parameters.

Entergy has analyzed the dryer for the most limiting set of these loads, the 100% power loads. By performing an analysis under the 100% power condition we determine the margin of the dryer to ASME fatigue endurance limit and use this information to calculate an allowable margin. This margin is then used to adjust the observed steam line frequency domain data. This then becomes a performance curve for monitoring acoustic signals during power ascension testing. This methodology provides reasonable assurance that the code limits addressed in the GE report will not be exceeded under EPU operation

RAI EMEB-B-43

On Page 23 of Attachment 6 to Supplement 26, GE states that there is more than 20% margin for any American Society of Mechanical Engineers (ASME) Level A or B load combination. Discuss this amount of margin in comparison to the uncertainties in the acoustic circuit and CFD analyses used in calculating the maximum loads on the VYNPS steam dryer during EPU operation. Also, discuss the potential for a pin-hole size break in the steam dryer outer hood face and the impact on steam dryer integrity from hydrodynamic forces due to steam flow being diverted through that hole.

Response to RAI EMEB-B-43

In Exhibit EMEB-B-143-1 Entergy addresses the uncertainties of acoustic circuit and CFD analysis loads. The ASME Code tables and FIV tables have been updated for revised 100% power CFD loads and new 120% power CFD loads. The minimum dryer margin in comparison to ASME limits, with consideration of load uncertainty, is addressed.

Concerning the second part of the RAI, i.e., the potential for a pin-hole size break in the dryer outer hood face, the Attachment 6 to Supplement 26 analysis of the VYNPS modified steam dyer demonstrates that there are large margins to both the ASME flow induced vibration acceptance criteria and the ASME Code Section III acceptance criteria at CLTP conditions. The Entergy power ascension test program will demonstrate that the dryer is also within the acceptance criteria at EPU steam flow conditions. Since the steam dryer will be demonstrated acceptable for EPU conditions, the possibility for any break or crack in the VYNPS steam dryer outer hood is negligible.

The differential pressure is less than 2.5 psid for normal operation and less than 7 psid during the main steam line break. Therefore, the impact of local flow forces from a pin-hole leak would be negligibly small in comparison with hydrodynamic and acoustic forces calculated as part the dryer stress analysis.

RAI EMEB-B-44

On Page 23 of Attachment 6 to Supplement 26, GE states that the finite element analysis for FIV stresses is a linear analysis. Provide the basis for this approach in light of the GE SMT results that reveal different excited frequencies appearing as the flow increases.

Response to RAI EMEB-B-44

Statement on Page 23 of Attachment 6 to Supplement 26 has been made only in connection to using linear elasticity as the analytical tool. Stresses and deformations stay under the endurance limits (no crack initiation and propagation occurs) and under the range that corresponds to non-linear deformations. This initial assumption has been shown by the calculations to be true.

No assumptions of linear dependency on any other parameter (e.g. flow rate) have been made in the report.

Entergy will monitor the change in acoustic loads in the steam lines during power ascension testing to identify if any non-linear acoustic spikes occur.

RAI EMEB-B-45

On Pages 12 and 13 of Attachment 7 to Supplement 26, Figures 3a and 3b show the power spectral density from the VYNPS MSL strain gauges at 100% power ranging up to about 0.2 pounds per square inch differential squared per Hertz (psid^2/Hz). On Pages 17 and 18 of Attachment 7, Figures 5a and 5b show the power spectral density from the VYNPS MSL venturi instrumentation ranging up to about 4 psid^2/Hz. Discuss the basis and significance of the difference in these two determinations of power spectral density.

Response to RAI EMEB-B-45

The important difference in the PSD's for the strain gage data and the corrected venturi pressure data is at or near 10 Hz. Above 20 Hz, the strain gage data has a noise floor of about 10^{-2} psid^2/Hz and the corrected venturi data for the most part is at or below this value. At or about 10 Hz, it is suspected that the pressure has or is near a loop at the venturi line and is at or near a node at the strain gage. Note that acoustic ¼ wave lengths are about 40 feet at 10 Hz. Note the increase in venturi pressures above 160 Hz where main steam line turbulence is being sensed by the venturi transducer.

Furthermore, the uncertainty in pressures obtained from the venturis is larger as described in Exhibit EMEB-B-18-1, which supports the fact that pressures obtained from venturi measurements appear larger than those obtained from strain gages.

RAI EMEB-B-46

On Pages 14 and 15 of Attachment 7 to Supplement 26, Figures 4a and 4b show power spectral density (psid²/Hz) versus frequency measured by strain gauges on each of the four MSLs at VYNPS for 80%, 90%, and 100% power levels. The plots indicate that power spectral density measured by the MSL strain gauges at specific frequencies does not vary linearly with power level. See, for example, (a) the MSL A strain gauge plot in Figure 4a which shows the highest power spectral density for 55 Hz to occur at 90% power; (b) the MSL B strain gauge plot in Figure 4a which shows the power spectral density for 10 Hz to be about equal at 80% and 90% power but to increase significantly at 100% power; (c) the MSL C strain gauge plot in Figure 4b which shows the power spectral density for 170 Hz to be about equal at 80% and 90% power but to decrease significantly at 100% power; and (d) the MSL D strain gauge plot which shows a power spectral density peak for 135 Hz at 100% power that does not appear at 80% and 90% power. Explain the consideration of nonlinearity of the strain gauge data in applying the acoustic circuit model and the GE SMT results to EPU conditions.

Response to RAI EMEB-B-46

Entergy and our contractors have looked at the strain gage and accelerometer signals at various power levels between 80 and 100% power. The data indicates that the signal amplitude has been predictably increasing with power. The exceptions cited by this RAI are valid points but very minor. The figures noted are log plots and much of this data is at the strain data acquisition noise floor.

The main steam line "A" strain gage plot in Figure 4a, which shows the highest power spectral density for 55 Hz, occurs at 90% power. The AC noise at 60 Hz was filtered from the signals. The 60 Hz filter resulted in some leakage into adjacent frequencies. Refined filtering of the AC noise was performed to maintain integrity of the data used in the 100% load definition. Signals of this magnitude ~.01 psid^2/Hz have negligible impact on the dryer load.

Main steam line "B" strain shows the power spectral density for 10 Hz to be about equal at 80% and 90% power but to increase at 100% power. This data was analyzed as a 2 Hz frequency bin and that depiction demonstrates that the power is changing very gradually. The PSD data cited is at a narrow frequency bin. The difference is 0.02 psi^2/Hz. Converting to Strain; 1/((3.902psi/ue)^2 x .02 .02 psi^2/Hz = 0.001 ue^2/Hz. The EPU data at QC1 and QC2 indicates strain gage readings at 1.0 ue^2/Hz. Therefore the changes cited in the strain gage plots are not significant.

On main steam line "C" strain gage plot at 170 Hz, the signal is at the noise floor. There is electrical noise from the reactor recirculation system that was filtered out at 170 Hz. The recirculation pump speed and associated electric noise is different for the three cases. The main steam line "D" strain gage plot shows a PSD peak less then 0.02 psi^2/Hz that leaked out of the recirculation pump electric noise filter at that frequency. In conclusion, 0.02 psi^2/Hz has an insignificant impact on the dryer load.

RAI EMEB-B-47

On Page 27 of Attachment 7 to Supplement 26, Figure 10 compares the power spectral density at 80%, 90%, and 100% power at the peak load locations on the A-B and C-D sides of the VYNPS steam dryer as determined by the acoustic circuit analysis. Discuss the consideration of nonlinearity in the change in steam dryer loading with power level, and the appearance of load peaks at specific frequencies at 100% power that did not appear at lower power levels (see, for example, 165 Hz on the A-B dryer side, and 145 and 185 Hz on the C-D dryer side).

Response to RAI EMEB-B-47

These dryer PSD values are 0.0001 psi^2/Hz at the 145 and 165 Hz frequencies, and 0.0003 psi^2/Hz at 185 Hz. The dryer data at QC2 at 790 MWe shows PSD's at approximately 0.01 psi^2/Hz, or ~30 to 100 times higher than the changes cited in the VYNPS data. The frequencies in question do not appear in the VYNPS strain gage data. Therefore it is expected that these changes at VYNPS are due to local turbulence near the venturi taps. Any growth of these points during power ascension due to an acoustic resonance will be identified by the VYNPS power ascension testing monitoring program before there would be a challenge to dryer integrity.

RAI EMEB-B-48

On Page 29 of Attachment 7 to Supplement 26, CDI compares the calculated steam dryer loads for Dresden Unit 2 and VYNPS. CDI indicates that, at 100% OLTP, the maximum pressure loads on the steam dryer in VYNPS are calculated to be 0.730 of the predicted loads in Dresden Unit 2. In light of the Dresden Unit 2 steam dryer loads under EPU conditions being sufficient to cause cracking that was identified during inspections of the original steam dryer in October 2003 and modified steam dryer in November 2004, discuss the potential for, and consequences of, the VYNPS steam dryer loads reaching or exceeding the Dresden Unit 2 loads at EPU conditions in light of the uncertainty range of the acoustic circuit analysis and the possibility of additional excited frequencies above OLTP conditions.

Response to RAI EMEB-B-48

All evidence is that VY loads are turbulent buffeting and should scale as a function of steam flow squared. If VYNPS proceeds to delta power (Δp) computed from $0.73(1 + \Delta p)^2 = 1$, or Δ p of about 17%, the loads should be comparable. However, the data analyzed to date does not show a load increase as power squared for VYNPS. The modified VYNPS dryer has incorporated improvements that were not present in the Dresden dryers that were damaged by FIV loads.

RAI EMEB-B-50

On Pages 30 and 31 of Attachment 7 to Supplement 26, Figures 12a and 12b show the power spectral density of the MSL strain gauges in VYNPS is higher than in Dresden Unit 2 for a large portion of the frequency spectra. On page 32, Figure 13 shows the maximum differential pressure and root mean square (RMS) pressure at the nodes on the steam dryer being lower in VYNPS at 100% power than in Dresden Unit 2 at pre-EPU and EPU power levels. Discuss the basis for the higher power spectral density and the lower pressure calculations for the steam dryer in VYNPS compared to the steam dryer in Dresden Unit 2.

Response to RAI EMEB-B-50

The VYNPS PSD is higher than the Dresden 2 (D2) data up to 20 Hz. Based on an assessment of the D2 data, this may be due to the high pass filter frequency used at D2. This frequency range portion of the VYNPS signal had little impact on the dryer loads. Entergy applies CFD loads to the VYNPS dryer load definition at < 20 Hz to capture the affect of turbulent buffeting at this low frequency region. The D2 data is then higher from 25 Hz through 60 Hz. Above 50Hz the VYNPS signal is at the noise floor of the data acquisition system [DAS]. It appears that the D2 DAS has a lower noise floor. The VY noise floor of .01 psid^2 is a very small pressure but it does result in additional projected ACA load that is applied in the structural analysis.

RAI EMEB-B-51

On Page 35 of Attachment 7 to Supplement 26, CDI states that the use of venturi instrumentation results in a conservatism that tends to increase with steam dryer loads. Discuss the basis for using venturi instrumentation that diverges from the actual results as the steam dryer loads increase.

Response to RAI EMEB-B-51

It is believed that improvements to the venturi correction model are over-correcting at higher frequencies (greater than 150 Hz) and this signal is really main steam line pipe turbulence that is then being transferred to a dryer loading as if it were of acoustic origin. Based on CDI experience, the effect of local turbulence will increase the projected load on the dryer. It is expected that the

MSL turbulence generated in the MSL boundary layer would dissipate quickly. This is supported by the fact that the signals do not appear at the strain gage sensing location. With the acoustic methodology, a conservative impact of the loads on the dyer is seen.

RAI EMEB-B-72

With regard to Section 3.1.1 of Attachment 6 to Supplement No. 26 (GE-NE-0000-0038-0936NP), the pressure data from the acoustic circuit analysis (ACA) prediction was translated to ANSYS load vectors for calculation of stresses due to acoustic loading. The translation was checked at key locations in the dryer and GE found that the load vectors were either exact matches or that the ANSYS values were conservative. Identify the conservative load vector and confirm whether and how frequency and phasing were preserved during translation.

Response to RAI EMEB-B-72

For a typical and representative location that does not show exact match between ANSYS input and benchmark, ANSYS and benchmark pressure time histories are plotted on Figure EMEB-B-72-1. On the graph, it is visual, and apparent, that ANSYS data correspond to the higher pressures. It is noted that the amplitude of the applied ANSYS pressure is significantly higher than the ACM pressure and therefore the phasing of the ACA pressure is insignificant.

In addition, Figure EMEB-B-72-2 shows Power Spectral Densities (PSD) obtained from the pressure data by Fast Fourier Transformation for both ANSYS data and the benchmark. ANSYS data PSD envelopes benchmark PSD in the whole 0 to 200 Hz range of frequencies used in the analysis. Therefore, load vector data used in the analysis is conservative.

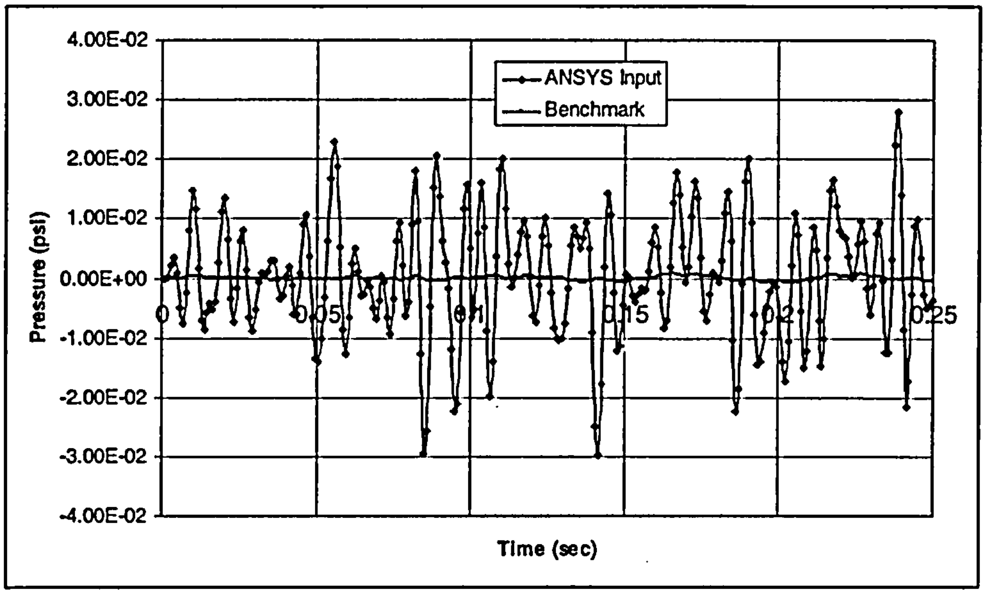

Figure EMEB-B-72-1. Pressure Time Histories Used in the Analysis

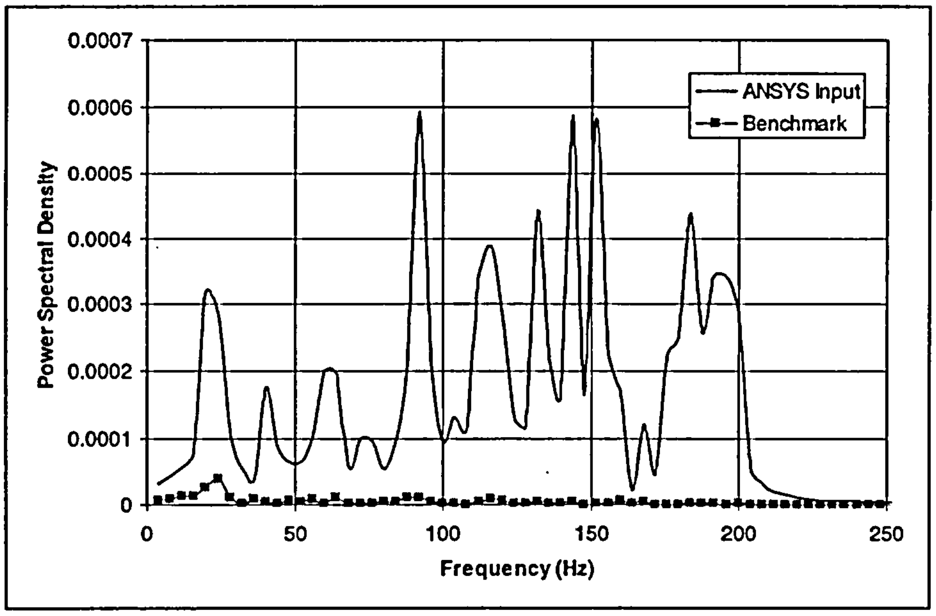

Figure EMEB-B-72-2. Power Spectral Density of Data Used in the Analysis

RAI EMEB-B-74

With regard to Section 3.1.2 of Attachment 6 to Supplement No. 26, Entergy should evaluate and submit the potential for the interaction of vortex shedding off the face of the dryer and the steam system acoustic modes. The evaluation should be based on an assessment of significant acoustic modes of the MSLs and dome contributing to pressure fluctuations on the steam dryer.

Response to RAI EMEB-B-74

The model developed by Fluent to evaluate VYNPS CFD loads was not designed to assess the potential for interaction between hydrodynamic forces and system acoustic characteristics. Accurate predictions of the propagation of pressure waves can be obtained if the time step is chosen such that the Courant number based on the speed of sound is close to unity. The time step chosen for the VYNPS CFD model was based on the fluid flow velocity rather than the speed of sound. The selected time step is about 10 times larger than required for tracking sound waves. With a large time step pressure waves are propagating at the speed of sound. However, a sharp pressure front could be diffused and attenuated with distance from its origin. The large time step relative to acoustic phenomena could have a damping effect on any acoustic signal.
An assessment of the steam dome acoustic modes was performed in response to RAI EMEB-B-142. The results show that the dome and the gap around the skirt interact to form an acoustic mode at 32Hz oscillating in the vertical direction. Additionally, a 45.5 Hz and 62.2Hz mode oscillates from one plenum to the opposite plenum. The assessment indicates that there is a modal component that moves circumferentially in the gap around the dryer.

RAI EMEB-B-76

In reference to Section 6.3.4 of NEDC-33192P, it shows that some MSL and steam dome modes are strongly coupled. Entergy should explain whether any considerations have been given to amplification of surface pressures on the dryer, by the coincident coupling of MSL sources and system acoustic modes.

Response to RAI EMEB-B-76

The strong coupling in a model test, where a highly absorptive steam water interface does not exist and dryer vanes and separators (which have high acoustic losses) are neglected, does not mean that the steam dome will couple strongly to the main steam lines. This is particularly true at VYNPS where the entire dryer load at CLTP appears to be turbulent rumbling which does not excite any discrete frequency oscillation that manifests itself in main steam system oscillations.

RAI EMEB-B-77

The Executive Summary of NEDC-33192P (Conclusions 8 - 10 for Plant Data and Conclusion 2 for SMT) mentions that existing data from VYNPS MSL strain gauges and venturi lines show no evidence of any "singing" in downstream valves. In other BWR-3 plants, and in the GE SMT data, singing in valves has been observed, and can lead to high acoustic pressure loads on the steam dryer. Entergy should explain whether there is a potential of acoustic pressure loads (on the dryer) induced by valve singing between pre-EPU and EPU conditions, and provide any estimates of valve singing frequencies (with respect to power level).

Response to RAI EMEB-B-77

Entergy evaluated the potential acoustic source frequencies in the VYNPS main steam lines by estimating the natural frequencies of known cavities and the shear wave instabilities caused by steam flow over the cavity openings. The cavity is excited and acts as a resonator when its natural frequency is matched by the frequency of the shear wave instability.

In order for a main steam relief valve standpipe resonance to generate an acoustic pressure loading on the steam dryer between pre-EPU and EPU conditions, a resonance must first be excited in the standpipe at the pre-EPU to EPU main steam line flow conditions and the valve must be acoustically coupled through the steam line to an acoustic mode shape within the vessel steam dome. The excitation of a resonance in the standpipe depends on the quarter wave resonance frequency (determined by the length of the standpipe and valve cavity), the diameter of the standpipe, and the velocity of the steam flow past the standpipe. The acoustic coupling between the valve and the vessel is dependent on the frequency of the valve resonance, the acoustic characteristics of the main steam line and the vessel, and the location of the valve along the main steam line. Not all relief valve resonances couple with the main steam system and produce acoustic pressure loads on the dryer. This coupling cannot be predicted using the currently available analytical methods and must be identified experimentally or by monitoring the plant response.

The VYNPS cavities of interest in the main steam lines are those that resemble "organ pipe" type geometries, including the HPCI and RCIC branch lines and SRV/SSV stub pipes and valve body cavity. The fundamental resonance frequencies of these cavities are calculated to be:

Cavity	Resonant Frequency (HZ)
HPCI	6.4
RCIC	10.5
SSV	165
SRV	185

The natural frequency of these potential resonators is a function of the speed of sound in the fluid and their geometry. These frequencies do not change as a function of changing fluid flow rates. The frequency of vortices generated by fluid flow over these cavities is proportional to the fluid velocity and therefore changes as a function of flow rate. Entergy's evaluation assumed sharp edges at the cavity entrance. The VYNPS installed SRV's and RCIC branch lines have a rounded edge Sweepolet providing a smoother transition which reduces the vortex shedding amplitude and broadens the frequency peaks. Similarly, the HPCI branch line connection consists of a welding tee also providing a smoother transition.

Results of the evaluation indicate that at the rated CLTP steam flow rate, the SRV stub pipes may potentially be excited at a shedding frequency of 187 Hz. HPCI cavity excitation may occur at 45 Hz, 97 Hz and 162 Hz. Excitation of the RCIC branch line could occur at 158 Hz. The SSV's natural frequency does not match the projected vortex shedding frequency. The VYNPS main steam strain gage and accelerometer data shows no evidence that these cavities are being excited at CLTP. At EPU steam flow rate, results indicate that neither SRV's nor SSV's should be excited. HPCI may be excited at 50 Hz, 120 Hz and 190Hz. RCIC may be excited at 190 Hz.

RAI EMEB-B-78

On Page 7 of Attachment 1 to Supplement No. 26, Entergy discusses measurement of MSL strains using strain gauges. Entergy should provide a justification that its measurement system can separate the dynamic acoustic pressure strains from those caused by the flow noise and the pipe vibrations. In particular, Entergy should provide estimates of the extraneous flow noise in the MSL, the frequencies of the MSL piping breathing mode and the lower frequency in-plane and out-of-plane bending modes, and the contribution of the extraneous in-plane bending mode strains to the hoop strain.

Response to RAI EMEB-B-78

At very low strain levels data from QC2 has demonstrated that the dynamic signal can vary azimuthally around the pipe. VY has two strain gages orientated in the hoop direction at one azimuth location. Data from Q2 with four strain gages 90 degrees apart, demonstrates that when there are high FIV signals the local pipe distortion can add significant content to the signal. Entergy has evaluated this data and assessed the additional signal introduced by this measurement method. This has been factored into the acoustic circuit model uncertainty assessment included as Exhibit EMEB-B-18-1.

RAI EMEB-B-80

In Attachment 7 to Supplement No. 26 (CDI Technical Memorandum No. 05-06), the MSL strain gauge time signals were shifted for each power condition based on a common reference (the leg A venturi line). Table 1 on page 4 provides a list of the time offsets applied to the strain gauge data. Entergy should provide examples of how the time shifts synchronize the strain gauge and venturi line data. The examples should include time correlation and/or frequency coherence functions showing how the time offsets were chosen.

Response to RAI EMEB-B-80

The signal from the venturi pressure transducer on the "A" main steam line was fed to both the strain gage data acquisition system as well as the pressure transducer data acquisition system. CDI found the offset of the start of the two data acquisition systems and plotted the data. Accurate alignment of the data demonstrates that the CDI offset was calculated correctly. Information from the CDI calculation file is included as Exhibit EMEB-B-80-1.

RAI EMEB-B-81

In Attachment 7 to Supplement No. 26, page 5 states that the MSL strain gauge data was filtered to reject signals associated with electrical noise and those associated with the recirculation pump vane passage frequency and its harmonics. Entergy should provide a list of the pump harmonics, along with an explanation of why the pump acoustic signals are not considered to be sources of steam dryer excitation. Also, Entergy should provide examples comparing the unfiltered and filtered MSL data to clearly show the filtering effects.

Response to RAI EMEB-B-81

The AC noise was filtered at 60, 120 and 180 Hz. The pump electrical noise was filtered at the following frequencies for the July 9th data used for the ACM input:

100%	Case:	56 Hz	168.25 Hz.
90%	Case	47.3 Hz	142 Hz.
80%	Case	36.25 Hz	109 Hz

Entergy reviewed additional acquired data sets to confirm the observed spikes in the data were from electrical interference. Figure EMEB-B-81-1 is a sample of the data from the "A" main steam line strain gage. The power is off to the Wheatstone bridge. This provides a measure of electrical noise. The reactor recirculation pump was at a different speed for this test. Pump noise is shown as 45.25 Hz 1X and 135.75 Hz 3X for the power off test below. The AC noise at 60 Hz and 180 Hz noise can also be noted.

Figures EMEB-B-81-2 and EMEB-B-81-3 provide examples comparing the unfiltered and filtered main steam line strain gage data to graphically demonstrate the filtering effects.

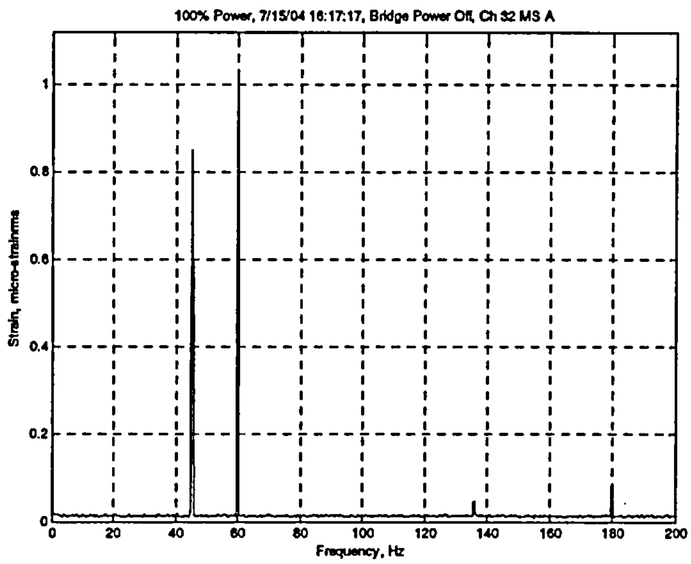

Figure EMEB-B-81-1: VYNPS "A" Main Steam Line Unfiltered Strain Gage Data 100% Power

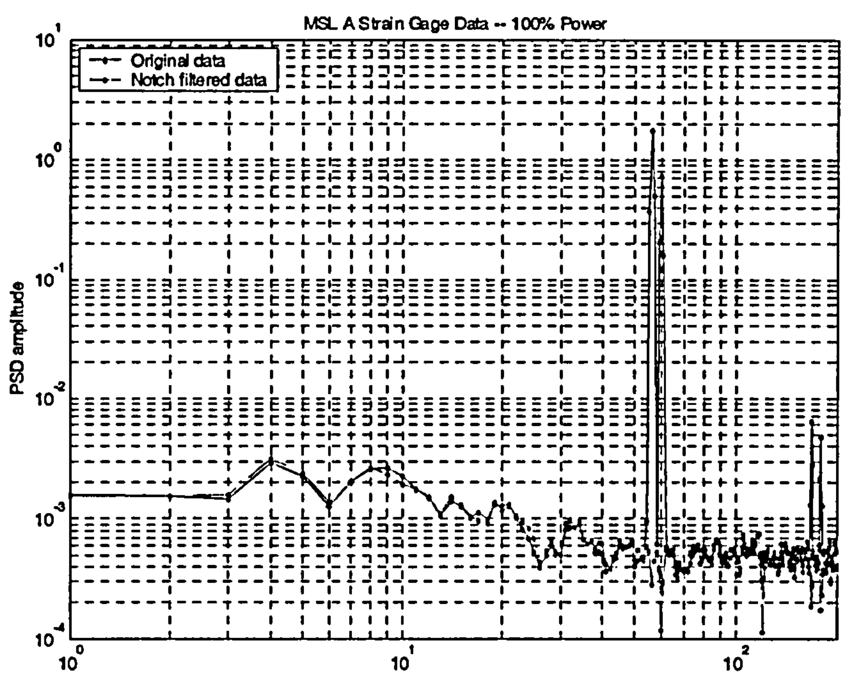

Figure EMEB-B-81-2: VYNPS Main Steam Line "A" Strain Gage Data 100% Power, Filtered and Unfiltered

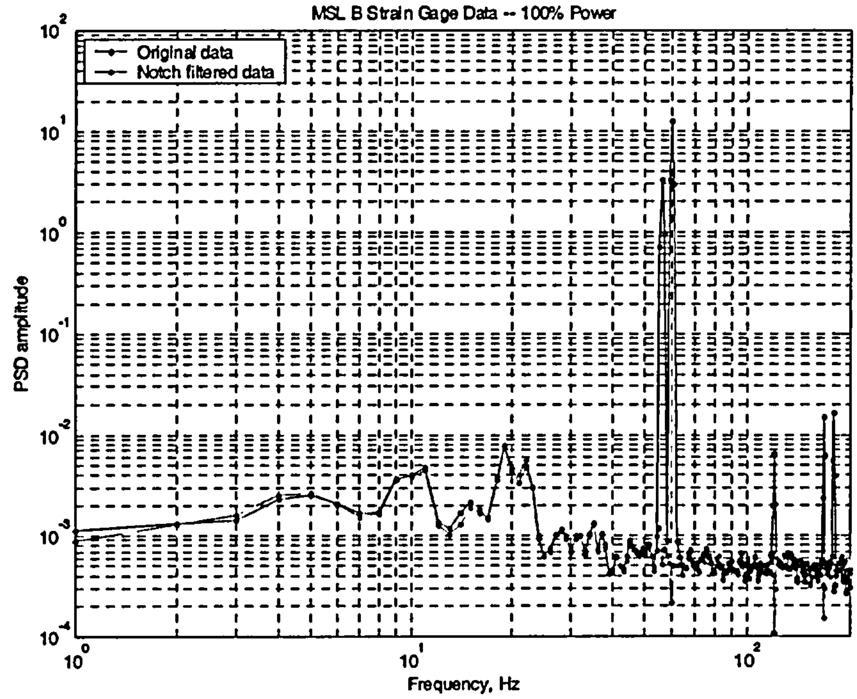

Figure EMEB-B-81-3: VYNPS Main Steam Line "B" Strain Gage Data 100% Power, Filtered and Unfiltered

RAI EMEB-B-82

Based on the compliance modeling of the venturi lines, an ACA of each line was performed to correct the fluctuating pressures measured at the ends of the line to those within the MSL fluid. CDI provides plots (Figures 2a and 2b on pages 10 and 11 of Attachment 7 to Supplement No. 26) of the four venturi line transfer functions and their variability with compliance. As compliance increases, the peaks and dips in the transfer functions become less pronounced. In later plots of venturi line pressure spectra, several low frequency pressure peaks coincide with transfer function peaks (10, 21, and 36 Hz), making the compliance a key variable in the ACA analysis. It is not apparent which compliance was actually applied to correct the venturi line data. Entergy should explain the application of a specific compliance for correcting the venturi line data.

Response to RAI EMEB-B-82

The transfer function denoted "Full Compliance" was the manufacturer published compliance for the instrument. This was the value used to correct the venturi line data. The uncertainty of compliance and other transfer function uncertainty issues are addressed in Exhibit EMEB-B-18-1.

RAI EMEB-B-83

MSL pressures inferred from strain gauge measurements (using calibrations documented on page 7 of Attachment 7 to Supplement No. 26), and MSL pressures, corrected from venturi line measurements, are plotted as PSD functions at 80, 90, and 100% power in Figures 3 - 6 on pages 12 - 20 of Attachment 7 to Supplement No. 26. At low frequency peaks (near 10, 21, and 36 Hz), the pressure levels in the venturi line spectra are consistently higher (2 - 3 psid^2/Hz) than those in the strain gauge data (0.06 - 0.16 psid^2/Hz). Entergy should explain why the strain gauge and venturi signals, which are closely spaced with respect to an acoustic wavelength, are so different at frequencies below 40 Hz.

Response to RAI EMEB-B-83

Below 40 Hz acoustic wave lengths are greater than 40 ft and ¼ wave lengths are greater than 10 ft. Each ¼ wave length has a pressure loop on one end and a node at the other. The distance between the strain gages and the venturi is approximately 40 feet so that nodes and loops can exist at the measured positions. See response to RAI EMEB-B-18 for additional information pertaining to the uncertainty associated with strain gage and venturi line measurements.

RAI EMEB-B-84

At frequencies above 50 Hz, the pressure spectra inferred from the MSL strain gauges are constant at about 0.008 psid^2/Hz (as shown on Figures 3 and 4 on pages 12 - 15 of Attachment 7 to Supplement No. 26), indicating a noise floor in the gauges (no actual pressure signal with amplitude lower than the noise floor can be measured). However, the corrected venturi data show peaks with amplitudes ranging from 0.1 to 1 psid^2/Hz at several frequencies above 50 Hz (see Figures 5 and 6 on pages 17-20 of Attachment 7 to Supplement No. 26). Entergy states that including the high frequency peaks in the venturi line data in their ACA analysis adds conservatism to the loads. However, if the venturi line transfer functions incorrectly add peaks to the pressure signals, they can also (and very likely do) remove peaks from the pressure signals (the transfer functions shown in Figure 2 contain many peaks and dips, which lower and increase the corrected pressure signal, respectively). Entergy should explain why a conservative lower bound on the transfer functions between 0 and 200 Hz (perhaps set to 0.1, which will uniformly increase the pressure signals input to the ACA) was not used.

Response to RAI EMEB-B-84

No predicted load on the dryer exceeds 10^{-4}psid^2/Hz over the 200 Hz frequency range, which corresponds to a RMS pressure less than 0.15 psid. The transfer function at higher frequencies is believed to be transferring noise to the MSL at the venturi location. The suggestion of setting a lower bound on the transfer function was not used but the uncertainty in transfer function is accounted for in the error analysis of the venturi line correction.

RAI EMEB-B-85

On page 9 of Attachment 7 to Supplement 26 it states, "For the most part, above 50 Hz, the strain gage data are at or below their noise floor. It appears that the primary loading of the [VYNPS] dryer will result from loads which have frequency content below 50 Hz." Entergy should explain why the venturi pressures, which are increasing with frequency above 100 Hz (see Figures 6a - 6d), do not contribute to the primary loading on the dryer. Entergy should discuss the sensitivity of the dryer loading to the MSL strain gauge data and venturi pressure data.

Response to RAI EMEB-B-85

The PSDs of the VY dryer load at max loading locations Figure 10 Attachment 7 to Supplement 26 averages 10^{-5} psid^2/Hz. Integrating over 0-200 Hz and taking the square root yields an RMS pressure of 0.05 psid. It would appear that these loads result from noise or random turbulence which, when transferred to the dryer by the ACM, cancel and result in small dryer loadings. VY has used CFD loads to calculate the turbulence loads on the dryer.

RAI EMEB-B-88

Entergy should provide schematics of the steam dome, dryer cavities and MSL including the key dimensions of the analysis to facilitate the review of Attachment 7 to Supplement No. 26.

Response to RAI EMEB-B-88

The figure and table below provide the key dimensions of the VYNPS acoustic circuit model.

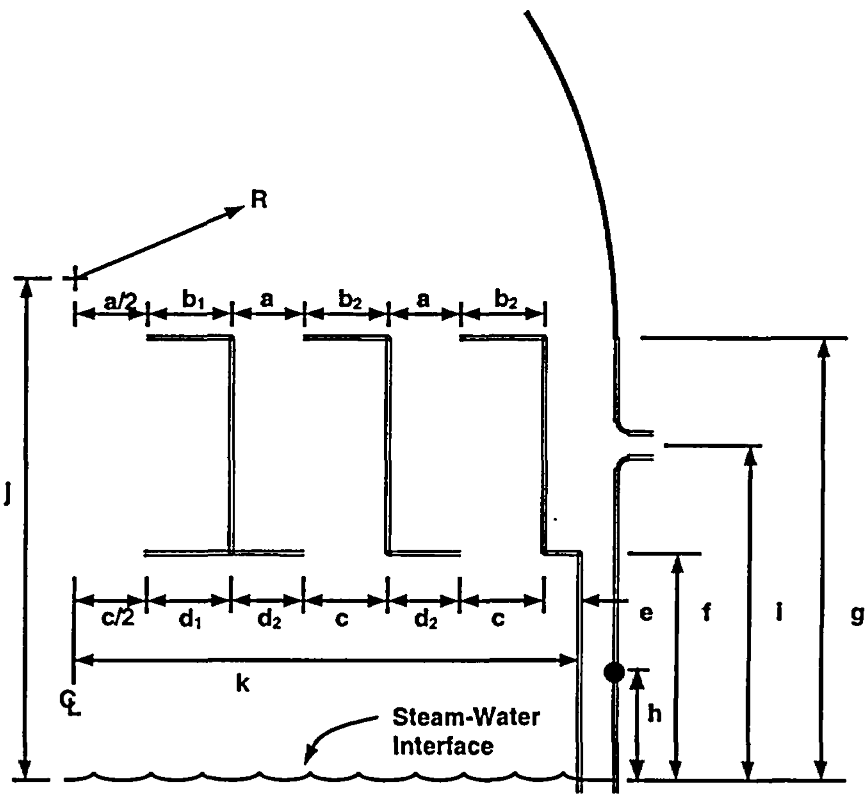

Cross-sectional description of the steam dome and dryer, with the dimensions a = 6.0 in, b_1 = 13.75 in, b_2 = 27.5 in, c = 18.0 in, d_1 = 7.75 in, d_2 = 15.5 in, e = 16.75 in, f = 75.5 in, g = 137.0 in, h = 35.5 in (reference legs), i = 88.5 in, j = 148.5 in, k = 100.5 in, and R = 102.5 in.

Table of Strain Gage and Venturi Locations on the Main Steam Lines from the Vermont Yankee Steam Dome

	MSL A	MSL B	MSL C	MSL D
Strain Gage Location (ft)	37.13	37.13	37.13	37.13
Venturi Line Entrance (ft)	96.84	80.88	80.88	96.84

RAI EMEB-B-89

Attachment 3 to Supplement No. 26 (CDI Report No. 04-09P, Revision 6), CDI asserts on page 4, based on Mach number and Strouhal number, that the possibility of significant direct hydrodynamic loading on the steam dryer can be rejected. The acoustic pressure is proportional to fluctuating particle velocity, while the hydrodynamic pressure is proportional to steady flow velocity. Therefore, it is doubtful that the two velocities would cancel in the manner suggested. Also, other parameters will affect the ratio of acoustic to hydrodynamic excitation significantly. The argument does support the importance of acoustic excitation, but does not conclusively discount hydrodynamic excitation. Entergy should address these points.

Response to RAI EMEB-B-89

Both acoustic and hydrodynamic loads are proportional to the fluctuating velocity. The proportionality constants are

ρa – for the acoustic pressure
ρU – for the hydrodynamic pressure

where ρ – mean steam density
a – acoustic speed in steam
U – mean steam velocity

The ratio of these proportionality constants are

$$\frac{hydro}{acoustic} \sim \frac{U}{a} < 0.1$$

If no acoustic excitation is observed, the only remaining unsteady loading is hydrodynamic. The hydrodynamic loads are however low and are of the order of tenths of a psid.

RAI EMEB-B-90

In Section 4.1 of Attachment 3 to Supplement No. 26, the acoustic cavity within the steam dome is assumed to have rigid boundary conditions at the walls of the dome and at the walls of the steam dryer. At the interface between the steam cavity and the water level surface, the normal pressure gradient is assumed to be proportional to the pressure itself via the ratio i*ω / a (as shown on page 10). The steam dome cavity is apparently assumed to be a system without losses. Entergy should define the steam dome cavity modeling further, specifically:

a) What is the basis for ignoring motion of the steam dryer walls in the steam cavity model? Are the walls assumed to be rigid? At steam dryer structural resonance conditions, how would the high amplitude motion of the walls affect the loading throughout the steam dryer?

b) What is the constant 'a' relating the pressure and pressure gradient at the water surface, the speed of sound in the steam or water? Also, what is the basis for selecting this boundary condition? How sensitive are the inferred loads to this choice of boundary condition?

c) What is the basis for assuming a "lossless" steam cavity? If losses were included in the steam cavity model, how would the steam dryer loads change? How sensitive are the inferred loads to the cavity loss coefficient?

Response to RAI EMEB-B-90

a) By neglecting steam dryer wall motion, the loads computed by the acoustic circuit methodology are rigid wall loads. In principle, the structural analysis could compute motion applying rigid wall loads and then compute the change in load that would occur as the structure is moved. By comparing the rigid load with the load which results as a consequence of dryer motion, the effect of FSI could be assessed. This assessment has not been carried out, as computed stresses are very low indicating low structural deflection which is indicative of low fluid structural interactions.

b) **CDI Proprietary Information**

CDI Proprietary Information

c) **CDI Proprietary Information**

CDI Proprietary Information

RAI EMEB-B-91

[[

]] Other reports, such as Fluent report TM-675, "CFD Modeling of the Vermont Yankee Steam Dryer," Section 4 (reference Attachment 1 to Supplement No. 29), and GE report NEDC-33191P, Revision 1, "Computational Fluid Dynamics Flow Visualization of Quad Cities Sub-scale Original Dryer Model As a Function of Reynolds Number," page 8-1 (reference Enclosure 1, Attachment 5 to Exelon letter RS-05-059, dated May 6, 2005), show strong evidence that the high-energy fluctuating vortices entering the MSLs are actually coherent over long distances, extending from the MSL inlets back to the steam dryers. [[

]]

Response to RAI EMEB-B-91

This response contains material proprietary to CDI

This response contains material proprietary to CDI

RAI EMEB-B-92

Entergy should provide a detailed description of how the acoustic circuit analysis model considered in Attachment 3 to Supplement No. 26 is assembled and solved at each time step, along with documentation of any quality assurance processes that:

a) Establish that no numerical transient effects are corrupting the analysis. Is the accuracy of the computations dependent on initial conditions? If so, how many time steps are required before accurate solutions are obtained? Alternatively, are the input time signals adjusted to gradually "ramp up" their amplitudes to avoid numerical transients that corrupt the solution?

b) Explain how the ACA approach responds to coherent and incoherent input signals, particularly those associated with background noise, such as the MSL strain gauge pressure data at frequencies above 50 Hz, as shown in Figures 3 and 4 of Attachment 7 to Supplement No. 26. Does random background noise lead to conservative, or non-conservative dryer loads at frequencies above 50 Hz?

Response to RAI EMEB-B-92

a) The acoustic circuit analysis is not undertaken in the time domain. Typically two seconds of in-plant data are Fourier decomposed and the analysis is undertaken in frequency space. This implies that the time signal repeats itself every two seconds. There is reason to believe that transients below several Hz may be introduced but signal levels here are very low and do not contribute to the dryer load.

b) The model has not been exercised to determine how random noise at each transducer becomes a steam dryer dynamic loading since this noise is turbulent in nature and at best a modest load. The fact that the model works well over 0-200 Hz (see figure for RAI #30 response) precludes the need to study transducer random noise sensitivity.

RAI EMEB-B-94

In Section 7 of Attachment 3 to Supplement No. 26, additional in-plant MSL pressure inputs inferred from strain gauge measurements in the Dresden Unit 2 plant are used to relax the assumptions used in prior ACA analyses that the source strengths at the MSL inlets are either completely in or out of phase. Entergy should provide a comparison of frequency spectra of selected dryer loads with and without the assumed source phasing and assess the influence of these assumptions on the dryer loads across frequencies between 0 and 200 Hz.

Response to RAI EMEB-B-94

Since Entergy did measure two independent pressures on each VYNPS main steam line, no assumption with regard to the phasing of the sources need to be made to utilize the ACM. Therefore it is unnecessary for Entergy to assess the sensitivity of source phasing assumptions.

RAI EMEB-B-95

Entergy should define the normalizing function, η_o', used in Section 7.2 of Attachment 3 to Supplement No. 26.

Response to RAI EMEB-B-95

The normalizing function is defined on Page 14 of Attachment 3 to Supplement No. 26.

RAI EMEB-B-108

The modifications to the VYNPS steam dryer are described in Section 2.0 of Attachment 5 to Supplement No. 26. These modifications use thicker plates, which are expected to reduce the FIV stresses significantly. However, at some locations, the FIV stresses in the modified dryer are higher. For example, according to Table 4.4-1 of Attachment 5, the modified top outer hood has higher stresses than the original one. Entergy should explain the differences between the stresses in the original and modified dryers at the key locations.

Response to RAI EMEB-B-108

The titles in Table 4.4-1 may have caused some confusion. The stress listed for Modified Top Outer Hood is the maximum stress in the new section of the top hood. The original top hood is the portion of the top hood that was not modified. The stresses are higher in the modified section because this section is in the area of higher loads.

The modified dryer was installed in the Spring of 2004. The stress report Attachment 5 to Supplement No. 26 includes the finite element analysis of the Modified Dryer for the CFD and Acoustic circuit loads developed this year using state of the art methods. The CFD loads were developed based on the modified geometry. There is no direct way to compare stresses in the old dryer with the new loads.

The new loads demonstrate that increasing the strength and stiffness of the face and coverplate provide margin against the vortex shedding loads in the lower plenum. The considerable margin in the modified design for ACM and CFD loads demonstrates that this design provides adequate margin for EPU.

RAI EMEB-B-109

The structural modifications in the VYNPS steam dryer, which are described in Section 2 of Attachment 5 to Supplement No. 26, have introduced several new weld locations that were not present in the original design. Entergy should explain whether a qualified welding procedure was followed for these underwater welds and whether the inspection results for these welds were acceptable.

Response to RAI EMEB-B-109

For the modifications performed to the VYNPS Steam dryer, welding was performed using qualified welding procedures, welders and certified filler material in accordance with ASME Section IX and XI (Code Case N516-2) and GE Energy Nuclear underwater welding specification P50YP244, Rev 10.

All inspection results for the welds performed for the modification were satisfactory. The inspections were performed by certified Quality Assurance representatives in accordance with the GE-UCC Nuclear Projects Quality Plan.

RAI EMEB-B-110

With regard to Attachment 5 to Supplement No. 26, Entergy should submit the information about the significant frequencies and mode shapes of the modified steam dryer.

Response to RAI EMEB-B-110

For one of the highest stress locations in Table 4.4-1 of Attachment 5 to Supplement No. 26, Modified Outer Hood Top Weld, Figure EMEB-B-110-1 shows power spectral density (PSD) distribution in the significant frequency range from [[ ]] The PSD shows peaks at [[ ]] This matches well with the peaks in the load response spectrum shown in Figure 10 of CDI 05-06 (Attachment 7 to Supplement No. 26). This demonstrates that the higher frequency loads above [[ ]] are having less impact on this structure. This supports the [[ ]] cut off frequency. It also demonstrates that the lower magnitude acoustic loads below [[ ]] are having a much smaller impact. The significant loads from the ACA are on the lower section of the vertical face. The two mode shapes that are likely excited by this load include [[ ]] These modes are depicted in the figures attached.

[[

[3]]]

Figure EMEB-B-110-1. PSD Distribution for the Modified Top Outer Hood Maximum Stress Location

[[

[3]]]

Figure EMEB-B-110-2. Mode Shape #121, 128.6 Hz. Outer Hood Plate

[[

[3]]]

Figure EMEB-B-110-3. Mode Shape #121, 128.6 Hz. VYNPS Steam Dryer Structure

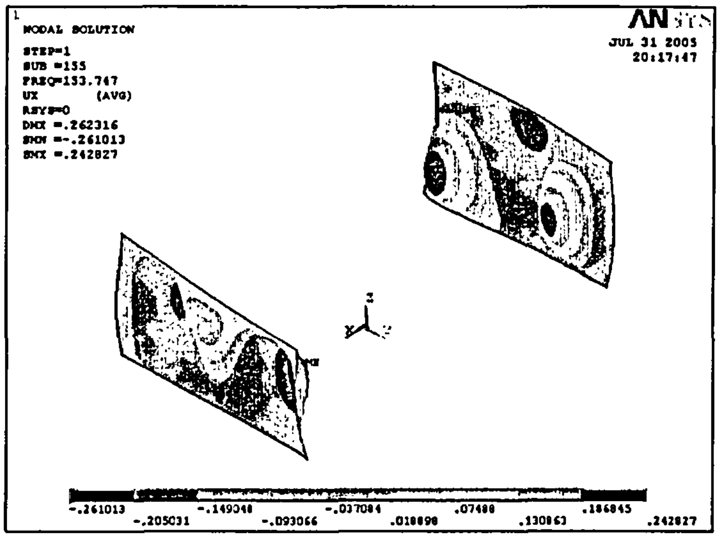

Figure EMEB-B-110-4. Mode Shape #155, 153.8 Hz. Outer Hood Plate

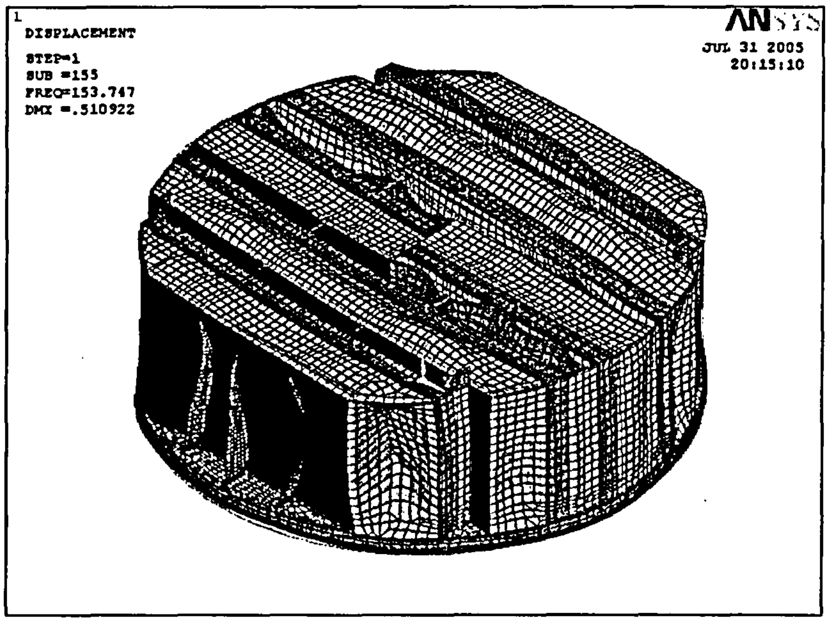

Figure EMEB-B-110-5. Mode Shape #155, 153.8 Hz. VYNPS Steam Dryer Structure

RAI EMEB-B-112

Entergy uses 1% of the critical damping in the finite element analysis of the steam dryer. Entergy should justify the use of 1% critical damping in the modal analysis of the VYNPS steam dryer and describe the sensitivity of the FIV stresses to the critical damping value.

Response to RAI EMEB-B-112

For the elastic dynamic finite element analysis of the VYNPS steam dryer subjected to fluid induced oscillating loading at CLTP and EPU conditions, a modal damping value of 1% of critical damping is used for all modes of the dryer. This damping value is selected mainly based on the review of three references:

1. Regulatory Guide 1.61 – Damping Values for Seismic Design of Nuclear Power Plants, October 1973.
2. "Kashiwazaki-6 Steam Dryer Hammer Test Final Report" GENE-F4100056-2, DRF F41-00056, February 1997.
3. "Tokai-2 Steam Dryer Vibration and Valve Closure Response" NEDE-24814, Class III, June 1980.

The 1% damping value report that was used for the VYNPS dryer analysis was previously transmitted to the NRC on the Exelon docket. The ADAMS ascension number is ML050980319.

Based on this assessment, the use of critical damping values of 1% is conservative and technically justified.

RAI EMEB-B-113

In Sections 3.4 to 3.6 of the steam dryer stress analysis report (pages 11 to 14 of Attachment 5 to Supplement No. 26), Entergy presents steam dryer design criteria, dryer loads, and load combinations. Entergy analyzes four different Level D conditions, two include faulted pressure, dead weight, ± safe shutdown earthquake (SSE), and FIV, whereas the other two include MSL break pressure, normal pressure, dead weight and ±SSE. Entergy should discuss the significance of including ±SSE loads in all four Level D conditions.

Response to RAI EMEB-B-113

The load combination and acceptance criteria are defined in GE 386HA931 document paragraph 5.2.3. This paragraph states "It may be assumed that SSE will cause whatever operational transients and LOCA events. Thus; stresses due to LOCA, stresses due to plant transient responses to LOCA, and stresses due to seismic vibratory motion shall be combined". Therefore, the SSE loads are included in all four Level D conditions to meet these criteria.

RAI EMEB-B-114

In two of the Service Level B conditions (see Table 3.6-1 of Attachment 5 to Supplement No. 26), loads due to turbine stop valve (TSV) events are considered, whereas in two other conditions, TSV flow-induced loads are considered. Entergy should explain the difference between TSV and TSV flow-induced loads.

Response to RAI EMEB-B-114

The turbine stop valve event produces two impact loads on the dryer. The first load is due to an acoustic wave that is caused by the rapid valve closure. The second load is a mass flow impact due to the flow reversal in the steamline. The acoustic wave travels down the steamline much faster than the reverse flow and impacts the dryer well before the flow impact. Because these loads are well separated in time, they are analyzed as separate load cases. The acoustic load is represented by the "TSV" term in load cases 4 and 5 (Levels B3 and B4). The flow impact load is represented by the "TSV flow-induced" term in load cases 6 and 7 (Levels B5 and B6).

RAI EMEB-B-115

In Section 3.8 (page 15 of Attachment 5 to Supplement No. 26), "FIV Stress Determination," Entergy selects 10 load case combinations for the alternating stress calculations based on the ANSYS results. Entergy further states that these cases are selected to maximize alternating stress but are also biased to later time points under the assumptions that, as time progressed, the CFD model would be converging on a steady-state solution. Entergy should explain how these load combinations were selected and why they are biased to later time points.

Response to RAI EMEB-B-115

The CFD static load cases have been replaced with transient CFD data, as described in response to EMEB-B-143.

RAI EMEB-B-116

In Tables 4.3-1 to 4.3-7 of Attachment 5 to Supplement No. 26, modified dryer stresses in different components are presented. Entergy should clarify the following items regarding these tables:

a) Explain whether these tables refer to stresses or stress intensities.

b) In these tables, local membrane stresses are considered but bending stresses are not considered. However, Columns 6 and 7 refer to primary bending stress. Explain this contradiction.

c) Explain why only local membrane stresses are multiplied by the weld stress factor, but FIV stresses are not.

d) Comparison of Table 4.3-1 and 4.4-1 shows that the FIV stresses in Table 4.3-1 (1st row, Column 5) is the sum of acoustic membrane stress (2nd row, Column 3, Table 4.4-1) and vortex shedding maximum surface stress (2nd row, Column 4, Table 4.4-1). Entergy should explain why acoustic maximum surface stress (Column 1, Table 4.4-1) is not considered in determining the FIV stresses in Table 4.3-1.

Response to RAI EMEB-B-116

a) These tables refer to stress intensities. The stress intensity is defined in NB-3213.1 [ASME Section III]. It is defined as twice the maximum shear stress. In other words, the stress intensity is the maximum difference between the algebraically largest principal stress and the algebraically smallest principal stress at a given point.

Table EMEB-B-116-1 is a list of ANSYS print out of principal stresses, stress intensities and SEQV for all the nodes in cover plate for Level B case 2 analysis. Due to the large volume of printout only these nodes near the maximum stress node 181 are included. This table is an example to show the detail stress calculation as shown in Table 4.3-1 Level B-2 column (A) stress, which is listed as 1842 psi, and to show it is localized stress.

From this table it can be seen that Node 181 has the following three principal stresses.

S1 = 654.16
S2 = -1.975
S3 = -1187.7

SI = 654.16-(-1187.7)
= 1841.9 psi

b) Table NB-3217-1, "Classification of Stress Intensity in Vessel for Some Typical Cases" is used as guideline for the dryer analysis. As an example, this table defines that near nozzle or other opening, the Local Membrane stress due to external load or moment is classified as P_L, and the bending stress is classified as Q, which is secondary. As shown in the above principal stress table, the membrane stress is the maximum stress at a node, which is localized stress, which is P_L, and the bending stress at that node is Q stress.

The allowable stress limits in Tables 4.3-1 to 4.3-7 are primary stress limits. Refer to Figure NB-3221-1, the primary stress limits are the sum of ($P_m + P_L + P_b$). It is agreed that these stress table more correctly label the column as ($P_m + P_L + P_b$), but is common practice to make the title shorter as ($P_m + P_b$). Therefore, there is no contradiction.

c) FIV stress is a high cycle reversing dynamic load. The stress is secondary in nature. This has been shown in EPRI/NRC/GE Piping and Fitting Dynamic Reliability Program, EPRI TR-102792, October 1994. The FIV stresses added to the primary stress are an extra conservatism required by NRC. In this analysis, there are two conservatisms included in the calculation. Refer to Table 4.4-1 of EPRI TR-102792. (1) The FIV stresses used in the primary stress tables are the absolute sum (ABS) of the acoustic membrane stress and vortex shedding maximum surface stress. Since they are two different sources of dynamic loads, the combination should be performed by square root of the sum of square (SRSS) method, instead of ABS. (2) Refer to Part B response, the membrane stress due to the vortex shedding should be used instead of maximum surface stress. With all the conservatisms as shown above, even the FIV stresses are not multiplied by the weld factors, the FIV stresses in these tables are still reasonably conservative.

d) The reason why acoustic maximum surface stress (Column 1, Table 4.4-1) is not considered in determining the FIV stresses in Table 4.3-1 has been explained in the item (b) response above. The maximum local surface stress is classified as "Q" stress per ASME Code. The response in (c) above explains it is very conservative to use ABS to combine the vortex shedding maximum surface stress and the dynamic loads.

Table EMEB-B-116 –1, ANSYS Printout for Stress Intensity Calculation

PRINT S NODAL SOLUTION PER NODE

***** POST1 NODAL STRESS LISTING *****

```
LOAD STEP=      4  SUBSTEP=      1

 TIME=    4.0000       LOAD CASE=   0

SHELL NODAL RESULTS ARE AT MIDDLE
```

NODE	S1	S2	S3	SINT	SEQV
1	925.32	30.590	-1.9750	927.30	911.45
2	43.941	-1.9750	-264.37	308.31	288.11
3	345.62	-1.9750	-522.18	867.80	756.48
4	264.08	-1.9750	-617.32	881.39	783.03
5	75.698	-1.9750	-528.30	604.00	569.16
178	836.05	-1.9750	-719.92	1556.0	1348.9
179	911.48	-1.9750	-395.63	1307.1	1161.4
180	484.55	-1.9750	-1027.9	1512.4	1337.3
181	**654.16**	**-1.9750**	**-1187.7**	**1841.9**	**1616.9**
182	857.60	-1.9750	-539.07	1396.7	1220.2
183	817.33	-1.9750	-733.32	1550.7	1343.6
MINIMUM VALUES					
NODE	6	67	84	82	82
VALUE	-1.9750	-143.06	-1230.5	93.078	88.111
MAXIMUM VALUES					
NODE	214	212	152	181	181
VALUE	985.19	308.61	-1.9750	**1841.9**	1616.9

RAI EMEB-B-117

In Attachment 2 to Supplement No. 26, Entergy describes its Steam Dryer Monitoring Plan (SDMP). In Table 1, Entergy proposes an hourly surveillance of MSL pressure data from strain gauges when initially increasing above a previously attained power. However, a similar surveillance frequency is not specified for MSL pressure data from pressure transducers. Entergy should explain the use of different surveillance frequencies for strain gauges and pressure transducers.

Response to RAI EMEB-B-117

The Supplement No. 26, Attachment 2, Table 1 specification for pressure transducer surveillance frequency corresponds to the 2.5% power ascension step evaluations described in Attachment 2. Pressure transducer data is needed at these evaluation hold points in the event that an ACA needs to be performed. If the rate of power ascension is small, collection of hourly strain gage data provides the ability to identify intermediate indications of trends between evaluation steps.

RAI EMEB-B-118

Table 2 of the SDMP (Attachment 2 to Supplement No. 26), presents VYNPS steam dryer performance criteria and required actions. One of the Level 2 performance criteria is that the pressure data do not exceed Level 2 spectra. Entergy should explain what are the Level 2 spectra and how the corresponding performance criterion is developed. Similarly, Entergy should explain the Level 1 spectra and the development of the corresponding performance criteria. Entergy should explain whether the performance criteria are based on the MSL strain gauge measurements, venturi pressure measurements, or both.

Response to RAI EMEB-B-118

The Level 2 and Level 1 performance criteria spectra are based on the 100% CLTP strain gage spectrum, extrapolated to the fatigue limit by a factor reflecting the stress analysis margin. See Exhibit EMEB-B-143-1 for details on development and application of the performance criteria. Pressure transducer data is not used in defining the acceptance criteria. The surveillance performance criteria listed in Table 2 of Supplement 26, Attachment 2 specify that the measured strain gage pressure data not exceed the Level 2 or Level 1 spectra. As stated in the Table 2 footnote, the Level 1 acceptance criteria spectrum is based on maintaining stresses less than or equal to the ASME allowable alternating stress value at 10^{11} cycles (i.e. 13.6 ksi). The Level 2 acceptance criteria spectrum is 80% of Level 1, or 10.88 ksi.

RAI EMEB-B-119

One of the Required Actions for Level 1 criteria listed in Table 2 of the SDMP is as follows: "Promptly initiate a reactor power reduction and achieve a previously acceptable power level within two hours, unless an engineering evaluation concludes that continued power operation or power accession is acceptable." Entergy should explain the Level 1 criteria and the corresponding Required Action.

Response to RAI EMEB-B-119

Refer to response to RAI EMEB-B-118 for an explanation of the Level 1 criteria. The required action to promptly initiate a reactor power reduction if the Level 1 criteria are exceeded is intended to ensure that the plant is operated at a condition where steam dryer structural integrity is known to be maintained. Exceeding the Level 1 acceptance criteria spectrum does not necessarily signify that any dryer component exceeds the stress limit. An engineering evaluation is needed to determine the amount of margin to the stress limit. Entergy proposes this required action to account for situations where unexpected response is seen and must be evaluated.

RAI EMEB-B-139

With regard to the work described in Attachment 1 to Supplement 29, please provide a case file for the Fluent simulations at 100% and 120% load condition for review by the NRC staff. In addition, a representative full data set for each load condition is requested. Finally, a mesh database (GAMBIT *.dbs) file is requested.

Response to RAI EMEB-B-139

Fluent data files for the VYNPS 100% and 120% load condition steam dryer simulations are enclosed with this submittal. These files are representative full data sets for the specified load conditions. Also included is a mesh database file. A copy of the Fluent code, such as that licensed to the NRC, is needed to access these files.

RAI EMEB-B-143

Since the CFD analyses at 120% of CLTP conditions reported in Figures 45 and 46 of Attachment 1 to Supplement 29 show large increases (about a factor of 10) in steam dryer loading at several discrete frequencies, Entergy is requested to provide corresponding maximum vortex shedding stresses (as defined in Table 4.4-1 in the report, 'VYNPS Modified Steam Dryer Analysis,' GE-NE-0000-0038-0936P, March 2005) for key dryer components.

Response to RAI EMEB-B-143

The maximum vortex shedding stresses have been calculated using the transient CFD model loads at 100% and 120% power. Exhibit EMEB-B-143-1 contains the updated vortex shedding stresses and an updated FIV stress summary.

RAI EMEB-B-144

On pages 14 and 15 of Attachment 3 to Supplement 26, [[

]]

Response to RAI EMEB-B-144

The CFD analysis has not saved the spatial velocity field as a function of time to permit the term for this source.

RAI EMEB-B-145

With regard to the work described in Attachment 1 to Supplement 29, [[

]]

Response to RAI EMEB-B-145

This response contains material proprietary to CDI

This response contains material proprietary to CDI

RAI EMEB-B-146

The CFD results indicated that the pressure PSD contains more peaks for the 120% of CLTP condition than the 100% of CLTP power condition. It is believed by Fluent that these peaks were introduced due to the interaction of the turbulent flow with the acoustic loading. Discuss the effects of the interaction between the acoustic and the hydrodynamic loadings on the forcing functions applying to the steam dryer.

Response to RAI EMEB-B-146

The hydrodynamic pressure fluctuations on the steam dryer are caused by vortex shedding or the formation of local vortices. The vortices create local pressure disturbances that act on the dryer surface. Acoustic loadings result from standing pressure waves as shown in response to EMEB-B-142. The sources that feed the acoustic waves can potentially be located at any point within the simulation domain. The time step chosen for the CFD model was based on the fluid flow velocity rather than the speed of sound and is about 10 times larger than required for tracking sound waves. The large time step relative to acoustic phenomena could have a damping effect on any acoustic signal. This did not allow the CFD model to address the interaction between the acoustic and hydrodynamic loadings on the forcing functions.

RAI EMEB-B-147

On page 3-4 of Attachment 4 to the application dated September 10, 2003, ASME Code Section XI, Subsection IWB-3641 is cited as the code requirements governing the stress analysis of the modification of the Core Spray nozzle and safe end. Please discuss the applicability of IWB-3641, which provides procedures for piping flaw evaluation, in lieu of the original Code of construction for analysis of modifications made to this component.

Response to RAI EMEB-B-147

During an ultrasonic examination conducted in April 1986, indications typical of intergranular stress corrosion cracking (IGSCC) were detected in the weld metal on the face of the nozzle. Since the weld material has been shown to be susceptible to IGSCC the joints were considered to be flawed. In May 1986 weld overlays were applied to the safe-end and to nozzle welds on the two core spray nozzles on the reactor pressure vessel. The weld overlay was designed in accordance with the requirements of the ASME Code, Section XI. Subsection IWB-3641was used in the evaluation. The design stress information was taken from the original stress report for the reactor pressure vessel.

By letter dated March 1, 1988, Vermont Yankee Nuclear Power Corporation (VYNPC) informed the NRC staff of its plans to continue operation and to confirm evaluation with regard to its long-term operation with core spray overlays. The NRC found these plans acceptable as documented in NRC letter to VYNPC dated May 9, 1988, "Core Spray Safe – End Inspection (TAC NO. 67522)".

RAI EMEB-B-148

On page 3-20 of Attachment 4 to the application dated September 10, 2003, the section addressing pipe stresses states: "For those systems that do not require a detailed analysis, pipe routing and flexibility was evaluated and determined to be acceptable."

a) Discuss the method used for evaluating flexibility of piping.

b) What acceptance criteria are applicable to the flexibility evaluation?

c) Which piping systems were evaluated with this approach?

Response to RAI EMEB-B-148

The piping that was evaluated by performing a review of pipe routing and available offsets in order to determine thermal flexibility acceptability in support of the September 10, 2003, application was limited to the following non-safety related piping:

- feedwater heater drain piping from the No.1 to the No. 2 heaters
- feedwater heater drain piping from the No. 2 to the No. 3 heaters
- moisture separator drain piping to the No. 2 heaters

As part of the feedwater heater replacement completed during the last refueling outage, detailed piping analyses of these lines were performed. Therefore the previous thermal flexibility evaluations for temperature increases due to power uprate are no longer applicable.

RAI EMEB-B-149

On page 3-35, Table 3-3, of Attachment 4 to the application dated September 10, 2003, the primary plus secondary stress level reported for the feedwater nozzle and safe end under constant pressure power uprate (CPPU) conditions is extremely close to the allowable ASME Code limit. Please discuss the general analytical approach used to calculate this stress. Also, explain the primary reasons for the 21% increase in stress over the CLTP stress reported, and why the feedwater nozzle CPPU stress and usage factor increases are so much larger than the increases for the other components listed in Table 3-3.

Response to RAI EMEB-B-149

The following discusses the methods used to perform the analysis and describes the steps necessary to determine the applicable stresses for comparison with the primary (P), primary plus secondary (P+Q), and primary plus secondary plus peak (P+Q+F) stress allowable listed in the ASME Code.

GE developed a "standard" technique to conservatively scale the original stress report stresses to account for changes in the original pressures, temperatures, and nozzle flows as a result of EPU. The standard technique of analysis linearly scales the stresses based on increases in temperatures and flows affecting a component. Pressure is not considered since this is a constant pressure power uprate (CPPU). This linear scaling method of calculating EPU stresses is an NRC-approved method (NEDO-32424[3]) and has been used in all GE nuclear power uprate projects. The scaled

---

3 GE Licensing Topical Reports, "Generic Guidelines for General Electric Boiling Water Reactor Extended Power Uprate," NEDC-32424P-A, Class III, (Proprietary) February 1999 (ELTR-1) and NEDO-32424, Class I (non-proprietary), April 1995

stresses were compared to the ASME B&PV Section III acceptance criteria.

The following provides a summary of the technique used:

- A scaling factor was determined based on the increase in flow and temperature for EPU conditions for this nozzle. The scaling factor was then used to conservatively calculate the stresses for the nozzle.
- An additional analysis was performed on the feedwater Nozzle to reduce conservatism in original calculations.
- The currently licensed thermal power (CLTP) nozzle stresses were separated from the piping reactions. The limiting piping loads were used in the evaluation.
- The nozzle stresses were conservatively scaled based on the increase in flow and temperature for EPU conditions for this nozzle.
- Even though the change in flow only influences the thermal stress, the pressure and thermal stresses are conservatively increased. The scaling factor was not applied to the piping loads.
  - The "adjusted" nozzle stresses were then added back to the piping reactions to determine the EPU "total" nozzle stresses.
  - When calculating the cumulative usage factor (CUF), the "new" EPU peak stress and the temperatures provided in the stress report were used.

The primary scaling factor stress increase in the feedwater nozzle is due to the increase in flow (from 3720 gpm to 4705 gpm) associated with the EPU conditions for this nozzle. [[
]]
The change in feedwater nozzle CPPU stress and usage factor is greater than the increase for the other components in PUSAR Table 3-3 because the change in flow and temperature is significantly greater. Additionally, some components in the "original" original licensed thermal power (OLTP) stress evaluation/report(s) conservatively considered higher temperatures and flows, resulting in either no or small EPU scaling factor for EPU conditions.

Attachment 8

Vermont Yankee Nuclear Power Station

Proposed Technical Specification Change No. 263 – Supplement No. 31

Extended Power Uprate

Response to Request for Additional Information

CDI Affidavit

Continuum Dynamics, Inc.

(609) 538-0444 (609) 538-0464 fax 34 Lexington Avenue Ewing, NJ 08618-2302

AFFIDAVIT

Re: Proprietary Responses to RAIs prepared by Continuum Dynamics, Inc. dated July 29, 2005 and August 1, 2005. (RAIs 90b, 90c, 91, 144 and 145)

I, Alan J. Bilanin, being duly sworn, depose and state as follows:

1. I hold the position of President and Senior Associate of Continuum Dynamics, Inc. (hereinafter referred to as C.D.I.), and I am authorized to make the request for withholding from Public Record the Information contained in the documents described in Paragraph 2. This Affidavit is submitted to the Nuclear Regulatory Commission (NRC) pursuant to 10 CFR 2.390(a)(4) based on the fact that the attached information consists of trade secret(s) of C.D.I. and that the NRC will receive the information from C.D.I. under privilege and in confidence.

2. The Information sought to be withheld, as transmitted to Entergy Vermont Yankee via email on July 29, 2005 and August 1, 2005. Responses to RAIs numbered 90b, 90c, 91, 144 and 145 are CDI Proprietary.

3. The Information summarizes:

   (a) a process or method, including supporting data and analysis, where prevention of its use by C.D.I.'s competitors without license from C.D.I. constitutes a competitive advantage over other companies;
   (b) Information which, if used by a competitor, would reduce his expenditure of resources or improve his competitive position in the design, manufacture, shipment, installation, assurance of quality, or licensing of a similar product;
   (c) Information which discloses patentable subject matter for which it may be desirable to obtain patent protection.

   The information sought to be withheld is considered to be proprietary for the reasons set forth in paragraphs 3(a), 3(b) and 3(c) above.

4. The Information has been held in confidence by C.D.I., its owner. The Information has consistently been held in confidence by C.D.I. and no public disclosure has been made and it is not available to the public. All disclosures to third parties, which have been limited, have been made pursuant to the terms and

conditions contained in C.D.I.'s Nondisclosure Secrecy Agreement which must be fully executed prior to disclosure.

5. The Information is a type customarily held in confidence by C.D.I. and there is a rational basis therefore. The Information is a type, which C.D.I. considers trade secret and is held in confidence by C.D.I. because it constitutes a source of competitive advantage in the competition and performance of such work in the industry. Public disclosure of the Information is likely to cause substantial harm to C.D.I.'s competitive position and foreclose or reduce the availability of profit-making opportunities.

I declare under penalty of perjury that the foregoing affidavit and the matters stated therein are true and correct to be the best of my knowledge, information and belief.

Executed on this 1 day of Aug 2005.

Alan B
Alan J. Bilanin
Continuum Dynamics, Inc.

Subscribed and sworn before me this day: 1st DAY OF AUGUST 2005

Eileen P. Burmeister
Eileen P. Burmeister, Notary Public

EILEEN P. BURMEISTER
NOTARY PUBLIC OF NEW JERSEY
MY COMM. EXPIRES MAY 6, 2007

Attachment 9

Vermont Yankee Nuclear Power Station

Proposed Technical Specification Change No. 263 – Supplement No. 31

Extended Power Uprate

Response to Request for Additional Information

GE Affidavits

General Electric Company

AFFIDAVIT

I, Robert E. Gamble, state as follows:

(1) I am Manager, ESBWR, General Electric Company ("GE"), have been delegated the function of reviewing the information described in paragraph (2) which is sought to be withheld, and have been authorized to apply for its withholding.

(2) The information sought to be withheld is contained in Enclosures 2 and 3 of GE letter, GE-VYNPS-AEP-394, *Responses to NRC RAIs EMEB-20, 26, 34, 35, 36, 37, 38, 39, 43, 44, 53, 55, 57, 71, 72, 75, 77, 97, 101, 107, 108, 109, 110, 112, 113, 114, 116, 149*, dated August 2, 2005. The proprietary information in Enclosure 2, *Responses to NRC RAIs EMEB-20, 26, 34, 35, 36, 37, 38, 39, 43, 44, 53, 55, 57, 71, 72, 75, 77, 97, 101, 107, 108, 109, 110, 112, 113, 114, 116, 149 (Proprietary)*, is delineated by a double underline inside double square brackets. Figures and large equation objects are identified with double square brackets before and after the object. The proprietary information in Enclosure 3 is the entire CD labeled *GE-VYNPS-AEP-394, GE RESPONSES TO NRC RAIs (EMEB-107) - GE Proprietary Information*[3]. In each case, the superscript notation[3] refers to Paragraph (3) of this affidavit, which provides the basis for the proprietary determination.

(3) In making this application for withholding of proprietary information of which it is the owner, GE relies upon the exemption from disclosure set forth in the Freedom of Information Act ("FOIA"), 5 USC Sec. 552(b)(4), and the Trade Secrets Act, 18 USC Sec. 1905, and NRC regulations 10 CFR 9.17(a)(4), and 2.390(a)(4) for "trade secrets" (Exemption 4). The material for which exemption from disclosure is here sought also qualify under the narrower definition of "trade secret", within the meanings assigned to those terms for purposes of FOIA Exemption 4 in, respectively, <u>Critical Mass Energy Project v. Nuclear Regulatory Commission</u>, 975F2d871 (DC Cir. 1992), and <u>Public Citizen Health Research Group v. FDA</u>, 704F2d1280 (DC Cir. 1983).

(4) Some examples of categories of information which fit into the definition of proprietary information are:

a. Information that discloses a process, method, or apparatus, including supporting data and analyses, where prevention of its use by General Electric's competitors without license from General Electric constitutes a competitive economic advantage over other companies;

b. Information which, if used by a competitor, would reduce his expenditure of resources or improve his competitive position in the design, manufacture, shipment, installation, assurance of quality, or licensing of a similar product;

c. Information which reveals aspects of past, present, or future General Electric customer-funded development plans and programs, resulting in potential products to General Electric;

d. Information which discloses patentable subject matter for which it may be desirable to obtain patent protection.

The information sought to be withheld is considered to be proprietary for the reasons set forth in paragraphs (4)a., and (4)b, above.

(5) To address 10 CFR 2.390 (b) (4), the information sought to be withheld is being submitted to NRC in confidence. The information is of a sort customarily held in confidence by GE, and is in fact so held. The information sought to be withheld has, to the best of my knowledge and belief, consistently been held in confidence by GE, no public disclosure has been made, and it is not available in public sources. All disclosures to third parties including any required transmittals to NRC, have been made, or must be made, pursuant to regulatory provisions or proprietary agreements which provide for maintenance of the information in confidence. Its initial designation as proprietary information, and the subsequent steps taken to prevent its unauthorized disclosure, are as set forth in paragraphs (6) and (7) following.

(6) Initial approval of proprietary treatment of a document is made by the manager of the originating component, the person most likely to be acquainted with the value and sensitivity of the information in relation to industry knowledge. Access to such documents within GE is limited on a "need to know" basis.

(7) The procedure for approval of external release of such a document typically requires review by the staff manager, project manager, principal scientist or other equivalent authority, by the manager of the cognizant marketing function (or his delegate), and by the Legal Operation, for technical content, competitive effect, and determination of the accuracy of the proprietary designation. Disclosures outside GE are limited to regulatory bodies, customers, and potential customers, and their agents, suppliers, and licensees, and others with a legitimate need for the information, and then only in accordance with appropriate regulatory provisions or proprietary agreements.

(8) The information identified in paragraph (2), above, is classified as proprietary because it contains detailed results and conclusions from analyses of the Vermont Yankee Steam Dryer which encompass and takes into account analyses and repairs utilizing analytical models and methods, including computer codes, which GE has developed. The development of these models and computer codes was achieved at a significant cost to GE, on the order of ½ million dollars.

The development of the evaluation process along with the interpretation and application of the analytical results is derived from the extensive experience database that constitutes a major GE asset.

(9) Public disclosure of the information sought to be withheld is likely to cause substantial harm to GE's competitive position and foreclose or reduce the availability of profit-making opportunities. The information is part of GE's comprehensive BWR safety and technology base, and its commercial value extends beyond the original development cost. The value of the technology base goes beyond the extensive physical database and analytical methodology and includes development of the expertise to determine and apply the appropriate evaluation process. In addition, the technology base includes the value derived from providing analyses done with NRC-approved methods.

The research, development, engineering, analytical and NRC review costs comprise a substantial investment of time and money by GE.

The precise value of the expertise to devise an evaluation process and apply the correct analytical methodology is difficult to quantify, but it clearly is substantial.

GE's competitive advantage will be lost if its competitors are able to use the results of the GE experience to normalize or verify their own process or if they are able to claim an equivalent understanding by demonstrating that they can arrive at the same or similar conclusions.

The value of this information to GE would be lost if the information were disclosed to the public. Making such information available to competitors without their having been required to undertake a similar expenditure of resources would unfairly provide competitors with a windfall, and deprive GE of the opportunity to exercise its competitive advantage to seek an adequate return on its large investment in developing these very valuable analytical tools.

I declare under penalty of perjury that the foregoing affidavit and the matters stated therein are true and correct to the best of my knowledge, information, and belief.

Executed on this 2nd day of August 2005.

Robert E. Gamble
General Electric Company

General Electric Company

AFFIDAVIT

I, George B. Stramback, state as follows:

(1) I am Manager, Regulatory Services, General Electric Company ("GE"), have been delegated the function of reviewing the information described in paragraph (2) which is sought to be withheld, and have been authorized to apply for its withholding.

(2) The information sought to be withheld is contained in Enclosure 2 of GE letter, GE-VYNPS-AEP-397, *Responses to NRC RAIs EMEB-143*, dated August 4, 2005. The proprietary information in Enclosure 2, *Responses to NRC RAIs EMEB-143*, is delineated by a double underline inside double square brackets. Figures and large equation objects are identified with double square brackets before and after the object. In each case, the superscript notation[3] refers to Paragraph (3) of this affidavit, which provides the basis for the proprietary determination.

(3) In making this application for withholding of proprietary information of which it is the owner, GE relies upon the exemption from disclosure set forth in the Freedom of Information Act ("FOIA"), 5 USC Sec. 552(b)(4), and the Trade Secrets Act, 18 USC Sec. 1905, and NRC regulations 10 CFR 9.17(a)(4), and 2.390(a)(4) for "trade secrets" (Exemption 4). The material for which exemption from disclosure is here sought also qualify under the narrower definition of "trade secret", within the meanings assigned to those terms for purposes of FOIA Exemption 4 in, respectively, Critical Mass Energy Project v. Nuclear Regulatory Commission, 975F2d871 (DC Cir. 1992), and Public Citizen Health Research Group v. FDA, 704F2d1280 (DC Cir. 1983).

(4) Some examples of categories of information which fit into the definition of proprietary information are:

a. Information that discloses a process, method, or apparatus, including supporting data and analyses, where prevention of its use by General Electric's competitors without license from General Electric constitutes a competitive economic advantage over other companies;

b. Information which, if used by a competitor, would reduce his expenditure of resources or improve his competitive position in the design, manufacture, shipment, installation, assurance of quality, or licensing of a similar product;

c. Information which reveals aspects of past, present, or future General Electric customer-funded development plans and programs, resulting in potential products to General Electric;

d. Information which discloses patentable subject matter for which it may be desirable to obtain patent protection.

The information sought to be withheld is considered to be proprietary for the reasons set forth in paragraphs (4)a., and (4)b, above.

(5) To address 10 CFR 2.390 (b) (4), the information sought to be withheld is being submitted to NRC in confidence. The information is of a sort customarily held in confidence by GE, and is in fact so held. The information sought to be withheld has, to the best of my knowledge and belief, consistently been held in confidence by GE, no public disclosure has been made, and it is not available in public sources. All disclosures to third parties including any required transmittals to NRC, have been made, or must be made, pursuant to regulatory provisions or proprietary agreements which provide for maintenance of the information in confidence. Its initial designation as proprietary information, and the subsequent steps taken to prevent its unauthorized disclosure, are as set forth in paragraphs (6) and (7) following.

(6) Initial approval of proprietary treatment of a document is made by the manager of the originating component, the person most likely to be acquainted with the value and sensitivity of the information in relation to industry knowledge. Access to such documents within GE is limited on a "need to know" basis.

(7) The procedure for approval of external release of such a document typically requires review by the staff manager, project manager, principal scientist or other equivalent authority, by the manager of the cognizant marketing function (or his delegate), and by the Legal Operation, for technical content, competitive effect, and determination of the accuracy of the proprietary designation. Disclosures outside GE are limited to regulatory bodies, customers, and potential customers, and their agents, suppliers, and licensees, and others with a legitimate need for the information, and then only in accordance with appropriate regulatory provisions or proprietary agreements.

(8) The information identified in paragraph (2), above, is classified as proprietary because it contains detailed results and conclusions from analyses of the Vermont Yankee Steam Dryer which encompass and takes into account analyses and repairs utilizing analytical models and methods, including computer codes, which GE has developed. The development of these models and computer codes was achieved at a significant cost to GE, on the order of 2 million dollars.

The development of the evaluation process along with the interpretation and application of the analytical results is derived from the extensive experience database that constitutes a major GE asset.

(9) Public disclosure of the information sought to be withheld is likely to cause substantial harm to GE's competitive position and foreclose or reduce the availability of profit-making opportunities. The information is part of GE's comprehensive BWR safety and technology base, and its commercial value extends beyond the original development cost. The value of the technology base goes beyond the extensive physical database and analytical methodology and includes development of the expertise to determine and apply the appropriate evaluation process. In addition, the technology base includes the value derived from providing analyses done with NRC-approved methods.

The research, development, engineering, analytical and NRC review costs comprise a substantial investment of time and money by GE.

The precise value of the expertise to devise an evaluation process and apply the correct analytical methodology is difficult to quantify, but it clearly is substantial.

GE's competitive advantage will be lost if its competitors are able to use the results of the GE experience to normalize or verify their own process or if they are able to claim an equivalent understanding by demonstrating that they can arrive at the same or similar conclusions.

The value of this information to GE would be lost if the information were disclosed to the public. Making such information available to competitors without their having been required to undertake a similar expenditure of resources would unfairly provide competitors with a windfall, and deprive GE of the opportunity to exercise its competitive advantage to seek an adequate return on its large investment in developing these very valuable analytical tools.

I declare under penalty of perjury that the foregoing affidavit and the matters stated therein are true and correct to the best of my knowledge, information, and belief.

Executed on this 4th of August 2005.

George B. Stramback
George B. Stramback
General Electric Company

Attachment 10

Vermont Yankee Nuclear Power Station

Proposed Technical Specification Change No. 263 – Supplement No. 31

Extended Power Uprate

Response to Request for Additional Information

Exhibits

Exhibit EMEB-B-18-1
Exhibit EMEB-B-80-1
Exhibit EMEB-B-143-1 (Proprietary)
Exhibit EMEB-B-143-1 (Non-Proprietary Version)

BVY 05-074
Docket No. 50-271

Exhibit EMEB-B-18-1

Dryer Load Uncertainty

Vermont Yankee Nuclear Power Station

Proposed Technical Specification Change No. 263 – Supplement No. 31

Extended Power Uprate

Response to Request for Additional Information

Acoustic Load Uncertainty

The performance of the Acoustic Circuit Model (ACM) has been benchmarked on the GE Scale Model Test (SMT) Facility and at Quad Cities Unit 2(QC2). These benchmarks provide information that supports Entergy's assessment of the performance of this model in predicting steam dryer loads based on dynamic or hydrodynamic steam line data.

There were differences in the method of determining the steam line pressure signals used in the SMT and QC2 benchmark tests and the VYNPS steam lines. This section will address the uncertainties introduced by these differences.

The uncertainty in the ACM loads is driven by the following sources:

1. UncACM1: Maximum of uncertainty of the ACM based on QC2 data and SMT benchmark data.

2. UncACM2: The uncertainty introduced by steam line pressure measurement method and location.

The purpose here is to define the uncertainty in the VYNPS calculated steam dryer load from each of these sources. These uncertainties will then be combined by the (SRSS) method to assess the ACM load uncertainty.

UncACM=Sqrt(UncACM1^2+ UncACM2^2)

This will be performed for the Root Mean Squared (RMS) uncertainty and the maximum load uncertainty. The maximum of these two will be used to define the UncACM uncertainty used in the limit curve factor assessment.

Uncertainty Identified in the SMT Benchmark Tests

The Entergy benchmark report, supplied in Attachment 1 to Supplement 27 (BVY 05-038 dated April 5, 2005), provided graphs comparing ACM predictions with SMT measurements in the form of power spectral density (PSD), RMS and maximum pressure values on all vertical faces and cover plate microphones. From the PSD plots it was found that the ACM was generally conservative at frequencies between 240 Hz (20 Hz full scale) and 3200 Hz (270 Hz full scale). The ACM was determined to be non-conservative below 240 Hz. The source of the signals below 240 Hz appears to be due to flow turbulence and is not associated with acoustic signals. Based on these findings, Entergy applied an unsteady CFD large eddy simulation (LES) analysis using the VYNPS plant and plant operating conditions as inputs to generate representative hydrodynamic loads. Both ACA and CFD loads were used in the structural evaluation of the VYNPS dryer. The uncertainty associated with the CFD loads are discussed in Exhibit EMEB-B-143-1.

In the process of assessing the ACM load uncertainty, it was noted that that the non-conservative RMS and maximum pressure conditions shown on the benchmark report plots involved test case conditions with flow: VY6RUN2, Burst with 81 CFM Flow and VY12R1, Chirp with 81 CFM Flow. Review of the PSDs also suggested the under predictions occurred at microphones associated with significant frequency content less than 240 Hz.

To assess this rigorously, the SMT data for VY6RUN2 and VY12R1 were reprocessed applying a 240 Hz High Pass filter. The revised, filtered plots Max and RMS signal plots are included as Figures EMEB-B-18-1-E1, EMEB-B-18-1-E2, EMEB-B-18-1-G1, and EMEB-B-18-1-G2. As noted with the low frequency turbulence signal removed, the RMS and maximum ACM predictions bound the measured data. This work has been independently reviewed by LMS.

As reported in Attachment 1 (VY-RPT-05-00006) to Supplement 27 the quantified SMT instrument uncertainties including microphone accuracy are less than 6% which is insignificant (~ one tenth) when compared to the overall ACM uncertainty and therefore not included in this assessment.

The data is also summarized for all conditions in the following Table EMEB-B-18-1-1.

BURST NO FLOW					
Source	(MaxCDI-MaxSMT)/MaxSMT			(RMSCDI-RMSSMT)/RMSSMT	
VY3R2	Max	53%		Max	52%
VY3R2	Min	2%		Min	19%
BURST & 81 CFM Filtered <240 Hz					
	(MaxCDI-MaxSMT)/MaxSMT			(RMSCDI-RMSSMT)/RMSSMT	
VY6RUN2	Max	55%		Max	31%
VY6RUN2	Min	4%		Min	3%
CHIRP & 81 CFM Filtered <240 Hz					
	(MaxCDI-MaxSMT)/MaxSMT			(RMSCDI-RMSSMT)/RMSSMT	
VY12R1	Max	67%		Max	40%
VY12R1	Min	1%		Min	8%
CHIRP NO FLOW					
	(MaxCDI-MaxSMT)/MaxSMT			(RMSCDI-RMSSMT)/RMSSMT	
VY13R1	Max	101%		Max	59%
VY13R1	Min	12%		Min	16%
Summary of all 4 Cases					
	(MaxCDI-MaxSMT)/MaxSMT			(RMSCDI-RMSSMT)/RMSSMT	
All Cases	Max	101%		Max	59%
All Cases	Min	1%		Min	3%

Table EMEB-B-18-1-1.

Summary of SMT Time Domain Signal Comparison

FiltApp_E_CompareVY6RUN2R1.xls

Acoustic Model Benchmark

7/30/2005

Appendix E Filtered <240 Hz, VY6RUN2 Burst Random with 81 CFM Flow

Microphone Mall Max

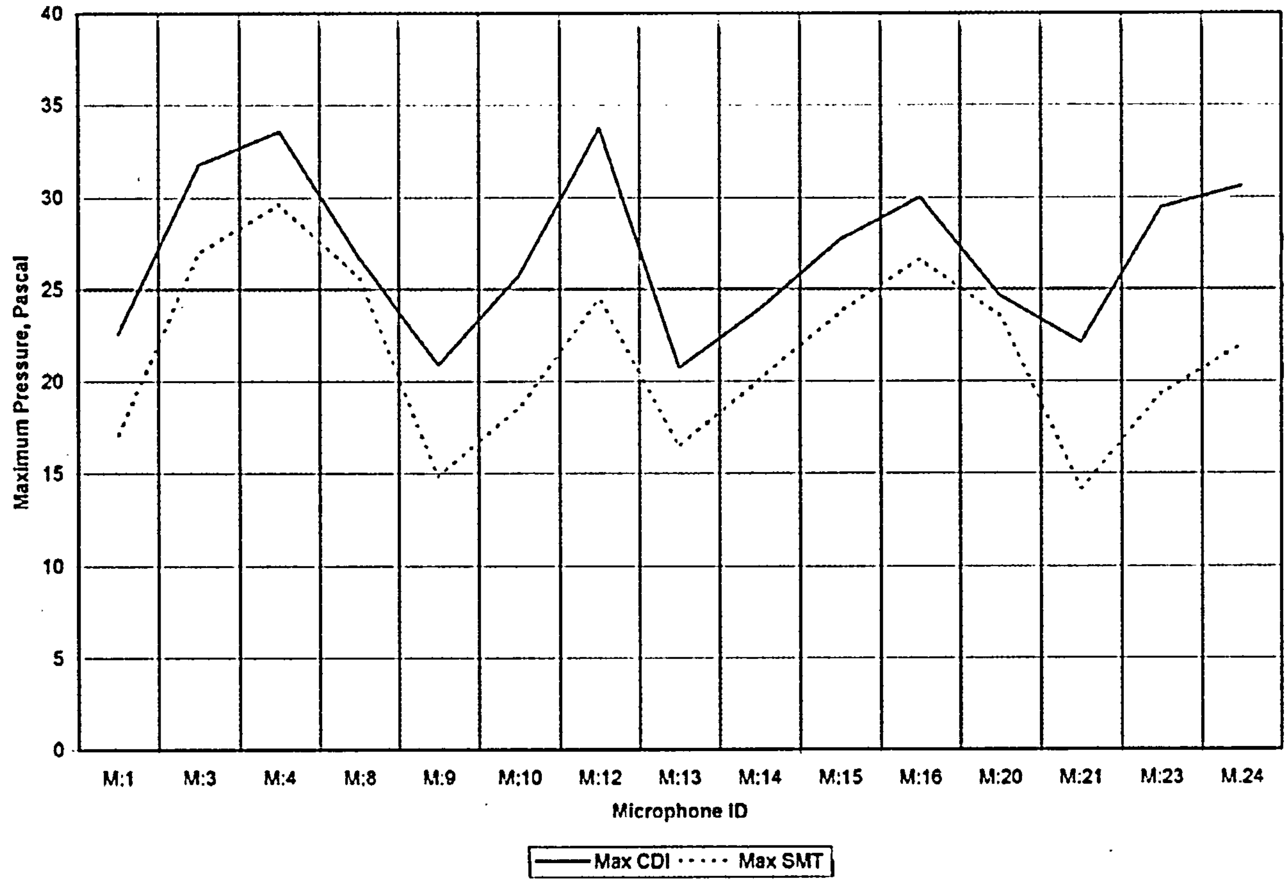

Figure EMEB-18-1-E1

Appendix E Filtered <240 Hz, VY6RUN2 Burst Random with 81 CFM Flow
Microphone Mall Prms

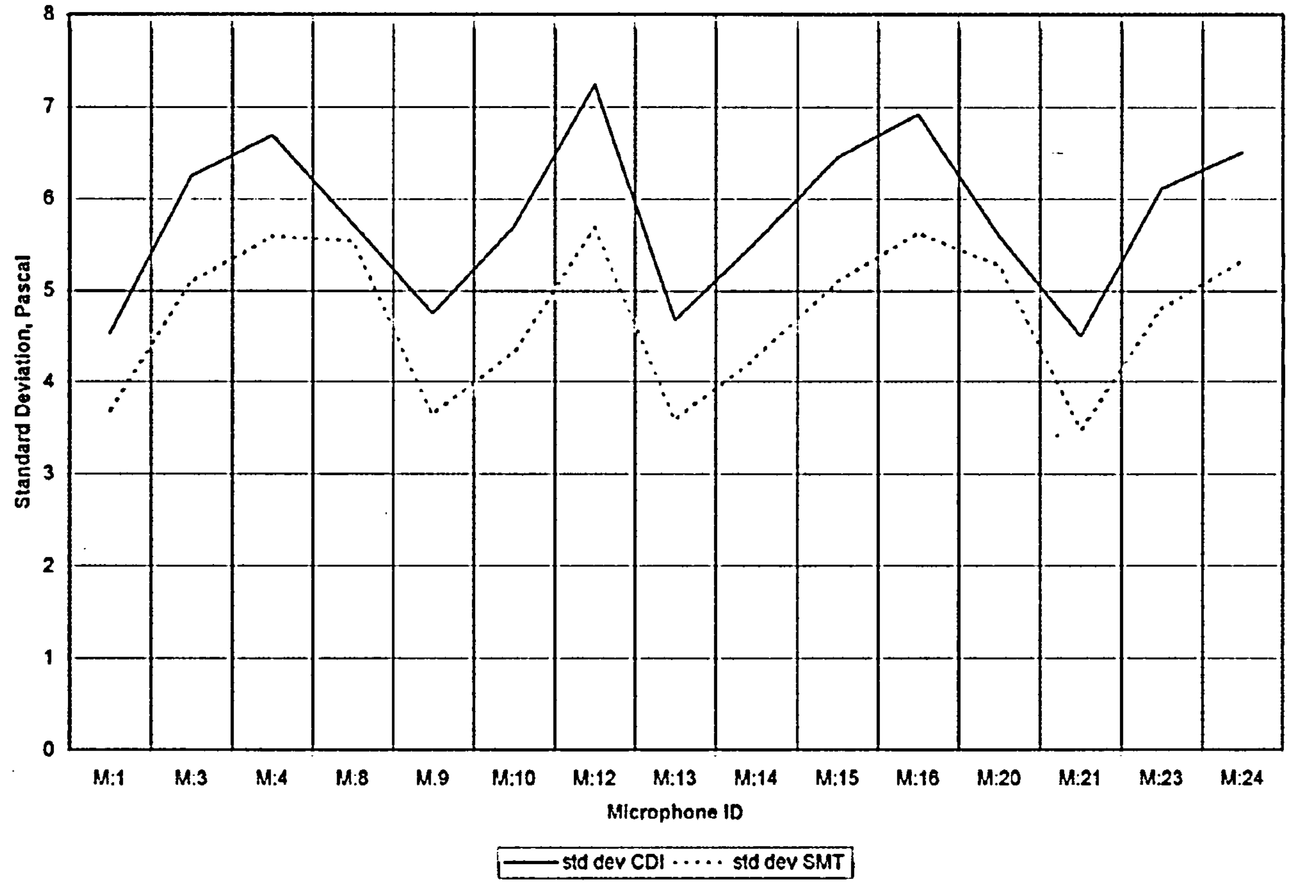

Figure EMEB-18-1-E2

Acoustic Model Benchmark
Appendix G Filtered <240 Hz, VY12R1 Chirp with 81 CFM Flow
Microphone Mall Max

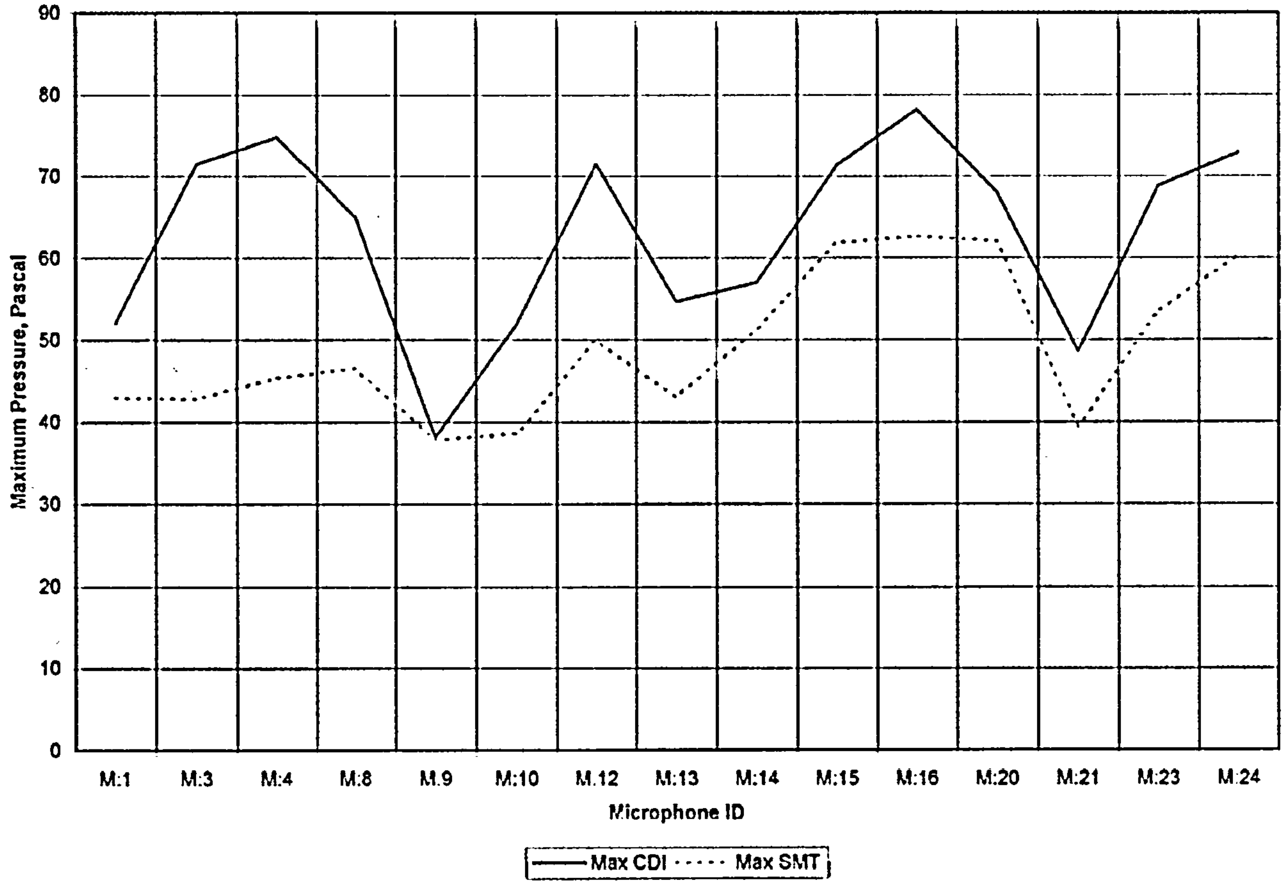

Figure EMEB-18-1-G1

Acoustic Model Benchmark
Appendix G Filtered <240 Hz, VY12R1 Chirp with 81 CFM Flow
Microphone Mall Prms

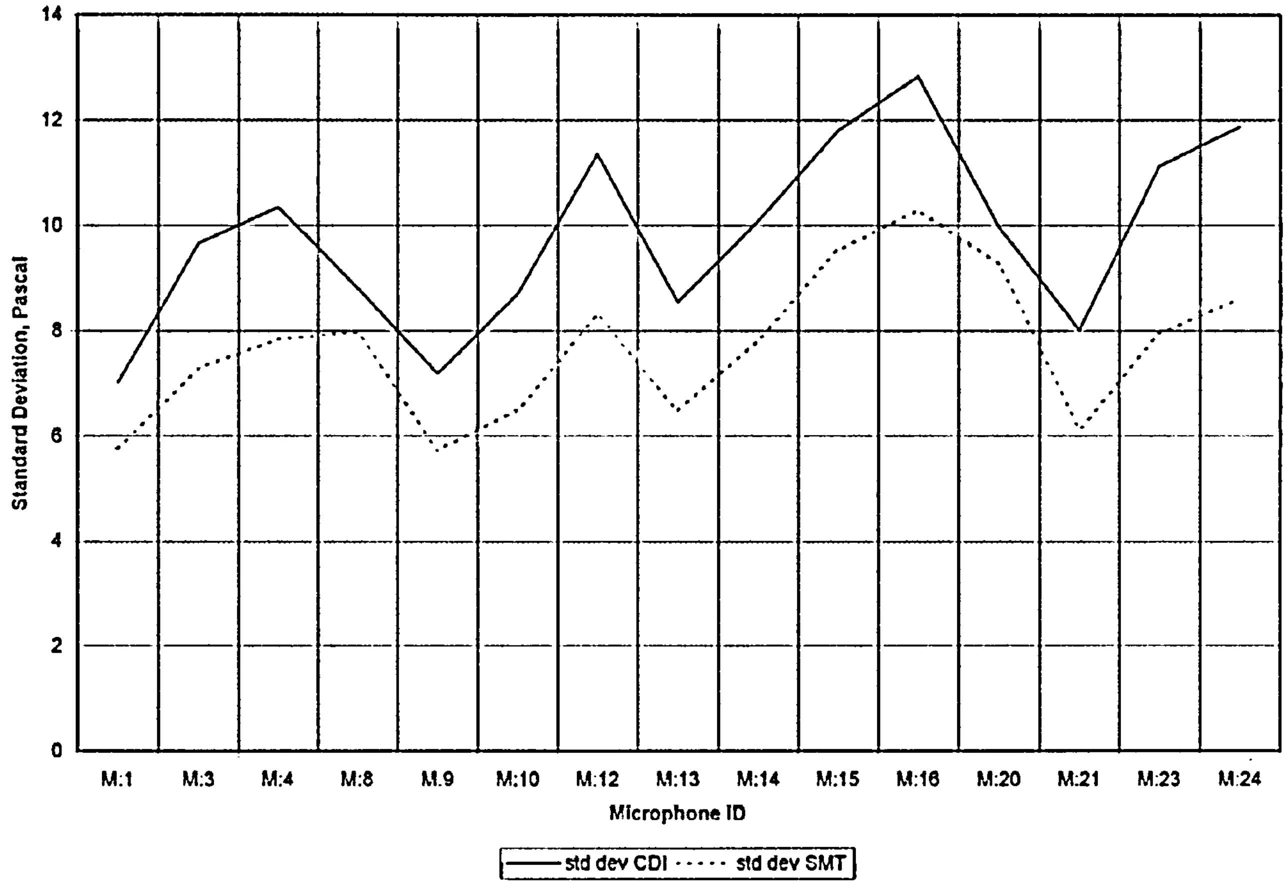

Figure EMEB-18-1-G2

Exhibit EMEB-B-18-1
VYNPS Steam Dryer Load Uncertainty
Page 6 of 22

Based on the cases studied, in terms of load magnitude between 240 Hz (20Hz Full Size) and 3200 Hz (280 Hz full scale), the ACM was conservative in maximum load prediction and RMS values for all four conditions. The minimum margin above 240 Hz was 1% based on the maximum load predictions. While no additional amplitude uncertainty should be required because the ACM was shown to be conservative, a 5% ACM load uncertainty was conservatively assigned from this test.

Entergy originally stated that the ACM enveloped most of the frequency content between 240 and 3200 Hz when a +/- 10% time step was applied. The VYNPS structural assessment indicated that application of the +/- 10 % time step in the VYNPS model resulted in an increase in peak stress range for a plus time step (and a decrease in load for a minus time step). The increase in stress, as shown below based on controlling locations on the dryer, results in a load uncertainty due to frequency mismatch of approximately 20%.

Frequency Uncertainty Peak Stress (PSI)	Base Case	+10% TS	%Change
Front Vertical Hood Top Weld	2417	2900	20%
Front Hood Gusset	3238	3535	9%

Table EMEB-B-18-1-2

The uncertainty is therefore estimated from the SMT benchmark is 20%.

Uncertainty Identified in the QC2 Benchmark Tests

The CDI benchmark report, CDI 95-10, provides a summary of blind benchmark predictions from QC2 at 790 MWe. At this power level, the average flow velocity in the main steamlines is about the same as that for VYNPS at EPU conditions. This ACM was done with the original parameters that matched damping, acoustic speed and reflective boundary assumptions used in the VYNPS load generation report (CDI 05-06). Therefore, this benchmark is applicable for the current VY ACA load uncertainty. It should be noted that Exelon updated their model based on this benchmark and additional tests at EPU power on QC2 to provide needed further improvements the accuracy of their ACA for their plants (not required for VYNPS).

The following Table includes a summary of results from the QC2 benchmark. This summary includes all pressure transmitter locations on the steam dryer face across from the steamline nozzles where VYNPS loads are significant (P3, P12, P20, and P21) as well as a pressure transmitter located on the dryer skirt (P24). It can be noted that the results are similar to the SMT benchmark where the ACM predictions are generally conservative in RMS and maximum value predictions.

Microphone	Max Abs Predicted (psig)	Max Abs Measured (psig)	(MaxCDI) /MaxQC2 %	RMS Predicted (psig)	RMS Measured (psig)	(RMSCDI)/ RMSQC2 %
P3	0.858	0.714	120%	0.216	0.189	114%
P12	0.955	0.78	122%	0.257	0.233	110%
P20	0.981	0.746	132%	0.257	0.213	121%
P21	1.313	1.017	129%	0.351	0.354	99%
P24	0.531	0.476	112%	0.107	0.109	98%
			(MaxCDI) /MaxQC2			(RMSCDI) /RMSQC2
		max	132%		max	121%
		min	112%		min	98%

Table EMEB-B-18-1-3
Summary of Vertical Face Loads for QC2 Blind Benchmark 790 MWe. (Data from CDI Report No. 05-10)

This benchmark was performed using the average signal from two of the four strain gages at each location. The in-plane pairs were used. Using 2 gages vs. 4 gages adds additional signal input to the ACM resulting in an overprediction of the loads. Therefore, the predicted loads ratios are adjusted by dividing the minimum predictions ratio by the average over prediction ratio of the Strain Gage (SG) signal.

Exelon made available the 4 sets of 4 strain gage signals from QC2. From available data it can be seen in the table below that the average over predicted signal ratio was 111% Max and 114% RMS. The minimum ratio of predicted to measured load was 112% Max and 98% RMS. Extrapolating these predictions by the average under prediction ratio of the SG results in uncertainties of 0% Max and 14% RMS. The assessment is summarized in the Table below.

Summary of QC 2 1/2 Bridge Data used in Analysis vs Averaged SG Data				
	Range	RMS	Range	RMS
Ave MSL B 651'	3.28	0.39	gage/ave	gage/ave
Ave S7/S9 MSL B 651'	3.66	0.42	112%	109%
Ave MSL B 621'	2.47	0.30	gage/ave	gage/ave
Ave S11/S11A MSL B 621'	2.91	0.35	118%	117%
Ave MSL C 651'	3.85	0.49	gage/ave	gage/ave
Ave S31/S33 MSL C 651'	3.62	0.45	94%	92%
Ave MSL C 621'	2.10	0.25	gage/ave	gage/ave
Ave S35/S35A MSL C 621'	2.56	0.34	122%	140%

			Range	RMS
			gage/ave	gage/ave
R1 = Average Overprediction of Signal		Average	111%	114%
From Table above			(MaxCDI)/ MaxQC2	(RMSCDI)/ RMSQC2
R2 = Min Predicted/Measured			112%	98%
Minimum Ratio of Predicted Dryer Load divided by Average Overprediction of Signal				
Ratio of R2 / R1			100%	86%

Table EMEB-B-18-1-4

From review of the CDI benchmark report the frequency comparison is better than the SMT benchmark for pressures that are above 10^{-4} $psid^2$ / Hz. The frequency match at the peak response is well within 10%. Therefore, the 20% frequency load uncertainty developed for VYNPS is +/-10% time step assessment remains valid.

The accuracy of the predicted load is based on relative location of sensing point in the steam line vs. the location of the sampling point used in the Benchmark Assessment. The following table compares the VY Sensing locations to those used in the SMT and QC2 Benchmarks.

Acoustic Model Pressure Sensor Location					
Facility	Description	MSL A	MSL B	MSL C	MSL D
VY Plant	Strain Gage Location (ft)	37.13	37.13	37.13	37.13
VY Plant	Venturi Line Entrance (ft)	96.84	80.88	80.88	96.84
GE SMT	P1 (ft)	1.474	1.391	1.391	1.474
GE SMT	P2 (ft)	4.438	5.094	5.161	4.438
GE SMT	P1 scaled By 17.3	25.50	24.06	24.06	25.50
GE SMT	P2 scaled By 17.3	76.78	88.13	89.29	76.78
QC2 Benchmark	Elev 651 (ft)	9.50	9.50	9.50	9.50
QC2 Benchmark	Elev 624 (ft)	41.00	41.33	41.33	41.00

Table EMEB-B-18-1-5

As noted the sensors in the QC2 benchmark were closer to the reactor steam nozzles than they are in the VY plant. Therefore due to acoustic losses in the steam line CDI performed an assessment of the uncertainty introduced in the benchmark load associated with this difference in location and the difference in optimal QC damping developed from the steam line QC 2 benchmark and the damping used in the VY model. The maximum uncertainty in QC nozzle loads from the assessment included in Attachments 1, 2, and 3 was an RMS uncertainty of 53%.

Maximum Uncertainty of the ACA Methodology

From this evaluation of the VYNPS SMT benchmark, QC2 benchmark, the VYNPS load step sensitivity results based on uncACM1 is calculated by the SRSS method to be 59%.

Bounding Uncertainties		
ACM Benchmark Uncertainty	QC2 790 BM	VY SMT BM
Frequency Peak Uncertainty	20	20
Minimum RMS/Max Uncertainty	14	5
Sensor Location uncertainty	53	N/A
SRSS of Uncertainty	59	21

Table EMEB-B-18-1-6

Uncertainty Introduced by the Measurement Method

A parametric study was performed by CDI to assess the variation in VYNPS dryer loads as a function of variation in input data magnitude. This study provided nine sets of time history loads across the dryer. The first set is the base case used in the analysis of the VYNPS dryer. The balance varied each of the eight sets that were derived by varying one input parameter by 10% and determined the impact on the dryer transient loads.

From the structural analysis it was observed that the dryer response under the acoustic loads was driven by loads on the vertical face of the dryer. The PSD of the dryer loads shown in CDI Report 05-06 shows that there are no outstanding acoustic signals of note from 0 through 200 Hz. The dryer load could be characterized as a broad band signal. Therefore, to assess the impact of input variations on dryer loads, peak response and RMS values were used to assess the change in dryer load as a function of input change. Points 7 and 99 as shown in Figure 9 of CDI report 05-06 are at the location of maximum

RMS and peak pressures on the dryer face. Therefore, these points were used in the assessment. The result of the CDI parametric evaluation is included as Attachment 1. Table EMEB-B-18-1-1-1 and 1-2 provide copies of the final values:

The venturi measurement uncertainty is driven by four sources:

1) UncVent1: The uncertainty acoustic modeling and methodology used to develop the transfer function of the sensing lines.
2) UncVent2: The uncertainty in the dynamic properties of the Rosemount transmitters mounted on the sensing lines, referred to here as compliance.
3) UncVent3: The accuracy of the instrumentation used in the mockup testing.
4) UncVent4: The accuracy of the instrumentation used to collect the plant data.

These uncertainties are then combined by the SRSS method to assess the venturi measurement uncertainty for both the RMS and maximum response of the signal.

$$UncVent=Sqrt\ (UncVent1^2 + UncVent2^2 + UncVent3^2 + UncVent4^2)$$

Attachment 2 provides the methodology to assess UncVent1, the transfer function uncertainty and UncVent2 the uncertainty in the steam transfer function as a function of the uncertainty in the Rosemount compliance.

The transfer function uncertainty was calculated based on evaluations performed on four steam line signals from QC2. In this uncertainty assessment Entergy used the maximum value from the four tests.

The Rosemont transmitters have isolation diaphragm that can be included in the steam acoustic model of the sensing system as a mass/spring/damper. The spring is the most important parameter and the combined characteristics are referred to as compliance. In CDI 95-06 the compliance values were based on published values by Rosemount along with detailed and proprietary information on the construction of the Rosemount transmitter that pertains to characterizing the dynamic properties of the transmitter. There was no uncertainty information available from Rosemount on the published stiffness data. The information supplied by CDI in Attachment B represents the change in the transferred signal based on a 1% change in the 100% compliance (value provided by the manufacturer). This acoustic load uncertainty assessment assumed an uncertainty of 30% in the compliance, UncVent2.

The test instruments used in the CDI mockup and the VYNPS plant were Sensotec high speed pressure transducers (0.25% accuracy) with a 16 bit data acquisition system. An uncertainty of 5% was used as a conservative bound to this equipment's uncertainty. It should be noted that the total uncertainty is primarily influenced by the transfer function uncertainty, uncVent1. Because the compliance uncertainty and pressure instrument uncertainty have a small impact on the total uncertainty, further refinement of these values was not deemed necessary.

Venturi RMS Signal Uncertainty							
		UncVent(RMS)	UncVent1	UncVent2		UncVent3	UncVent4
		Venturi Line Total Uncertainty	Maximum Transfer Function Uncertainty	Instrument Compliance Uncertainty	Transfer Function Error Due to % Compliance Uncertainty	Uncertainty due to Instrument Error at Mockup	Uncertainty due to Instrument Error at in Plant
A	Venturi Inlet	179%	177%	30%	82%	5.00%	5.00%
B	Venturi Inlet	177%	177%	30%	33%	5.00%	5.00%
C	Venturi Inlet	177%	177%	30%	35%	5.00%	5.00%
D	Venturi Inlet	179%	177%	30%	86%	5.00%	5.00%
Venturi Maximum Signal Uncertainty							
		UncVent	UncVent1	UncVent2		UncVent3	UncVent4
		Venturi Line Total uncertainty	Maximum Transfer Function Uncertainty	Instrument Compliance Uncertainty	Tranfser Function Error Due to % Compliance Uncertainty	Uncertainty due to Instrument Error at Mockup	Uncertainty due to Instrument Error at in Plant
A	Venturi Inlet	128%	128%	30%	25%	5.00%	5.00%
B	Venturi Inlet	128%	128%	30%	23%	5.00%	5.00%
C	Venturi Inlet	128%	128%	30%	32%	5.00%	5.00%
D	Venturi Inlet	128%	128%	30%	30%	5.00%	5.00%

Table EMEB-B-18-1-7

Uncertainty in the dryer loads is driven by uncertainty in the input pressure as calculated from VYNPS SG data. The uncertainty is from two sources:

a. UnSG1: The uncertainty of using the VYNPS equipment to measure pressure in the pipe. Entergy has used strain gages and a National Instrument DAS acquisition to collect stain gage data and correlate that data to average hoop strain and pressure. This uncertainty value includes the uncertainty of the strain acquisition equipment and the uncertainty in pipe thickness.
b. UncSG2: At very low strain levels, data from QC2 demonstrated that the dynamic signal can vary azimuthally around the pipe. VYNPS has two strain gages orientated in the hoop direction at one azimuth location. Data from QC2 with four strain gages 90 degrees apart demonstrate that when there are high flow

induced vibration (FIV) signals the local pipe distortion can add significant content to the signal. This uncertainty is added to reflect the non-conservative uncertainty introduced by using a single strain input to assess average circumferential strain.

The UncSG1 uncertainty values were developed by Structural Integrity Associate (SIA) in Calculation VY-13Q-305. Based on VYNPS pipe thickness data and the accuracy of the VYNPS SG data acquisition equipment, SIA calculated a measurement uncertainty of 8.74%. We therefore conservatively assigned UncSG1 = 10%.

On QC2 Exelon collected data 4 (¼ bridge) temporal SG signals at pipe locations for a total of 16 signals. Data from QC2 with four strain gages 90 degrees apart, demonstrate that when there are high FIV signals, the local pipe distortion can add significant content to the signal.

To assess the uncertainty the strain from the four strain gages at each location was averaged and compared, with the data from each SG. That evaluation is included in the following table. As noted, both the RMS and range data from a single strain gage are, in all cases, more conservative than the averaged data. Entergy has elected to conservatively assign a 10% uncertainty to the UncSG2 value for VYNPS.

Summary of QC 2 data Comparing Averaged SG Data to the data from Each Gage				
	Range	RMS	Range	RMS
Ave MSL B 651'	3.28	0.39	gage/ave	gage/ave
S7	4.42	0.49	35%	26%
S9	4.99	0.68	52%	75%
S8	3.78	0.50	15%	30%
S10	5.68	0.76	73%	98%
	Range	RMS	Range	RMS
Ave MSL B 621'	2.47	0.30	Gage/ave	gage/ave
S11	4.74	0.58	92%	96%
S11A	3.03	0.38	23%	30%
S12	4.30	0.51	74%	72%
S12A	4.77	0.60	93%	104%
	Range	RMS	Range	RMS
Ave MSL C 651'	3.85	0.49	Gage/ave	gage/ave
S31	4.03	0.58	5%	18%
S33	5.96	0.58	55%	17%
S32	5.77	0.87	50%	77%
S34	5.73	0.75	49%	51%
	Range	RMS	Range	RMS
Ave MSL C 621'	2.10	0.25	Gage/ave	gage/ave
S35	3.04	0.38	45%	54%
S35A	4.30	0.58	104%	136%
S36	3.84	0.50	83%	103%

S36A	4.48	0.54	113%	118%
			Range	RMS
			Gage/ave	gage/ave
		Minimum	5%	17%
		Maximum	113%	136%

Table EMEB-B-18-1-8

These uncertainties were combined by the SRSS method to assess the SG Measurement Uncertainty for both the RMS and Maximum Response of the signal. The resulting strain gage signal uncertainty values are summarized in the table below. Note these values are the same for the four steam lines.

Strain Gage (SG) RMS Signal Uncertainty				
		UncSG	UncSG1	UncSG2
		SG Signal Total Uncertainty	SG Uncertainty due to Instrument and Thickness	SG Uncertainty due to 1 vs 4 SG Sensors
A	StrainGage	14%	10%	10%
B	StrainGage	14%	10%	10%
C	StrainGage	14%	10%	10%
D	StrainGage	14%	10%	10%
Strain Gage (SG) Maximum Signal Uncertainty				
		UncSG	UncSG1	UncSG2
		SG Signal Total Uncertainty	SG Uncertainty due to Instrument and Thickness	SG Uncertainty due to 1 vs 4 SG Sensors
A	StrainGage	14%	10%	10%
B	StrainGage	14%	10%	10%
C	StrainGage	14%	10%	10%
D	StrainGage	14%	10%	10%

Table EMEB-B-18-1-9

In the following Tables the SG RMS and venturi RMS signal uncertainties for each line are multiplied by the sensitivity values to determine the impact on dryer loads. Because the transfer function uncertainty could be related to a common characteristic of the ACA of the sensing line, the venturi uncertainty from each of the four lines is first added by absolute sum. Then this absolute sum is combined by the SRSS method with the affect of the SG uncertainty on each line to find the total load uncertainty due to signal error on each side of the dryer. This is done to both RMS and maximum uncertainty values. Then the maximum uncertainty value determined from both sides of the dryer and both the RMS and maximum uncertainties is used to represent the uncertainty on dryer loads due to signal uncertainty.

Dryer Load Uncertainty due to Venturi RMS Signal Uncertainty						
		P7 Side	P99 Side	Del Ld/Del Signal	Del Ld/Del Signal	Venturi Line Total Uncertainty
		Un=F1 x TU	Un=F2 x TU	F1	F2	TU
A	Venturi Inlet	0%	4%	0	0.024	179%
B	Venturi Inlet	0%	37%	0	0.208	177%
C	Venturi Inlet	48%	0%	0.27	0	177%
D	Venturi Inlet	3%	0%	0.014	0	179%
	abs sum	50%	41%			
Dryer Load Uncertainty due to Strain Gage SG RMS Signal Uncertainty						
		P7 Side	P99 Side	Del Ld/Del Signal	Del Ld/Del Signal	SG Signal Total Uncertainty
		Un=F1 x TU	Un=F2 x TU	F1	F2	TU
A	Strain Gage	0%	6%	0	0.397	14%
B	Strain Gage	0%	6%	0	0.403	14%
C	Strain Gage	5%	0%	0.374	0	14%
D	Strain Gage	5%	0%	0.372	0	14%

Dryer Load Uncertainty due to Venturi Maximum Signal Uncertainty						
		P7 Side	P99 Side	Del Ld/Del Signal	Del Ld/Del Signal	Venturi Line Total uncertainty
		Un=F1 x TU	Un=F2 x TU	F1	F2	TU
A	Venturi Inlet	0%	1%	0	0.01	128%
B	Venturi Inlet	0%	39%	0	0.307	128%
C	Venturi Inlet	14%	0%	0.106	-0.001	128%
D	Venturi Inlet	1%	0%	0.011	-0.001	128%
	abs sum	15%	40%			
Dryer Load Uncertainty due to Strain Gage SG Maximum Signal Uncertainty						
		P7 Side	P99 Side	Del Ld/Del Signal	Del Ld/Del Signal	SG Signal Total Uncertainty
		Un=F1 x TU	Un=F2 x TU	F1	F2	TU
A	Strain Gage	0%	3%	0	0.24	14%
B	Strain Gage	0%	6%	0	0.444	14%
C	Strain Gage	5%	0%	0.36	0	14%
D	Strain Gage	7%	0%	0.521	0	14%
UncACM2 = SRSS Dryer Load Uncertainty					**P7 Side**	**P99 Side**
SRSS (ABS Venturi and SRSS SG RMS Signal Uncertainty)					**51%**	**42%**
SRSS (ABS Venturi and SRSS SG MAX Signal Uncertainty)					**17%**	**41%**
Bounding Uncertainty RMS, Max, Either Side					**51%**	

Table EMEB-B-18-1-10

Total ACM Uncertainty

Based on the Table presented below the total measurement uncertainty was calculated to be 78 %.

Final ACM Uncertainty	
UncACM1: Maximum Benchmark Uncertainty	59%
UncACM2: Signal Uncertainty	51%
SRSS(UncACA1, UncACA2)	78%

Table EMEB-B-18-1-11

Attachments

Attachment 1: CDI Parametric Assessment of Dryer Loads as a Function of Instrument Uncertainty

Attachment 2: CDI Uncertainty Assessment of Venturi Instrument Line Transfer Function

Attachment 3: CDI Uncertainty Assessment of Sensing Point Distance from RPV

Attachment 1
Vermont Yankee Error Analysis

The error analysis is carried out at locations on the outer bank hood directly between the steam lines at the cover plate elevation (low resolution node numbers 7 and 99). The acoustic circuit analysis can be used directly to access errors in load predictions based on errors in measurement. Using the 100% power data set, the change in predicted RMS pressures are computed as a function of changing the strain gage and venturi pressure measurements, with results shown in the first table. Results for a similar calculation, for predicted peak pressures, are shown in the second table.

Pressure Data Location on MSL	$\Delta\%(P_7/P_{7RMS}) / \Delta\%$	$\Delta\%(P_{99}/P_{99RMS}) / \Delta\%$
A Venturi Inlet	0.000	0.024
B Venturi Inlet	0.000	0.208
C Venturi Inlet	0.270	0.000
D Venturi Inlet	0.014	0.000
A Strain Gage	0.000	0.397
B Strain Gage	0.000	0.403
C Strain Gage	0.374	0.000
D Strain Gage	0.372	0.000
SRSS	0.593	0.603

Table EMEB-B-18-1-1-1
Sensitivity of RMS Dryer Loads to Errors in Main Steam Line (MSL) Pressures

Pressure Data Location on MSL	$\Delta\%(P_7/P_{7Peak}) / \Delta\%$	$\Delta\%(P_{99}/P_{99Peak}) / \Delta\%$
A Venturi Inlet	0.000	0.010
B Venturi Inlet	0.000	0.307
C Venturi Inlet	0.106	-0.001
D Venturi Inlet	0.011	-0.001
A Strain Gage	0.000	0.240
B Strain Gage	0.000	0.444
C Strain Gage	0.360	0.000
D Strain Gage	0.521	0.000
SRSS	0.642	0.591

Table EMEB-B-18-1-1-2
Sensitivity of Peak Dryer Loads to Errors in MSL Pressures

Attachment 2
Vermont Yankee Instrument Line Error Analysis

The instrument line error analysis is carried out by comparing the transfer function developed by the instrument line experiment and the instrument line acoustic circuit model (which was subsequently applied to the VY instrument lines). The instrument line experiment was patterned after the four venturi instrument lines in Quad Cities Unit 2; thus, the EPU data available from Exelon for these lines were used to compute the sensitivity of RMS and peak pressure predictions at the four main steam lines. Here, subscript "mod" refers to the transfer function developed by acoustic circuit methodology, while subscript "emp" refers to the transfer function developed empirically.

The rationale for the analysis is based on the premise that the venturi line mocked up in CDI's laboratories when modeled by acoustic circuit analysis introduces the same amount of uncertainty as would be introduced by modeling a venturi line in a plant. By experimentally measuring the transfer function (see Ref. B-1) with two transducer errors Δ_T, and comparing the pressure predicted at the MSL of Quad Cities Unit 2 computed from the ACM (P_{RMSmod}) to that computed using the empirically determined transfer function P_{RMSemp} (with error Δ_E) provides an estimate of the acoustic circuit error in correcting the venturi measurement. The error fraction $\Delta_{TransFunct}$ is shown for venturi data taken on all four lines (A-D)

Results are shown in the following tables.

Pressure Data Location	$\lvert(P_{RMSmod}-P_{RMSemp}) / P_{RMSemp}\rvert = \Delta_{TransFunct}$
A Venturi	0.475
B Venturi	0.639
C Venturi	0.581
D Venturi	0.278
Average	0.493

Table EMEB-B-18-1-2-1
Error RMS MSL Pressures to Transfer Function Accuracy in Instrument Lines

Pressure Data Location	$\lvert(P_{Peakmod}-P_{Peakemp}) / P_{Peakemp}\rvert = \Delta_{TransFunct}$
A Venturi	0.524
B Venturi	0.561
C Venturi	0.434
D Venturi	0.321
Average	0.460

Table EMEB-B-18-1-2-2
Error Peak MSL Pressures to Transfer Function Accuracy in Instrument Lines

Compliance Effects

The tests conducted as described in Ref. B-1 did not include transducers that exist on branch lines on the instrument racks. However, manufacturer supplied data indicate that these transducers in the frequency range (0-200 Hz) introduce a compliance (spring) into the system.

The compliance error analysis is carried out by running the instrument line code for various percent compliance ($\Delta\%$), and computing the sensitivity of RMS and peak pressure predictions at the four main steam lines. Results are shown in the following tables.

Pressure Data Location	$\lvert \Delta\%(P/P_{RMS}) / \Delta\% \rvert$
A Instrument Line	0.817
B Instrument Line	0.330
C Instrument Line	0.347
D Instrument Line	0.864
Average	0.590

Table EMEB-B-18-1-2-3
Sensitivity of RMS MSL Pressures to Compliance in Instrument Lines

Pressure Data Location	$\lvert \Delta\%(P/P_{Peak}) / \Delta\% \rvert$
A Instrument Line	0.251
B Instrument Line	0.233
C Instrument Line	0.319
D Instrument Line	0.296
Average	0.275

Table EMEB-B-18-1-2-4
Sensitivity of Peak MSL Pressures to Compliance in Instrument Lines

The total error in RMS measured venturi instrument line data corrected to the main steam line consists of four terms:

$$\text{Error} = \text{SRSS}\left(\Delta_T + \lvert \Delta_{TransFunct} \rvert + \Delta_e + \left| \frac{\Delta\%(P/P_{RMS})}{\Delta\%} \right| \times \Delta_C\right)$$

where Δ_T is the pressure transducer error, associated with the measurement of the empirically determined transfer function, $\Delta_{TransFunct}$ is the transfer function error provided in Tables EMEB-B-18-1-2-1 and 2, Δ_e is the pressure measurement error of the transducer in the plant, and $\left|\dfrac{\Delta\%(P/P_{RMS})}{\Delta\%}\right|$ is the sensitivity of compliance error provided in Tables EMEB-B-18-1-2-3 and 4. The last term is multiplied by Δ_C, the compliance error as a fraction of the compliance specified by the manufacturer.

Attachment 3
Vermont Yankee Instrument Position Uncertainty

With pressures measured at two locations on a MSL, it is possible to compute the pressure at a third location. This is used to estimate the error associated with measuring the pressure on the MSL at the venturi location which is further downstream than strain gage pressure measurements which were made at QC1 and QC2.

The error analysis is carried out by first computing the pressure on the main steam lines at the same location of the first strain gage location in Quad Cities Unit 2 (9.50 feet from the steam dome), using the VY strain gage data (at 37.13 feet) and the pressure at the venturi instrument line entrance (at 96.84 feet for main steam lines A and D, and 80.88 feet for main steam lines B and C). Comparisons of this pressure are made with model predictions for the VY acoustic circuit model and the benchmarked acoustic circuit model with modeling parameters used for Quad Cities. The difference in prediction estimates the error associated with moving the measurement to the venturi location. An error analysis (for Quad Cities) showed that a 5.03% error in strain gage RMS pressure measurements results in a 3.56% change in RMS dryer loads. This factor (0.708) is then applied to the difference in predictions, and an error associated with instrument locations is determined, as shown in the table.

Venturi Location	$(P_{VY}-P_{QC})/P_{VY}$	Dryer Load Error Fraction
A	0.437	0.309
B	0.736	0.521
C	0.738	0.523
D	0.468	0.331
Average	0.595	0.421

Table EMEB-B-18-1-3-1
Error - RMS Dryer Loads to Instrument Position Uncertainty

Reference

B-1. "Test Report for Validating an Instrumentation Line Acoustic Transmission Model," Revision 0, CDI Report No. 04-12 prepared for Exelon Generation LLC, July 2004.

Exhibit EMEB-B-80-1

CDI Signal Offset

Vermont Yankee Nuclear Power Station

Proposed Technical Specification Change No. 263 – Supplement No. 31

Extended Power Uprate

Response to Request for Additional Information

ENGINEERING CALCULATIONS

Continuum Dynamics, Inc. Page 1 of 11

Subject/Title Pressure Data Correction

Revision Level 6

Contract No. F155

Preparer [signature] Date 2/3/05
Signature

Checker/Verifier [signature] Date 3Feb2005
Signature

Objective of this Calculation To verify that VY pressure data has been corrected for the delay between Reactor Building and Strain Gage data acquisition systems. Corrected pressure data has been shifted in time and resampled. Corrected data stored in new data file.

Input Sources: (1) VY pressure (PT) data
(2) VY strain gage data
(3) Engineering calc "Plant Data Resampling Procedure"

Verification Method:

✓ Line by Line
Alternate Calculation
Parallel Analysis

Assumption:	Concurrence Needed?	Concurred by
none		

QA23a, Rev. 2, 9/93

Inputs –

1) strain gage data:

columns in text file
sampled at 1024 Hz

2) pressure data

column-oriented text files (e.g. prXXX-2.txt) — xxx = power level
sampled at 2000 Hz
shifted relative to strain gage data by time τ

Procedure –

1) Using common channel between strain gage & reactor building systems, (high speed venting signal – column 5 in pressure data & column C in strain gage data), calculate time delay from phase of cross-spectrum as follows

$$\text{phase} = 2\pi f \tau$$

f = frequency in Hz
τ = time shift (+ve if pressure leads strain pressure)

See write-up on following pages for add'l discussion. Verify by alternate analysis (check plots)

2) Corrected (shifted) pressure data is resampled using Matlab "resample" function from 2000 Hz to 1024 Hz. Approach verified in input source [3].

3) Output corrected (shifted & resampled) data to text file with file name

prxxx-2-corr.txt — xxx = power level

p3/11

Since pressure and strain gage data were acquired independently, but contained a common signal (high speed venturi in MSL A), it is possible to correct the data for the time delay to account for the phasing between signals when analyzing the data. The pressure data from the reactor building was corrected to accommodate the analysis by resampling the data from 2000 samples per second to the strain gage sample rate of 1024 samples per second and shifting the data in time by a constant delay. Note that the pressure data were filtered before resampling to minimize aliasing of the high frequency content in the original pressure data. The delays were determined by analyzing the common channel in the frequency domain to estimate the phase delay based on spectral analysis methods. The estimated time delays are tabulated in Table A below and were typically less than 1 second. A comparison between the estimated phase delay between the uncorrected and corrected pressure data and the duplicate signal in the strain gage data acquisition system are plotted in Figures V through Z for plant power levels of 100%, 95%, 90%, 85%, and 80%. Note that the phase delay for the uncorrected data increases linearly with frequency, which is expected for a pure time delay. The phase delay for the corrected data is approximated zero, which confirms that the data are properly corrected for the time delay.

— using Matlab "resample" [illegible] [illegible] [illegible] high [illegible]
JSK 2/1/5

Table A: Summary of estimated time delays between measured reactor building pressure and strain gage data (positive delay implies that the pressure data leads the strain gage data).

Plant power	Test number	Delay, sec
80%	1	0.639
80%	2	0.462
80%	3	0.512
85%	1	-0.96
85%	2	0.444
85%	3	0.0451
90%	1	1.161
90%	2	0.196
90%	3	0.766
95%	1	0.0256
95%	2	0.750
95%	3	0.689
100%	1	0.889
100%	2	0.404
100%	3	0.170

Only datasets used
JSK 2/1/05

C.D.I. NUCLEAR CONTRACT NO. F317
DONE BY JSK DATE 2/1/05
VERIFIED BY [illegible] DATE 3 Feb 2005

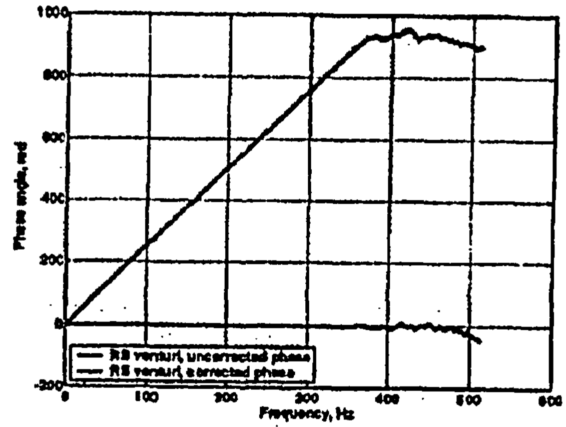

Figure V: Phase delay between uncorrected and corrected pressure data and duplicate signal in strain gage data acquisition system, 100% power, Test 2.

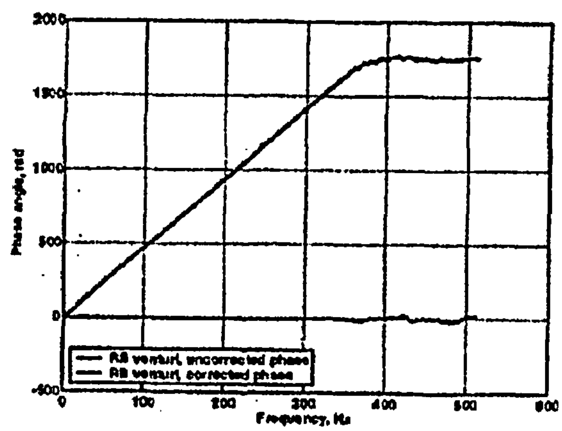

Figure W: Phase delay between uncorrected and corrected pressure data and duplicate signal in strain gage data acquisition system, 95% power, Test 2.

C.D.I. NUCLEAR CONTRACT NO. 5131
DONE BY SAS DATE 2/3/05
VERIFIED BY AB DATE 3/5/2005

p5/11

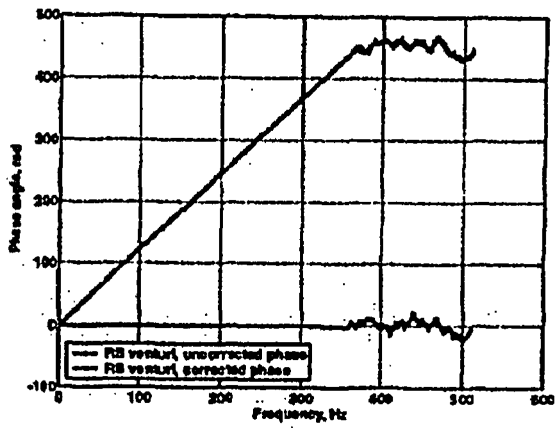

Figure X: Phase delay between uncorrected and corrected pressure data and duplicate signal in strain gage data acquisition system, 90% power, Test 2.

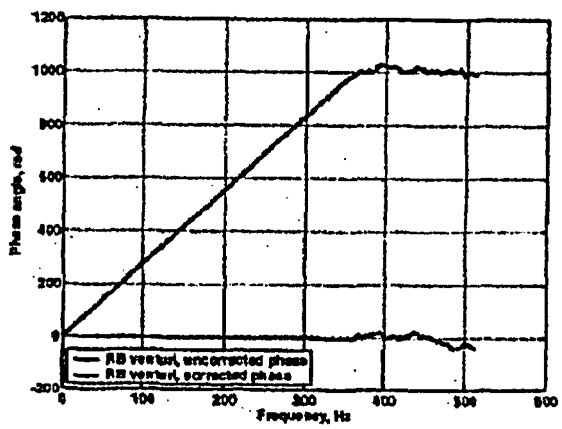

Figure Y: Phase delay between uncorrected and corrected pressure data and duplicate signal in strain gage data acquisition system, 85% power, Test 2.

C.D.I. NUCLEAR CONTRACT NO. F117
DONE BY JK DATE 2/3/05
VERIFIED BY JZ DATE 3/26/2005

pcl.

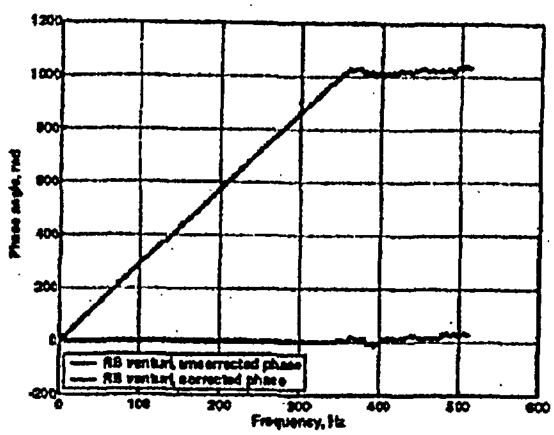

Figure Z: Phase delay between uncorrected and corrected pressure data and duplicate signal in strain gage data acquisition system, 80% power, Test 2.

C.D.I. NUCLEAR CONTRACT NO. F507
DONE BY SAX DATE 7/1/05
VERIFIED BY DT DATE 3 Feb 2005

p7/1

uncorrected : pr100_2.txt
corrected : pr100_2_cor.txt

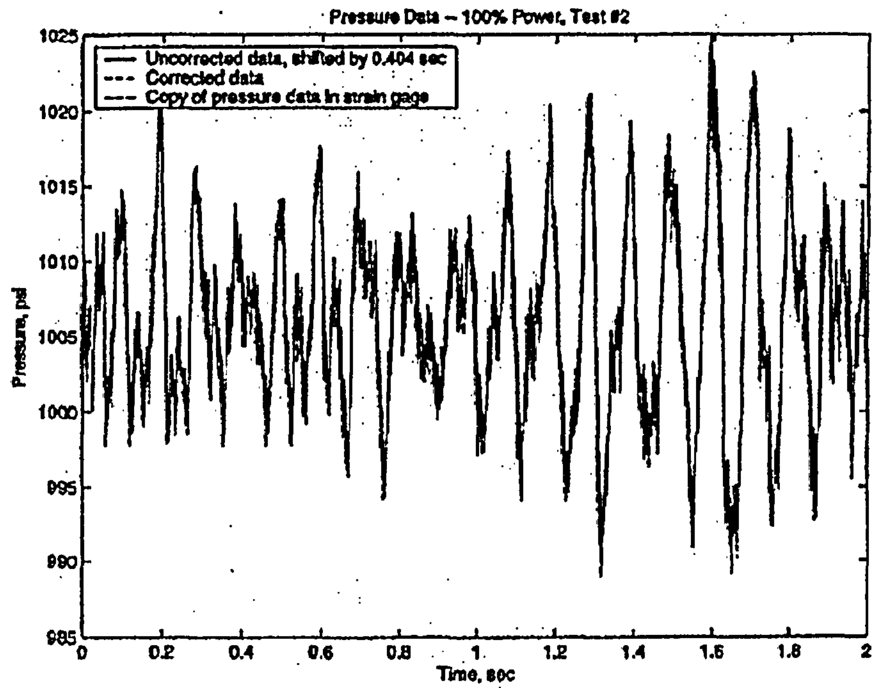

C.D.I. NUCLEAR CONTRACT NO. E3?
DONE BY SMK DATE 2/1/05
VERIFIED BY ___ DATE 3 Feb 2005

p 8/4

Uncorrected: pr095_2.txt
corrected: pr095_2.corr.txt

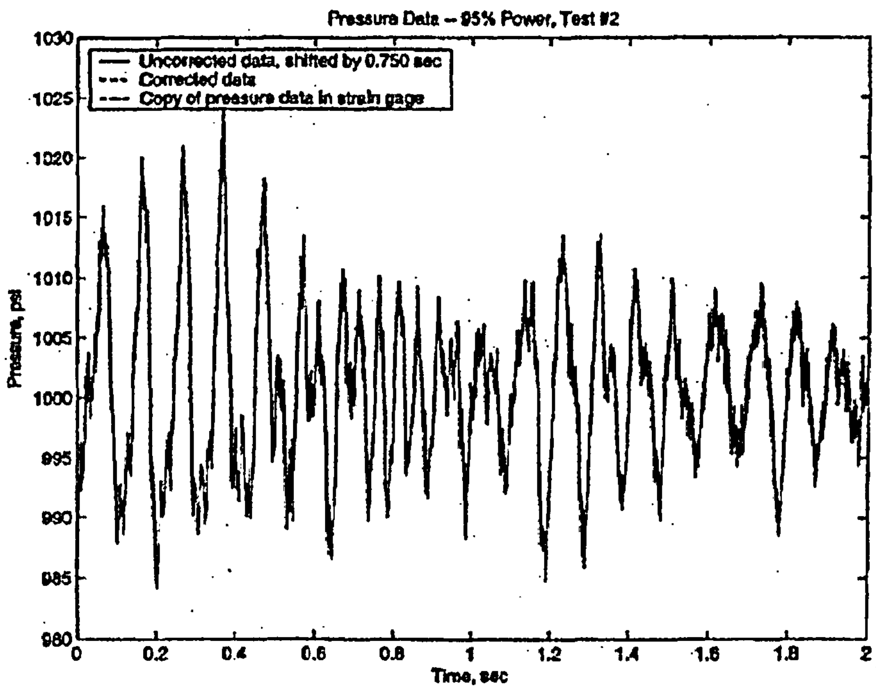

C.D.I. NUCLEAR CONTRACT NO. [illegible]
DONE BY [illegible] DATE [illegible]
VERIFIED BY [illegible] DATE 3 Feb 2005

p9/11

Uncorrected: prd6_2.txt
Corrected: prd6_2_corr.txt

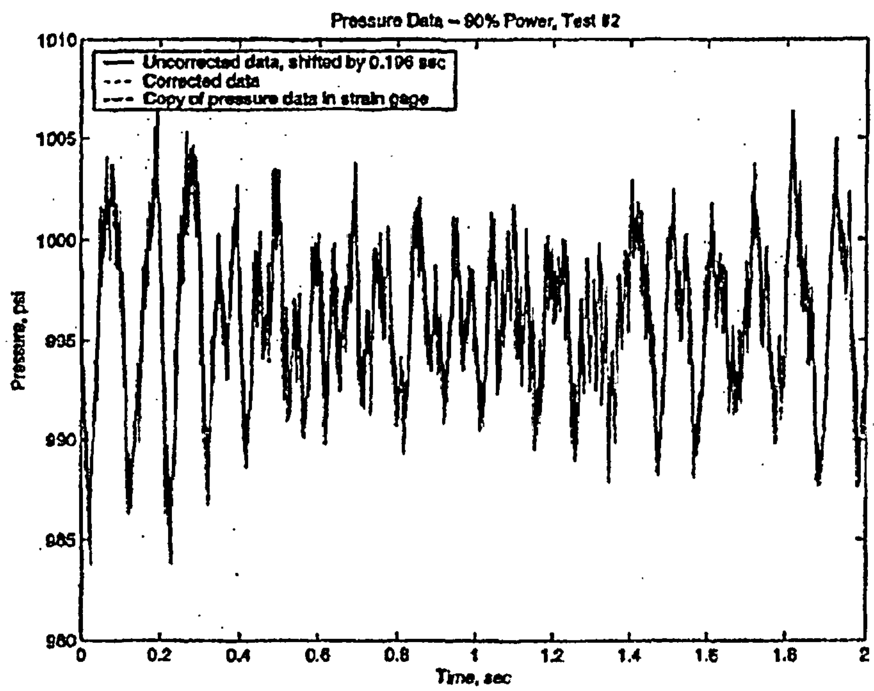

C.D.I. NUCLEAR CONTRACT NO. 5113
DONE BY SIK DATE 7/31/05
VERIFIED BY [illegible] DATE 8/5/05

p 16/16

Uncorrected : press_2.txt
Corrected : press_2.cor.txt

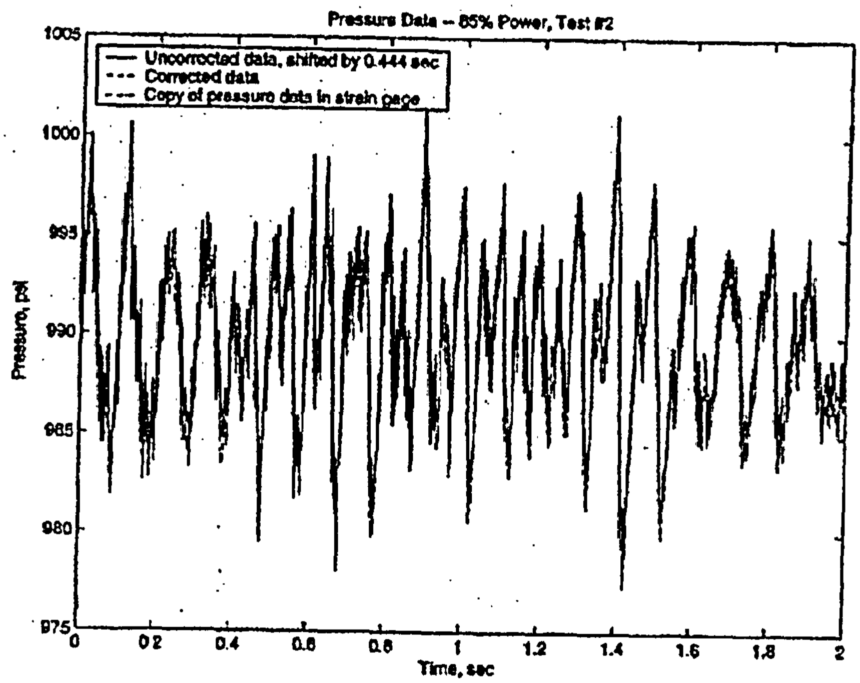

C.D.I. NUCLEAR CONTRACT NO.
DONE BY DATE
VERIFIED BY DATE

uncorrected: pr80-2.txt
corrected: pr680-2-corr.txt

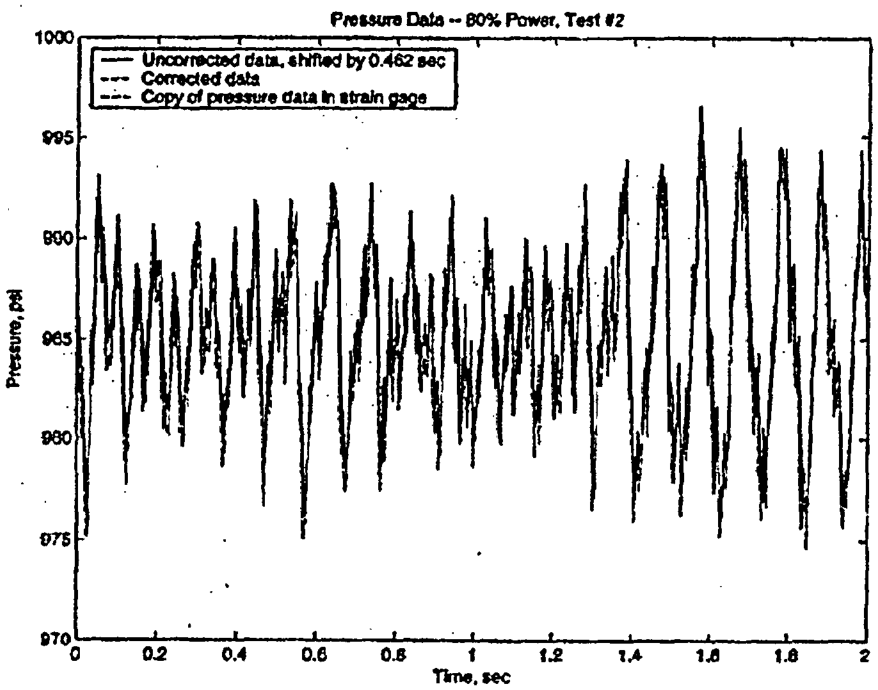

C.D.I. NUCLEAR CONTRACT NO. ____
DONE BY ____ DATE ____
VERIFIED BY ____ DATE ____

Exhibit EMEB-B-143-1

Revised FIV Stress Summary

Vermont Yankee Nuclear Power Station

Proposed Technical Specification Change No. 263 – Supplement No. 31

Extended Power Uprate

Response to Request for Additional Information

NON-PROPRIETARY VERSION

Exhibit EMEB-B-143-1: Revised FIV Stress Summary to Incorporate 100% and 120% CFD Transient Loads and Load Uncertainty

NON-PROPRIETARY VERSION

Overview

This Exhibit summarizes the updated structural analysis of the VYNPS dryer for CFD loads that include data at both 100% and 120% power conditions. The stress report submitted in Attachment 5 to Supplement 26 (BVY 05-034 dated March 31, 2005) included analysis for 100% power (CLTP) CFD data. That report included a structural review of 17 time point snap shot cases to assess the magnitude of turbulent forces in the VYNPS dryer plenum. After submitting the stress report Entergy and Fluent continued to run the CFD analysis over the next two months and developed dynamic, transient solutions for both the 100% (CLTP) and 120% (EPU) power conditions. The structural analysis was updated with the new CFD loads.

Entergy also performed +/-10% time step evaluations of the CFD loads to assess the sensitivity of the results for load and structural frequency uncertainty.

This Exhibit also summarizes the evaluation of Acoustic and CFD load uncertainty. This evaluation is applicable only to the VYNPS dryer analysis and reflects the specific measurement and analytical methods used by Entergy. These uncertainties were used to calculate an uncertainty value for the limit curve factor, for application to the power ascension to confirm the structural integrity of the VYNPS modified steam dryer. To respond to NRC questions about VYNPS methodology uncertainty, the final limit curve factor is determined by subtracting uncertainty from the most limiting factor of any dryer component. If the100% plant steam line data stays below the limit curve factor between 100% and 120% operation, the attached information demonstrates that Code limits will be met and structural integrity will be maintained. This response demonstrates that the VYNPS modified dryer maintains considerable margin against code limits even with bounding uncertainties applied.

Summary

The following conservative uncertainty values were determined for the CFD and acoustic loads used in this assessment:

CFD Load Uncertainty	16%
ACM Load Uncertainty	78%

The load factor shown below is the minimum load factor considering all dryer components and both 100% and 120% CFD load conditions that could be applied to the acoustic circuit loads to maintain the peak stress limits shown:

Acceptance Level	Level 1	Level 2
Peak Stress Limit	13,600 psi ASME C Limit LCF1	0.8 x 13,600 80% of ASME C Limit LCF2
Minimum Load Factor	6.8	5.2
Uncertainty of Load Factor	3.1	2.4
Load Factor Minus Uncertainty	3.7	2.8

Exhibit EMEB-B-143-1: Revised FIV Stress Summary to Incorporate 100% and 120% CFD Transient Loads and Load Uncertainty

NON-PROPRIETARY VERSION

The major contribution to the load factor uncertainty value [versus limit curve factor] is not from the acoustic circuit methodology but from the instrumentation and transfer functions associated with the steam line signals used as input.

Normally in fatigue analysis, mean values of expected loads are used. The margin for uncertainty is contained in the conservative fatigue limits included in the ASME Code. These contain a factor of two for stress and ten for the number of cycles. The load factor uncertainties shown above have been subtracted from the minimum load factors to demonstrate that the VYNPS modified steam dryer maintains considerable Code margin for EPU operation.

Discussion

The VYNPS steam dryer loads are generated from two fluid models; an acoustic circuit model (ACM) and a computational fluids dynamics model (CFD). Benchmarking of the ACM model demonstrated that it does a reasonable job of predicting loads above 20 Hz. Loading above 20 Hz is predominantly acoustic. The CFD model was used to establish the VYNPS load definition below 20 Hz, where fluid momentum effects are prevalent. Stress from both load cases are combined in the VYNPS dryer FIV assessment.

Development of CFD Loads

Transient data from the CFD simulation was saved at a .0001 sec time interval for dryer dP forces as well as steam line mass flow and other key parameters. Signal analysis of the new data demonstrated that the plenum region was experiencing more high frequency load content than indicated by the two discrete data points previously used to monitor results. Based on this difference, Entergy decided to use the new data to evaluate the dryer dynamically.

The CFD model was developed to depict hydrodynamic forces. The time step and model boundary conditions were selected to properly model hydrodynamic forces. The modeling however assumed compressible steam properties to provide a more realistic depiction of the turbulence at the outlet of the steam dome. The compressible properties also resulted in acoustic forces along with the hydrodynamic loads. The CFD load energy above 30 Hz, as depicted by the PSD charts in Attachment 1 to Supplement 29, is considered to predominantly reflect acoustic ringing.

Key stress results from three of the cases evaluated are summarized in Table EMEB-B-143-1-1, including:

- ACM results from the Supplement 26 stress report
- CFD analysis 100% power
- CFD analysis 120% power
- CFD analysis 120% power with a shortened time step. (The plus time step results were analyzed but not summarized because they had no increase to stress on limiting components.)
- CFD results for 100% and 120% power with filtered data

Exhibit EMEB-B-143-1: Revised FIV Stress Summary to Incorporate 100% and 120% CFD Transient Loads and Load Uncertainty

NON-PROPRIETARY VERSION

It is noted that the CFD stress is still low, but the transient analysis stress is higher than the static load developed from the original time point snap shot case data. There is not a significant difference between the stresses from CFD transient analysis at 100% and 120% power.

The time step change sensitivity assessment did not have a significant impact on the components most limiting from the standpoint of limit curve factor. The most limiting component was the modified top outer hood. Here the stress increased from 1112 psi to 1155 psi, or 4%.

The purpose of the CFD analysis was to define the hydrodynamic loads. The CFD model included compressibility and as a result a sizeable portion of the load above 30 Hz was determined to be acoustic ringing. The ACM model was used to define acoustic loads. To help characterize the impact of the CFD acoustic loads on the dryer stress the critical component of the CFD alternating stress was identified for all key stress locations. The stress data was then low-pass filtered at 30 Hz. A stress ratio was then calculated between the peak stress with filtering and peak stress before filtering. This ratio was then used to factor the CFD peak stress to remove the acoustic load.

These factored stresses are presented in the stress summary to help quantify the affect of hydrodynamic versus acoustic loads on fatigue stress. The significant reduction in the CFD stress supports the industry position that the important dryer loads are acoustic. The filtered stress was not used in the evaluation of combined stress or the limit curve factors presented here.

Calculation of FIV Loads

In order to address the issue of ACA load prediction capability at < 20 Hz and adequately quantify low frequency loads, Entergy decided to add the CFD hydrodynamic loads to the stress analysis. Since the acoustic signals in the VYNPS steam lines are very low the hydrodynamic forces could be a significant part of the dryer load.

Supplement 26 (BVY 05-034 dated March 31, 2005) reflected 17 time point snap shot load cases from the earlier CFD 100% run. The CFD loads were combined by absolute sum with the acoustic model stress results and compared with Code stress limits. This evaluation combines the results from the ACA and CFD transient analyses, two dynamic transient runs that are based on independent load sets. The SRSS combination is consistent with the VYNPS design basis for RPV internals. The acoustic and CFD loadings have frequency content that does not overlap. Therefore, a SRSS approach to combine the calculated stresses from these two sources is justified. Also, the SRSS approach is typically used to combine responses from various dynamic loads. For conservatism the maximum alternating value from each load set without credit for stress orientation is used.

Exhibit EMEB-B-143-1: Revised FIV Stress Summary to Incorporate 100% and 120% CFD Transient Loads and Load Uncertainty

NON-PROPRIETARY VERSION

Stress Equation for FIV Loads:

$$(CFD^2 + (LCF*ACM)^2)^{1/2} *Wf * Sif = Lf * Salt$$

Where:

LCF= Limit Curve Factor

Lf = Code Factor

Lf (Limit Curve 1)= Lf = 1.0

Lf (Limit Curve 2)= Lf = 0.8

Salt = Allowable Alternating Stress=13,600 psi

Wf=Weld Geometry Factor

Sif= Stress Intensification Factor

CFD = half the stress range from ANSYS analysis for CFD transient loads, psi. Both 100% power and 120% power were used.

ACM = half the stress range from ANSYS analysis for ACM transient loads, psi. Based on Plant 100% power Steam Line Data.

The stress summaries for the ACA loads with 100% and 120% CFD Loads are included in Tables EMEB-B-143-1-2 and EMEB-B-143-1-3. The stress summaries for ASME load combinations at selected locations and comparison with allowable values are shown in Tables EMEB-B-143-1-4 (a) through (g) for CLTP case. Tables EMEB-B-143-1-5 (a) through (g) show the corresponding values for the EPU case (120% power).

Note that the following revisions were considered in these revised tables:

- The FIV primary stress now includes weld size factor when combining with other loads to obtain total stress
- The faulted condition load combinations in these tables include the revision where combinations D3 and D4 include FIV stress instead of combinations D1 and D2.
- The acoustic and CFD stresses are combined by the square-root-of-sum-of-squires (SRSS) method rather than by conservative absolute sum method used in the March 2005 stress report.

The design basis event for Level D is the main steamline break outside containment. There are two basic load combinations on the dryer for this event. The first load combination is the acoustic rarefaction wave that is generated by the pipe opening. The second load combination is the two-phase level swell impact caused by the flashing of the water in the RPV. These two loads are separated in time and are analyzed

Exhibit EMEB-B-143-1: Revised FIV Stress Summary to Incorporate 100% and 120% CFD Transient Loads and Load Uncertainty

NON-PROPRIETARY VERSION

separately. Load combinations D1 and D2 represent the level swell impact phase of the event. Load combinations D3 and D4 represent the acoustic wave impact phase of the event.

Earlier the load combinations D1 and D2 had the FIV stress included. However, the FIV stress need not be included in these combinations because the level swell in the annulus between the dryer and vessel wall and subsequent introduction of two-phase flow in the steamline will disrupt the acoustic sources that dominate the FIV load component.

On the other hand, for load combinations D3 and D4, where the acoustic loading from postulated break is considered, the FIV loading needs to be included. The arrival of the acoustic wave is the first indication to the dryer that the break has occurred. At the time of the acoustic wave impact, the normal operation DP and the normal operation FIV loads are present; therefore, FIV is now included in the faulted combinations D3, D4.

Method of Solution Considering Uncertainty

In the development of the limit curve factor, the following methodology was utilized to evaluate the uncertainty in this factor. Given $a \pm \sigma_a$ and $b \pm \sigma_b$, the following methodology is used by Entergy to evaluate the propagation of errors.

Addition

$$Q = a + b$$

$$\sigma_Q = [(\sigma_a)^2 + (\sigma_b)^2]^{1/2}$$

Subtraction

$$Q = a - b$$

$$\sigma_Q = [(\sigma_a)^2 + (\sigma_b)^2]^{1/2}$$

Multiplication

$$Q = a \cdot b$$

$$\sigma_Q = a \cdot b \cdot [(\sigma_a/a)^2 + (\sigma_b/b)^2]^{1/2}$$

Square

$$Q = a^2$$

$$\sigma_Q = a \cdot a \cdot [(\sigma_a/a)^2 + (\sigma_a/a)^2]^{1/2}$$

$$\sigma_Q = \mathrm{sqrt}(2)\, a^2 \cdot (\sigma_a/a)$$

Exhibit EMEB-B-143-1: Revised FIV Stress Summary to Incorporate 100% and 120% CFD Transient Loads and Load Uncertainty

NON-PROPRIETARY VERSION

Division to Assess Minimum Value (Minimum of Q-σ_Q)

$Q = a / b$

$\sigma_Q = a / b - (a-\sigma_a) / (b+\sigma_b)$

Evaluation of the limit curve factor with load uncertainty

Stress Equation for FIV Loads:

$(CFD^2 + (LCF*ACM)^2)^{1/2} *Wf * Sif = Lf * Salt$

Rearranging, the limit curve factor is derived:

$LCF = [((Lf*Salt)/(Wf*Sif))^2 - CFD^2)^{1/2}]/ACM$

Load Uncertainty Rations

UncCFD = CFD Load Uncertainty Ratio
= s_{cfd} / CFD (expressed in percent).

UncACM = ACM Load Uncertainty Ratio
= s_{acm} / ACM (expressed in percent).

Conservative code SIF and Code allowable limits maintained.

Step 1 solve the following term:

$a1= ((Lf*Salt)/(Wf*Sif))^2 - CFD^2)$

The only uncertainty term to consider here is with the CFD term.

The uncertainty associated with CFD^2 is expressed as

$s_1 = sqrt(2) * CFD^2 * s_{cfd} / CFD = sqrt(2) * CFD^2 * UncCFD$

Step 2 solve the following term:

$a2= ((Lf*Salt)/(Wf*Sif))^2 - CFD^2)^{1/2} = (a1)^{1/2}$

Here it is necessary to assess the uncertainty associated with performing the square root of a1. This is expressed as the inverse of the square expression used in step 1.

$s_2 = (s_1 * a2)/ (sqrt(2) * a1)$

NON-PROPRIETARY VERSION

Step 3 solve the following term:

$LCF = [((Lf*Salt)/(Wf*Sif))^2 - CFD^2)^{1/2}]/ACM$

a3= a2/ACM

Here it is necessary to assess the uncertainty associated with performing division.

$s_3 = a2 / a3 - (a2 - s_2) / (ACM + s_{acm})$

$s_{acm} = UncACM * ACM$

$s_3 = a2 / a3 - (a2 - s_2) / (ACM + UncACM * ACM)$

Development Uncertainty Values used in this assessment

The ACM uncertainty was calculated in 78% in the ACA Uncertainty assessment included as Exhibit EMEB-B-18-1. Based on information from the CFD model sensitivity evaluation, Entergy has determined a CFD uncertainty value of 15% for the projected CFD loads. The comparison of the turbulence energy in the LES runs was shown to be higher than in RANS comparison runs. The CFD analysis with the +/- 10% change in load step had an impact to the limiting stress of 4%. Therefore the CFD frequency uncertainty is determined to be 4%. The total CFD uncertainty; uncCFD= sqrt(15^2 + 4^2) = 16%.

In Supplement 26, load step run was used to find the maximum acoustic load stress on the dryer. When looking at uncertainty it is more appropriate to express the nominal stress based on the best estimate of load and structural frequencies and use of the +/- time step solutions to assess the uncertainty in the stress as a result of the frequency uncertainty. Therefore Table 5.1-2 of Attachment 5 to Supplement 26 has not been revised for this update.

Based on CFD/ACM load uncertainties of 16% and 78% respectively, Tables EMEB-B-143-1-2 and EMEB-B-143-1-3 provide a summary of the limit curve factors and limit curve factor uncertainty for ACA loads combined with both the CFD 100% power and CFD 120% power loads. The most limiting values from these two assessments were used as the final recommended values included in the summary above.

The derived uncertainty in the acoustic loading is 78% and that in the CFD loading is 16%. Thus the acoustic loading stress was increased by 78% and the CFD loading stress was increased by 16% and then combined by SRSS method. The results at one limiting location are shown in Table EMEB-B-143-6. It is seen that there is still significant margin to allowable. The limiting primary stress margin (for Load Combination B3) case was further evaluated to determine the margin for ACM load.

It was determined that for the B3 load combination, the available margin to allowable stress is 171% in terms of the overall FIV stress. In other words, the FIV stress of 872 psi can increase by 171% before the allowable upset condition stress of 20588 psi is reached. It is noted that the calculated FIV stress of 872 psi already includes a 78% uncertainty on the acoustic stress and 16% uncertainty on the CFD stress.

The limiting component for ACM increase is B3 for the Long Gussets. The ACM available margin to allowable stress is 289% in terms of the overall FIV stress (see Table EMEB-B-143-7). In other words, the FIV stress can increase by a factor of 3.89 before the allowable upset condition stress of 20588 psi is reached. It is noted that the calculated FIV stress of 1943 psi already includes a 78% uncertainty on the acoustic stress and 16% uncertainty on the CFD stress. This clearly illustrates that even at the limiting location, significant structural margin exists to compensate any unforeseeable change in calculated acoustic loading stress. In addition the pressure stress used in the level B evaluation is based on a conservative value (see Appendix A). The 3.89 factor is higher than the minimum factor minus uncertainty (3.7) calculated for the fatigue stress assessment. Therefore fatigue margin is controlling in terms of ACM loading.

Assessment of Structural Response to CFD transient Loads

The PSD plots CFD load time histories are shown in Figures EMEB-B-143-1-1 and EMEB-B-143-1-2. These figures demonstrate that the CFD load has significant frequency content above 30 Hz. Of particular importance for the dryer is the load peak at 62 Hz. Figure EMEB-B-143-1-3 provides a PSD for key stress locations under the CFD load condition. Most of the frequency content of the stress is at 62 Hz.

Figure EMEB-B-143-1-4 depicts the transient response of a key stress component. Here again the sinusoidal response demonstrates that most of the response is at 62 Hz. The structural response is also shown for the +/- time step sensitivity assessments. The results indicate shortening of the load period, corresponding to the 0.7273 millisecond time step, results in higher stresses. Lengthening the load period by 10% has relatively little impact. The PSD spectrum of Figure EMEB-B-143-1-3 shows energy peaks at 46, 55 and 62 Hz. The 55Hz peak is relatively minor.

The structural mode shapes with a strong component normal to the front face are shown in Figures EMEB-B-143-1-5, EMEB-B-143-1-6 and EMEB-B-143-1-7. Of particular note is mode 22 shown in Figure EMEB-B-143-1-6. This mode has a frequency of 62.7 Hz, well aligned with the 62 Hz peak in the CFD load.

The overall effect of shortening the load period is to 'push' these peaks upwards in frequency with resultant higher stresses. Lengthening the load period 'pushes' these peaks downwards in frequency. In both instances, the 62 Hz peak continues to contribute, but the 46 and 55 Hz peaks are further away from the 62.7 Hz with lengthened load period and closer with shortened load period.

Exhibit EMEB-B-143-1: Revised FIV Stress Summary to Incorporate 100% and 120% CFD Transient Loads and Load Uncertainty

NON-PROPRIETARY VERSION

Table EMEB-B-143-1: ANSYS Stress Results, Alternating Stress Amplitude		ACM CLTP Max Surface Stress (psi)	Acoustic Mem-brane Stress (psi)	Vortex Shedding Max Surface Stress (psi)				
				CFD 100% Pwr	CFD 120% Pwr	CFD at 120% 10% Time Step	CFD 100% Pwr Filterd >30 Hz	CFD 120% Pwr Filtered >30 Hz
	Horizontal plates:							
1	Inner hood base plate	588	288	314	624	470		
2(a)	Modified outer cover plate5/8", both tips 4"	896	116	492	437	325	133	149
2(b)	Modified outer cover plate, exclude tips	530	75	492	439	325		
4(a)	Original top hood (all hood)	412	147	888	943	255		
4(b)	Modified top hood (outer hood)	403	71	935	1112	1155	94	167
4(c)	Hood top plates(Inner hood)	456	405	1987	1964	1555	40	39
	Vertical plates:							
5(a)	Original outer Hood, strips	989	173	68	108	96	3	2
5(b)	Modified outer hood, top weld	430	57	381	301	364	42	60
5(c)	Modified outer hood, bottom weld	475	130	621	725	260	81	131
5(d)	Hood vertical plates (inner hood)	484	123	1214	761	905		
6	Hood end plates.(inner hood)	446	319	1040	536	1273		
7	Hood end plates (outer hood)	1,029	340	713	322	185		
8	Outer Hood Brackets(gussets)	719	446	736	573	165	74	74
10	Steam 'dam'	399	16	818	807	730		
11	Steam 'dam' gussets	537	352	1598	941	793		
0	Other Plates							
12	Hood partition plates	288	116	149	94	233		
13	Baffle plates	686	24	1311	1144	2034	92	80
14	Outlet plenum ends	536	425	1806	1891	1411	54	95
0	Ring, Beams & Gussets							
15	Dryer support ring	527	not req	730	675	400		
16	Bottom cross beams	226	not req	368	135	274		
17	Cross beam gussets	626	40	778	414	1061		
	Gussets for outer Cover plate and hood							
18(c)	New gusset on cover plate and front hood	1,071	952	730	820	907	204	221
18(a)	Gusset	350		1187	295	406	427	121
18(b)	Gusset foot weld to cover plate	471	440	599	490	244		

Table EMEB-B-143-1-1
ANSYS Stress Results, Alternating Stress Amplitude

Exhibit EMEB-B-143-1: Revised FIV Stress Summary to Incorporate 100% and 120% CFD Transient Loads and Load Uncertainty

NON-PROPRIETARY VERSION

Table EMEB-B-143-2: FIV Alternating Stress Summary with Hydrodynamic (CFD) Loads 100% Power		Part A: Fatigue Stress Assessment CFD Loads 100% Pwr						
		ACM CLTP Max Surface Stress (psi)	Vortex Shedding Max Surface Stress (psi)	Weld Conc. Factor	Plate Thickness (in)	Weld Size (in)	Under-size Factor	Peak Stress (psi) (*1)
ID	Dryer Component Name	(1)	(3)	(5)			(6)	
	Horizontal plates:							
1	Inner hood base plate	588	314	1.8	0.5	0.5	1.00	1200
2(a)	Modified outer cover plate5/8", both tips 4"	896	492	1.8	0.625	0.625	1.00	1840
2(b)	Modified outer cover plate, exclude tips	530	492	1.8	0.625	0.5	1.56	2034
4(a)	Original top hood (all hood)	412	888	1.8	0.5	0.5	1.00	1762
4(b)	Modified top hood (outer hood)	403	935	1.8	1	0.625	2.56	4692
4(c)	Hood top plates(Inner hood)	456	1987	1.4	0.5	0.5	1.00	2854
	Vertical plates:							
5(a)	Original outer Hood , strips	989	68	1.8	0.5	0.5	1.00	1784
5(b)	Modified outer hood, top weld	430	381	1.8	1	0.625	2.56	2647
5(c)	Modified outer hood, bottom weld	475	621	1.8	-	-	-	2034
5(d)	Hood vertical plates (inner hood)	484	1214	1.4	0.5	0.5	1.00	1830
6	Hood end plates,(Inner hood)	446	1040	1.8	0.5	0.5	1.00	2037
7	Hood end plates (outer hood)	1029	713	1.8	0.5	0.5	1.00	2253
8	Outer Hood Brackets(gussets)	719	736	1.4	0.5	0.5	1.00	1440
10	Steam 'dam'	399	818	1.8	0.5	0.5	1.00	1638
11	Steam 'dam' gussets	537	1598	1.8	0.5	0.5	1.00	3034
	Other Plates							
12	Hood partition plates	288	149	1.8	0.5	0.5	1.00	584
13	Baffle plates	686	1311	1.8	0.5	0.5	1.00	2663
14	Outlet plenum ends	536	1806	1.8	0.5	0.5	1.00	3391
0	Ring, Beams & Gussets							
15	Dryer support ring	527	730	1.8	3	3	1.00	1621
16	Bottom cross beams	226	368	1.8	3	3	1.00	777
17	Cross beam gussets	626	778	1.8	0.5	0.5	1.00	1797
	Gussets for outer Cover plate and hood							
18(c)	New gusset on cover plate and front hood	1071	730	1.8	0.5	0.75	1.00	2333
18(a)	Gusset	350	1187	1	0.5	0.75	1.00	1238
18(b)	Gusset foot weld to cover plate	471	599	1.8	0.5	0.375	1.78	2438

Notes *1: Peak Stress = SRSS ((1), (3)) x (5) x (6)

Table EMEB-B-143-1-2

FIV Alternating Stress Summary with Hydrodynamic (CFD) Loads 100% Power

Exhibit EMEB-B-143-1: Revised FIV Stress Summary to Incorporate 100% and 120% CFD Transient Loads and Load Uncertainty

NON-PROPRIETARY VERSION

Table EMEB-B-143-2: FIV Alternating Stress Summary with Hydrodynamic (CFD) Loads 100% Power		Part B: Limit Curve Factor minus Uncertainty CFD Loads 100% Pwr					
		Level 1			Level 2		
ID	Dryer Component Name	LCF1	sig3	LCF1-sig3	LCF2	sig3	LCF2-sig3
	Horizontal plates:						
1	Inner hood base plate	12.8	5.6	7.2	10.3	4.5	5.8
2(a)	Modified outer cover plate5/8", both tips 4"	8.4	3.7	4.7	6.7	3.0	3.8
2(b)	Modified outer cover plate, exclude tips	9.1	4.0	5.1	7.2	3.2	4.1
4(a)	Original top hood (all hood)	18.2	8.0	10.2	14.5	6.4	8.1
4(b)	Modified top hood (outer hood)	6.9	3.1	3.8	5.4	2.4	2.9
4(c)	Hood top plates(Inner hood)	20.9	9.2	11.6	16.5	7.3	9.2
	Vertical plates:						
5(a)	Original outer Hood , strips	7.6	3.3	4.3	6.1	2.7	3.4
5(b)	Modified outer hood, top weld	6.8	3.0	3.8	5.4	2.4	3.0
5(c)	Modified outer hood, bottom weld	9.1	4.0	5.1	7.2	3.2	4.1
5(d)	Hood vertical plates (inner hood)	19.9	8.8	11.2	15.9	7.0	8.9
6	Hood end plates,(inner hood)	16.8	7.4	9.4	13.4	5.9	7.5
7	Hood end plates (outer hood)	7.3	3.2	4.1	5.8	2.6	3.3
8	Outer Hood Brackets(gussets)	13.5	5.9	7.6	10.8	4.7	6.0
10	Steam 'dam'	18.8	8.3	10.6	15.0	6.6	8.4
11	Steam 'dam' gussets	13.8	6.1	7.7	10.9	4.8	6.0
	Other Plates						
12	Hood partition plates	26.2	11.5	14.7	21.0	9.2	11.8
13	Baffle plates	10.8	4.8	6.1	8.6	3.8	4.8
14	Outlet plenum ends	13.7	6.1	7.6	10.8	4.8	6.0
0	Ring, Beams & Gussets						
15	Dryer support ring	14.3	6.3	8.0	11.4	5.0	6.4
16	Bottom cross beams	33.4	14.6	18.8	26.7	11.7	15.0
17	Cross beam gussets	12.0	5.3	6.7	9.6	4.2	5.4
	Gussets for outer Cover plate and hood						
18(c)	New gusset on cover plate and front hood	7.0	3.1	3.9	5.6	2.5	3.1
18(a)	Gusset	38.7	17.0	21.7	30.9	13.6	17.3
18(b)	Gusset foot weld to cover plate	8.9	3.9	5.0	7.1	3.1	4.0
Notes *1: Peak Stress = SRSS ((1), (3)) x (5		MinLCF1-sig3			Min LCF2-sig3		
		3.81			2.93		

Table EMEB-B-143-1-2

FIV Alternating Stress Summary with Hydrodynamic (CFD) Loads 100% Power

Exhibit EMEB-B-143-1: Revised FIV Stress Summary to Incorporate 100% and 120% CFD Transient Loads and Load Uncertainty

NON-PROPRIETARY VERSION

Table EMEB-B-143-3: FIV Alternating Stress Summary with Hydrodynamic (CFD) Loads 120% Power		Part A: Fatigue Stress Assessment CFD Loads 120% Pwr						
		ACM CLTP Max Surface Stress (psi)	Vortex Shedding Max Surface Stress (psi)	Weld Conc. Factor	Plate Thickness (in)	Weld Size (in)	Under-size Factor	Peak Stress (psi) (*1)
ID	Dryer Component Name	(1)	(3)	(5)	0.00	0	(6)	0
	Horizontal plates:							
1	Inner hood base plate	588	624	1.80	0 5	0.5	1.00	1543
2(a)	Modified outer cover plate5/8", both tips 4"	896	437	1.80	0.625	0.625	1.00	1794
2(b)	Modified outer cover plate, exclude tips	530	439	1.80	0 625	0.5	1.56	1936
4(a)	Original top hood (all hood)	412	943	1.80	0.50	0.50	1.00	1852
4(b)	Modified top hood (outer hood)	403	1112	1.80	1	0.625	2.56	5450
4(c)	Hood top plates(inner hood)	456	1964	1.40	0.5	0.5	1.00	2823
	Vertical plates:							
5(a)	Original outer Hood , strips	989	108	1.80	0.50	0.5	1.00	1791
5(b)	Modified outer hood, top weld	430	301	1.80	1.00	0.625	2.56	2419
5(c)	Modified outer hood, bottom weld	475	725	1.80	-	-	-	1936
5(d)	Hood vertical plates (inner hood)	484	761	1.40	0.50	0.5	1.00	1263
6	Hood end plates,(inner hood)	446	536	1.80	0.50	0.5	1.00	1255
7	Hood end plates (outer hood)	1029	322	1.80	0 50	0.5	1.00	1941
8	Outer Hood Brackets(gussets)	719	573	1.40	0 50	0.5	1.00	1287
10	Steam 'dam'	399	807	1.80	0.50	0.5	1.00	1620
11	Steam 'dam' gussets	537	941	1.80	0.50	0.5	1.00	1950
	Other Plates							
12	Hood partition plates	288	94	1.80	0.50	0.5	1.00	545
13	Baffle plates	686	1144	1.80	0.50	0.5	1.00	2401
14	Outlet plenum ends	536	1891	1.80	0.50	0.5	1.00	3538
0	Ring, Beams & Gussets							
15	Dryer support ring	527	675	1.80	3.00	3	1.00	1541
16	Bottom cross beams	226	135	1.80	3 00	3	1.00	474
17	Cross beam gussets	626	414	1.80	0.50	0.5	1.00	1351
	Gussets for outer Cover plate and hood							
18(c)	New gusset on cover plate and front hood weld	1071	820	1.80	0.5	0.75	1.00	2428
18(a)	Gusset	350	205	1.00	0.5	0.75	1.00	458
18(b)	Gusset foot weld to cover plate	471	490	1.80	0.5	0.375	1.78	2175

Notes *1: Peak Stress = SRSS ((1), (3)) x (5) x (6)

Table EMEB-B-143-1-3
FIV Alternating Stress Summary with Hydrodynamic (CFD) Loads 120% Power

Exhibit EMEB-B-143-1: Revised FIV Stress Summary to Incorporate 100% and 120% CFD Transient Loads and Load Uncertainty

NON-PROPRIETARY VERSION

Table EMEB-B-143-3: FIV Alternating Stress Summary with Hydrodynamic (CFD) Loads 120% Power		Part 3B: Limit Curve Factor minus Uncertainty CFD Loads 120% Pwr					
		Level 1			Level 2		
ID	Dryer Component Name	LCF1	sig3	LCF1-sig3	LCF2	sig3	LCF2-sig3
	Horizontal plates:						
1	Inner hood base plate	12.8	5.6	7.2	10.2	4.5	5.7
2(a)	Modified outer cover plate5/8", both tips 4"	8.4	3.7	4.7	6.7	3.0	3.8
2(b)	Modified outer cover plate, exclude tips	9.1	4.0	5.1	7.3	3.2	4.1
4(a)	Original top hood (all hood)	18.2	8.0	10.2	14.5	6.4	8.1
4(b)	Modified top hood (outer hood)	6.8	3.1	3.7	5.2	2.4	2.8
4(c)	Hood top plates(inner hood)	20.9	9.2	11.6	16.5	7.3	9.2
	Vertical plates:						
5(a)	Original outer Hood , strips	7.6	3.3	4.3	6.1	2.7	3.4
5(b)	Modified outer hood, top weld	6.8	3.0	3.8	5.4	2.4	3.1
5(c)	Modified outer hood, bottom weld	9.1	4.0	5.1	7.3	3.2	4.1
5(d)	Hood vertical plates (inner hood)	20.0	8.8	11.2	16.0	7.0	9.0
6	Hood end plates,(inner hood)	16.9	7.4	9.5	13.5	5.9	7.6
7	Hood end plates (outer hood)	7.3	3.2	4.1	5.9	2.6	3.3
8	Outer Hood Brackets(gussets)	13.5	5.9	7.6	10.8	4.7	6.1
10	Steam 'dam'	18.8	8.3	10.6	15.0	6.6	8.4
11	Steam 'dam' gussets	14.0	6.1	7.8	11.1	4.9	6.2
	Other Plates						
12	Hood partition plates	26.2	11.5	14.7	21.0	9.2	11.8
13	Baffle plates	10.9	4.8	6.1	8.7	3.8	4.8
14	Outlet plenum ends	13.6	6.1	7.6	10.7	4.8	5.9
0	Ring, Beams & Gussets						
15	Dryer support ring	14.3	6.3	8.0	11.4	5.0	6.4
16	Bottom cross beams	33.4	14.6	18.8	26.7	11.7	15.0
17	Cross beam gussets	12.1	5.3	6.8	9.6	4.2	5.4
	Gussets for outer Cover plate and hood						
18(c)	New gusset on cover plate and front hood weld	7.0	3.1	3.9	5.6	2.5	3.1
18(a)	Gusset	38.8	17.0	21.8	31.1	13.6	17.5
18(b)	Gusset foot weld to cover plate	9.0	3.9	5.0	7.1	3.1	4.0
Notes	*1: Peak Stress = SRSS ((1), (3)) x 5	MinLCF1-sig3			Min LCF2-sig3		
		3.71			2.77		

Table EMEB-B-143-1-3

FIV Alternating Stress Summary with Hydrodynamic (CFD) Loads 120% Power

Exhibit EMEB-B-143-1: Revised FIV Stress Summary to Incorporate 100% and 120% CFD Transient Loads and Load Uncertainty

NON-PROPRIETARY VERSION

[[

]]

Table EMEB-B-143-1-4 (a)

ASME Code Stresses at CLTP

Exhibit EMEB-B-143-1: Revised FIV Stress Summary to Incorporate 100% and 120% CFD Transient Loads and Load Uncertainty

NON-PROPRIETARY VERSION

[[

]]

Table EMEB-B-143-1-4 (b)

ASME Code Stresses at CLTP

Exhibit EMEB-B-143-1: Revised FIV Stress Summary to Incorporate 100% and 120% CFD Transient Loads and Load Uncertainty

NON-PROPRIETARY VERSION

[[

]]

Table EMEB-B-143-1-4 (c)

ASME Code Stresses at CLTP

Exhibit EMEB-B-143-1: Revised FIV Stress Summary to Incorporate 100% and 120% CFD Transient Loads and Load Uncertainty

NON-PROPRIETARY VERSION

[[

]]

Table EMEB-B-143-1-4 (d)

ASME Code Stresses at CLTP

Exhibit EMEB-B-143-1: Revised FIV Stress Summary to Incorporate 100% and 120% CFD Transient Loads and Load Uncertainty

NON-PROPRIETARY VERSION

[[

]]

Table EMEB-B-143-1-4 (e)

ASME Code Stresses at CLTP

Exhibit EMEB-B-143-1: Revised FIV Stress Summary to Incorporate 100% and 120% CFD Transient Loads and Load Uncertainty

NON-PROPRIETARY VERSION

[[

]]

Table EMEB-B-143-1-4 (f)
ASME Code Stresses at CLTP

Exhibit EMEB-B-143-1: Revised FIV Stress Summary to Incorporate 100% and 120% CFD Transient Loads and Load Uncertainty

NON-PROPRIETARY VERSION

[[

]]

Table EMEB-B-143-1-4 (g)

ASME Code Stresses at CLTP

Exhibit EMEB-B-143-1: Revised FIV Stress Summary to Incorporate 100% and 120% CFD Transient Loads and Load Uncertainty

NON-PROPRIETARY VERSION

[[

]]

Table EMEB-B-143-1-5 (a)

ASME Code Stresses at EPU

Exhibit EMEB-B-143-1: Revised FIV Stress Summary to Incorporate 100% and 120% CFD Transient Loads and Load Uncertainty

NON-PROPRIETARY VERSION

[[

]]

Table EMEB-B-143-1-5 (b)

ASME Code Stresses at EPU

Exhibit EMEB-B-143-1: Revised FIV Stress Summary to Incorporate 100% and 120% CFD Transient Loads and Load Uncertainty

NON-PROPRIETARY VERSION

[[

]]

Table EMEB-B-143-1-5 (c)

ASME Code Stresses at EPU

Exhibit EMEB-B-143-1: Revised FIV Stress Summary to Incorporate 100% and 120% CFD Transient Loads and Load Uncertainty

NON-PROPRIETARY VERSION

[[

]]

Table EMEB-B-143-1-5 (d)

ASME Code Stresses at EPU

Exhibit EMEB-B-143-1: Revised FIV Stress Summary to Incorporate 100% and 120% CFD Transient Loads and Load Uncertainty

NON-PROPRIETARY VERSION

[[

]]

Table EMEB-B-143-1-5 (e)

ASME Code Stresses at EPU

Exhibit EMEB-B-143-1: Revised FIV Stress Summary to Incorporate 100% and 120% CFD Transient Loads and Load Uncertainty

NON-PROPRIETARY VERSION

[[

]]

Table EMEB-B-143-1-5 (f)

ASME Code Stresses at EPU

Exhibit EMEB-B-143-1: Revised FIV Stress Summary to Incorporate 100% and 120% CFD Transient Loads and Load Uncertainty

NON-PROPRIETARY VERSION

[[

]]

Table EMEB-B-143-1-5 (g)

ASME Code Stresses at EPU

Exhibit EMEB-B-143-1: Revised FIV Stress Summary to Incorporate 100% and 120% CFD Transient Loads and Load Uncertainty

NON-PROPRIETARY VERSION

[[

]]

Table EMEB-B-143-1-6

ASME Code Stresses at EPU with 78%/16% ACM/CFD Uncertainty

Exhibit EMEB-B-143-1: Revised FIV Stress Summary to Incorporate 100% and 120% CFD Transient Loads and Load Uncertainty

NON-PROPRIETARY VERSION

[[

]]

Table EMEB-B-143-1-7

ASME Code Stresses at EPU with 78%/16% ACM/CFD Uncertainty

Exhibit EMEB-B-143-1: Revised FIV Stress Summary to Incorporate 100% and 120% CFD Transient Loads and Load Uncertainty

NON-PROPRIETARY VERSION

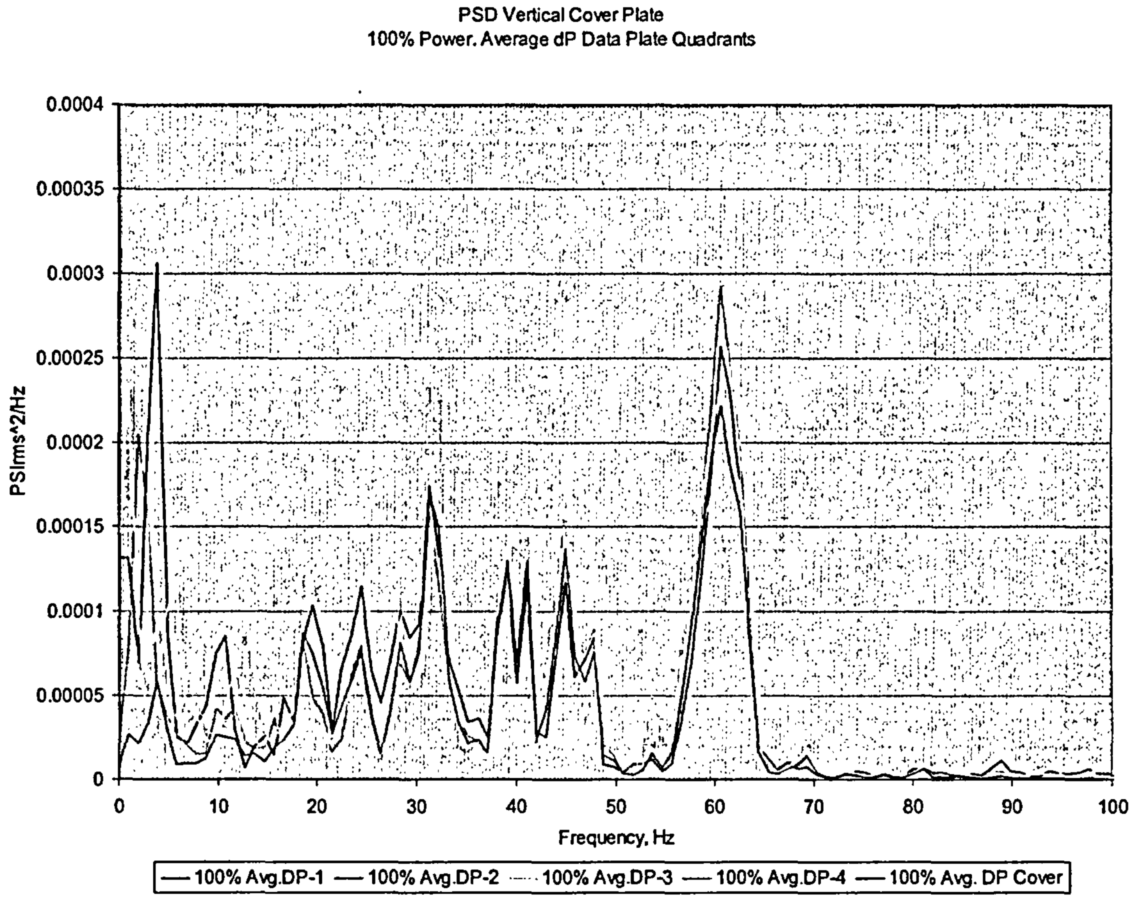

Figure EMEB-B-143-1-1

Four Quadrants of Cover Plate, Average Pressure Load, 100% Power PSD

Exhibit EMEB-B-143-1: Revised FIV Stress Summary to Incorporate 100% and 120% CFD Transient Loads and Load Uncertainty

NON-PROPRIETARY VERSION

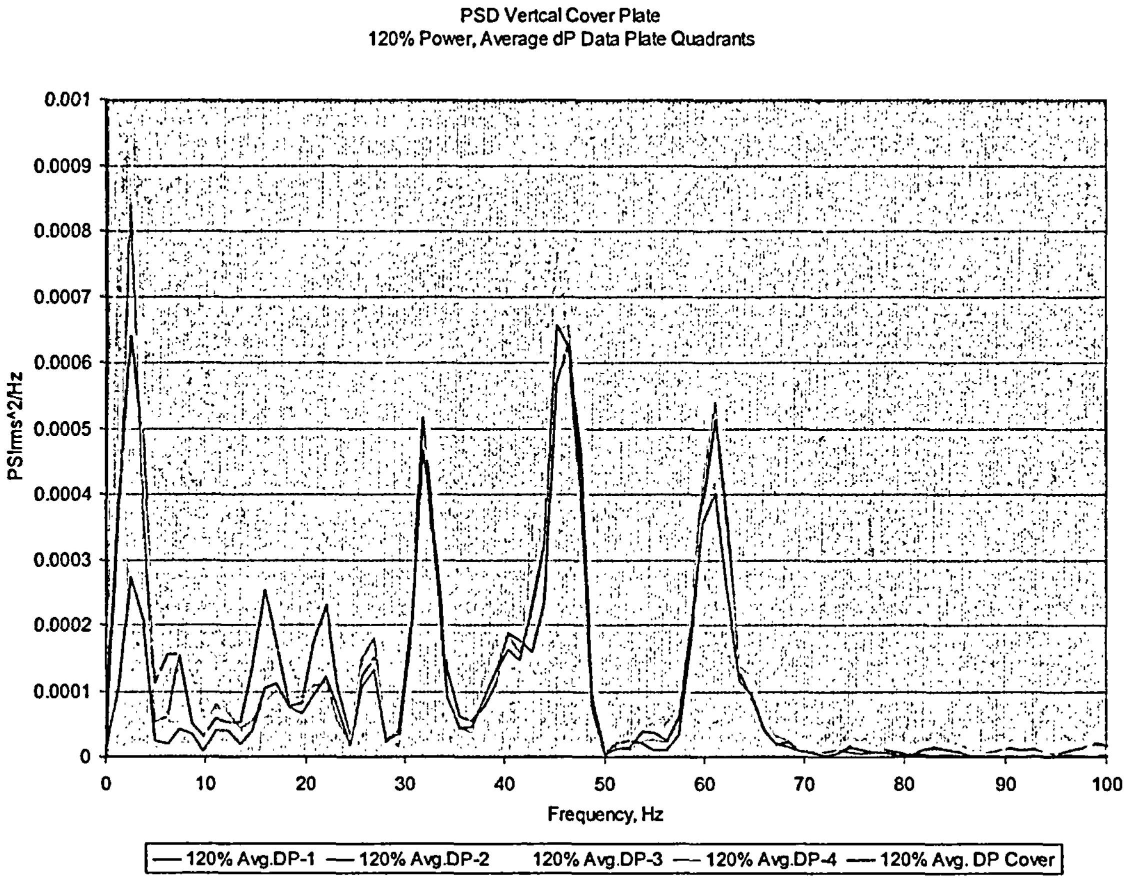

Figure EMEB-B-143-1-2

Four Quadrants of Cover Plate, Average Pressure Load, 120% Power PSD

Exhibit EMEB-B-143-1: Revised FIV Stress Summary to Incorporate 100% and 120% CFD Transient Loads and Load Uncertainty

NON-PROPRIETARY VERSION

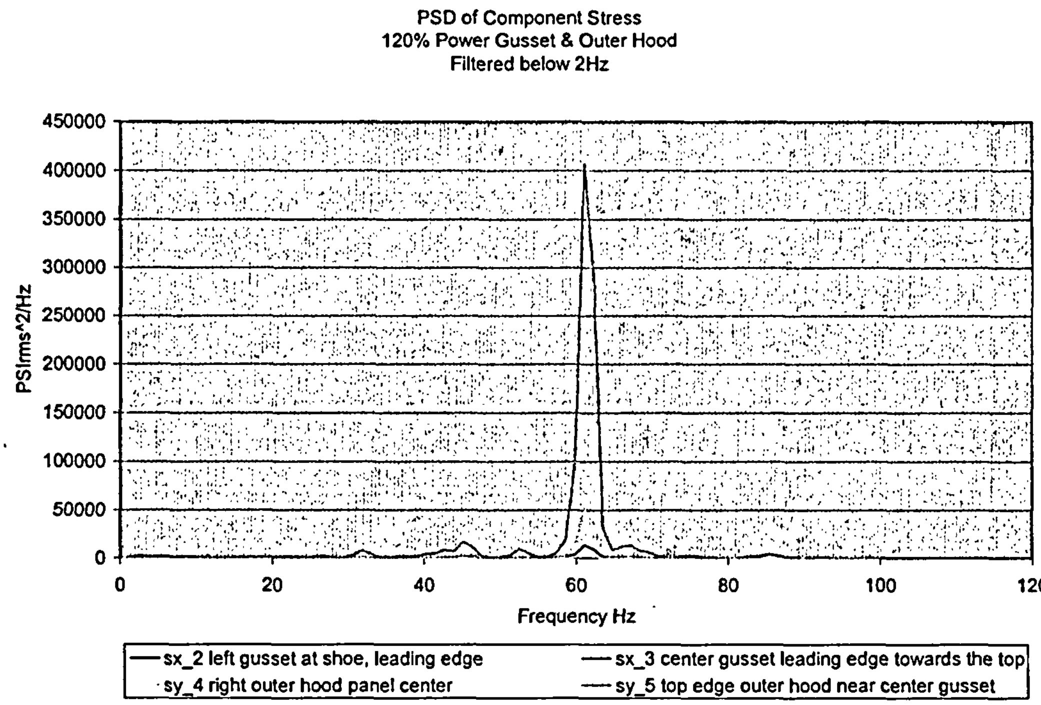

Figure EMEB-B-143-1-3

PSD of Component Stress Under CFD 120% Power Loads

Exhibit EMEB-B-143-1: Revised FIV Stress Summary to Incorporate 100% and 120% CFD Transient Loads and Load Uncertainty

NON-PROPRIETARY VERSION

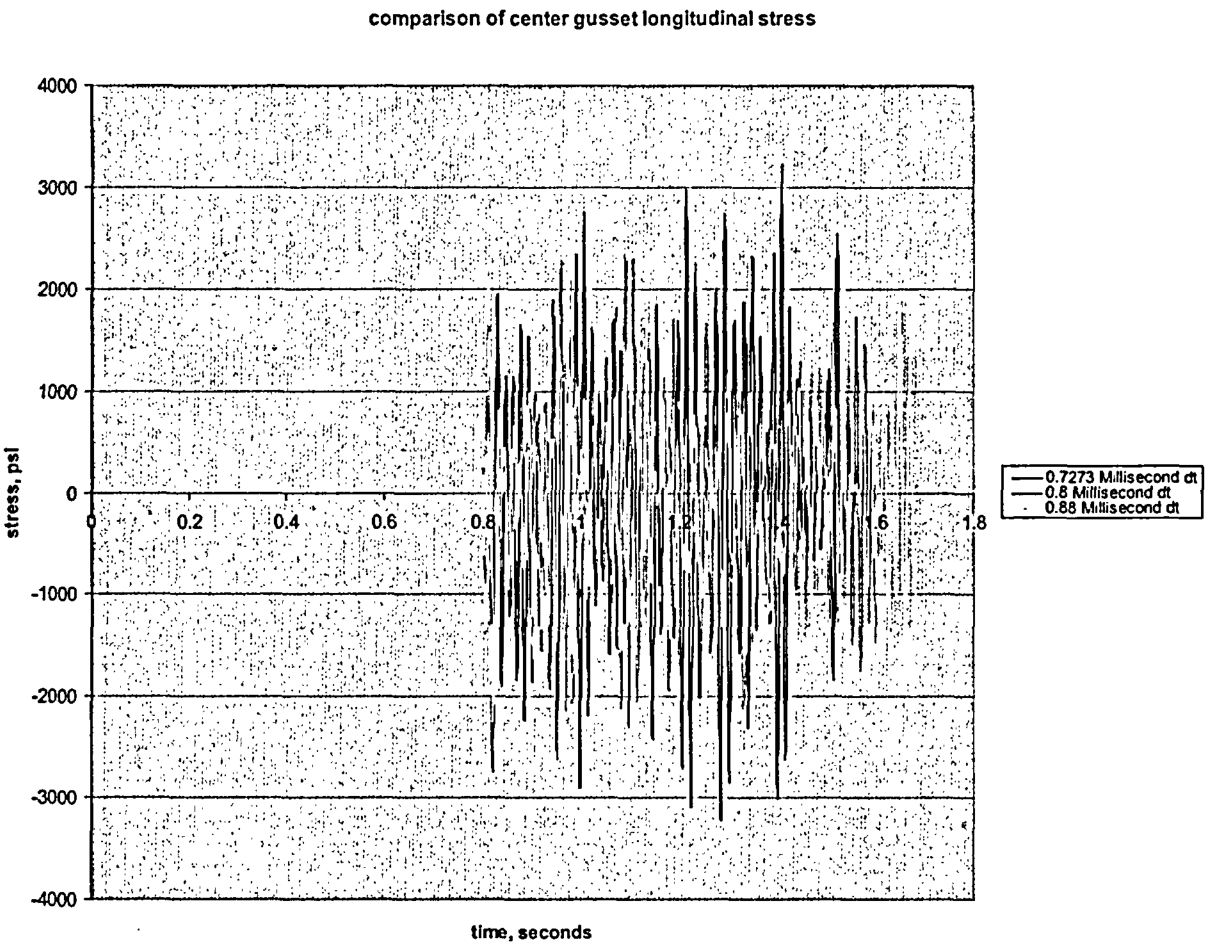

Figure EMEB-B-143-1-4

Stress Time History results 120% Power and +/- 10% Time Step Variation

Exhibit EMEB-B-143-1: Revised FIV Stress Summary to Incorporate 100% and 120% CFD Transient Loads and Load Uncertainty

NON-PROPRIETARY VERSION

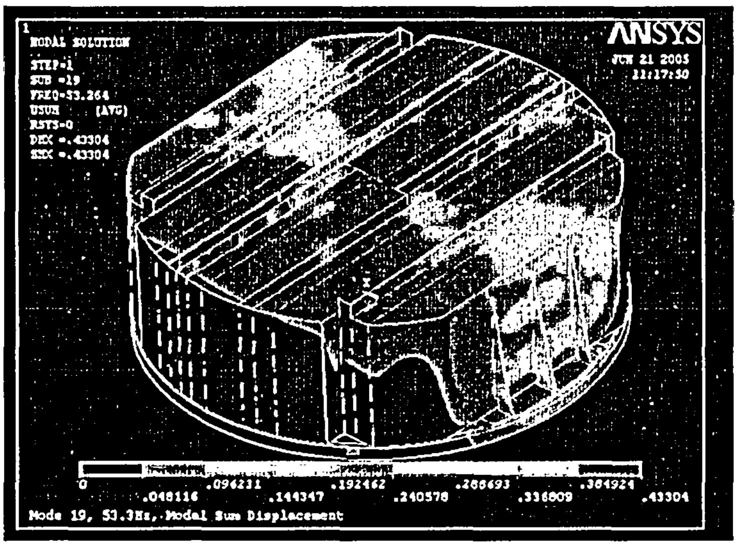

JAR Associates 6/22/05 VY Dryer
CFD Transient Analysis, Rev B

9

Figure EMEB-B-143-1-5

CFD Model Mode 19

Frequency 53.3 Hz

Exhibit EMEB-B-143-1: Revised FIV Stress Summary to Incorporate 100% and 120% CFD Transient Loads and Load Uncertainty

NON-PROPRIETARY VERSION

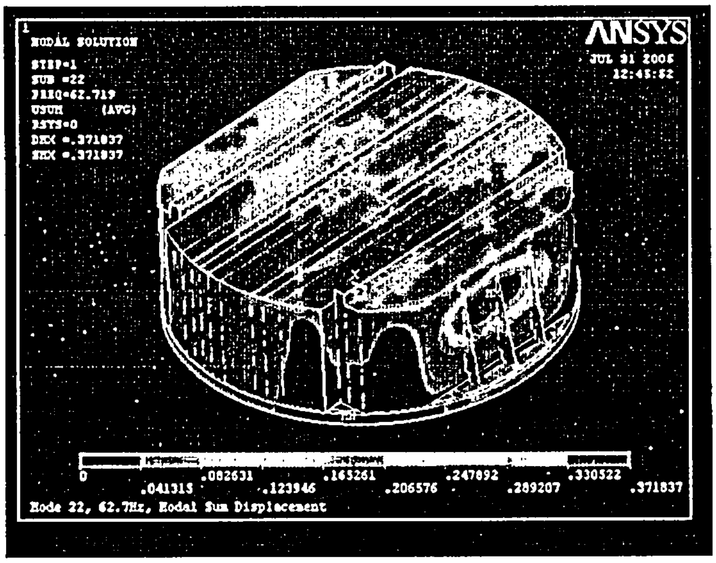

JAR Associates 6/22/05 VY Dryer
CFD Transient Analysis, Rev B

11

Figure EMEB-B-143-1-6
CFD Model Mode 22
Frequency 62.7 Hz

Exhibit EMEB-B-143-1: Revised FIV Stress Summary to Incorporate 100% and 120% CFD Transient Loads and Load Uncertainty

NON-PROPRIETARY VERSION

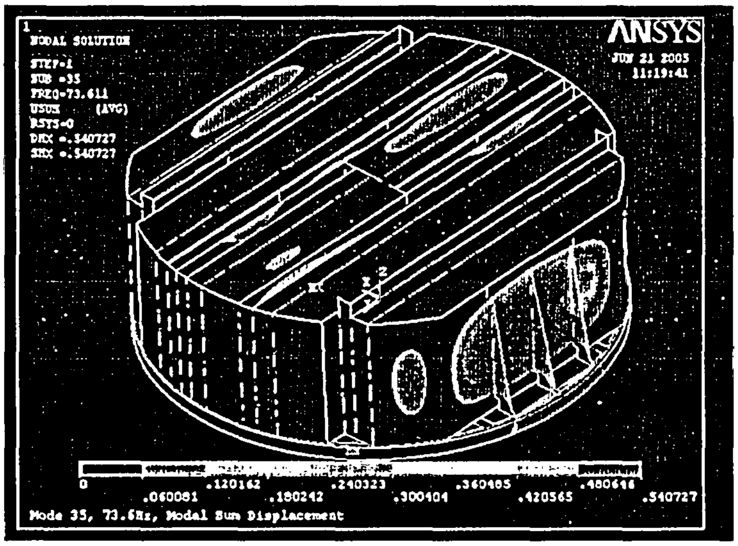

JAR Associates 6/22/05 VY Dryer
CFD Transient Analysis, Rev B

12

Figure EMEB-B-143-1-7
CFD Model Mode 35
Frequency 73.6Hz